

國立臺灣大學醫學院微生物學所微生物及免疫學組

碩士論文

Graduate Institute of Microbiology

College of Medicine

National Taiwan University

Master Thesis

探討鷹架蛋白 IQGAP2 在 EB 病毒感染中所扮演的角  
色

The Roles of Scaffold Protein IQGAP2 in Epstein-Barr  
Virus Infection

林楷敏

Kai-Min Lin

指導教授：蔡錦華 博士

Ching-Hwa Tsai, PhD

中華民國 104 年 7 月

July, 2015



國立臺灣大學（碩）博士學位論文  
口試委員會審定書

中文題目：探討鷹架蛋白IQGAP2在EB病毒感染  
中所扮演之角色

英文題目：The Roles of Scaffold Protein IQGAP2  
in Epstein-Barr Virus Infection

本論文係林楷毅君（學號R02445114）在國立臺灣大學  
微生物學所完成之碩（博）士學位論文，於民國104年7月17日  
承下列考試委員審查通過及口試及格，特此證明

口試委員：

林楷毅 鄧述謨 林孝芳

（簽名）

（指導教授）

林孝芳


林孝芳

系主任、所長

鄧述謨

（簽名）


## 摘要



EB 病毒是第一個被發現與腫瘤高度相關的 DNA 病毒，可以作為研究病毒致癌分子機制的範本，對病毒如何調控細胞因子來幫助其感染、潛伏於宿主，甚至使宿主細胞癌化的研究，有很大的助益。近年的研究逐漸發現，EB 病毒的致病機制，除了與其潛伏期有關，病毒的裂解複製期，亦能對 EB 病毒相關疾病的產生造成影響，惟 EB 病毒在宿主細胞內複製、進入裂解期的分子機制尚未完全明瞭。我們利用人類白血球濃厚液分離出的 B 細胞，感染 EB 病毒，發現細胞內一個鷹架蛋白 IQGAP2 的表現量增加。IQGAP2 目前被認為腫瘤抑制因子，所以在致癌 EB 病毒感染中會增加讓人好奇。除了病毒感染，當病毒進入裂解期時，IQGAP 的表現量也會增加。我們接著發現 EB 病毒的裂解轉活化因子 Rta 會讓細胞內的 IQGAP2 增加。實驗結果顯示，Rta 可能透過 IQGAP2 驅動子上的 Rta 反應元素來調控其轉錄。有趣的是，我們發現 Rta 會將 IQGAP2 蛋白帶入細胞核內，而 Rta 與 IQGAP2 在細胞核的複合體，會影響 EB 病毒裂解期蛋白的表現。Rta 會和 IQGAP2 共同作用，並且調控 EB 病毒進入裂解期。最後，我們發現在 EB 病毒感染而不朽化的類淋巴母細胞中，IQGAP2 能透過鈣黏蛋白 E 影響細胞之間的團聚。綜上所述，我們發現當 EB 病毒進入裂解期時，其裂解轉活化因子 Rta 會透過 IQGAP2 驅動子上的作用而使細胞核內的 IQGAP2 蛋白增加。這樣的一個 Rta-IQGAP2 複合體會在細胞核內調控 Rp 的活化。我們的發現找出一個新的參與 EB 病毒進入裂解期，使其進入複製期的調控因子，這些結果對我們了解 EB 病毒的生活史，有助於控制 EB 病毒的複製知相關研究。

關鍵字: EB 病毒, Rta (BRLF1), IQGAP2, 裂解期

## Abstract



As the first defined human oncogenic virus, Epstein-Barr virus (EBV) provides a good model to investigate how pathogens “hijack” cellular factors to promote their infection, persistence and even tumorigenesis. Although prolonged latency is the key feature of EBV, growing evidence suggests that lytic replication is crucial to EBV pathogenesis, yet how the virus promotes lytic cycle is not fully elucidated. In our B cell EBV infection model, we found that IQGAP2, a scaffold protein recognized as a tumor suppressor, was up-regulated after EBV infection. EBV lytic activation also increases IQGAP2 expression. We then identified that EBV immediate-early transactivator Rta was responsible to this up-regulation, most likely through a putative Rta responsive element (RRE) on IQGAP2 promoter. Surprisingly, we demonstrated that Rta was able to recruit IQGAP2 to the nucleus. This nuclear complex may play a role in lytic activation since lytic protein expression decreased when IQGAP2 transcription was suppressed due to impaired Rta auto-activation. Furthermore, in LCLs, IQGAP2 mediate cell-to-cell adhesion through regulation of adhesion molecule E-cadherin. To sum up, we found that, upon lytic stimuli, Rta increased IQGAP2 expression and translocalized it to the nucleus. The Rta-IQGAP2 complex activated Rta promoter (Rp) and promote lytic progression. This novel finding shed lights on a new path to understanding the intricate mechanism of EBV lytic cycle.

Key words:

Epstein-Barr virus (EBV); Rta (BRLF1); IQ-motif containing GTPase activating-like protein 2 (IQGAP2); lytic replication

# Table of Contents



摘要	I
Abstract	II
Table of Contents	III
Introduction	1
1. Epstein-Barr virus	1
1.1 Discovery	1
1.2 Classification, viral structure, and genome	1
1.3 Life cycle	2
1.4 Regulation of lytic reactivation	3
1.5 EBV-associated diseases	4
2 Rta	5
2.1 Structure	5
2.2 Transactivation ability	5
2.3 Cellular effects	6
3 IQGAP	7
3.1 IQGAP family	7
3.2 IQGAP1	8

3.3 IQGAP2	9
3.4 IQGAP3	11
3.5 Interaction of IQGAP1 with viruses	11
4 Study aim	11
<b>Materials and Methods</b>	<b>13</b>
1 Materials	13
1.1 Cell lines	13
1.2 Competent cells	14
1.3 DNA plasmids	14
1.4 Primers	16
1.5 Antibodies	17
1.6 Chemicals and reagents	18
1.7 Kits	20
1.8 Buffers	20
2 Methods	24
2.1 Cell culture	24
2.2 Polymerase chain reaction (PCR)	25
2.3 Plasmid construct	25





2.4 Transformation	26
2.5 Plasmid preparation	26
2.5.1 QIAGEN plasmid midi kit	26
2.5.2 Presto mini plasmid kit	27
2.6 NTRII transfection	28
2.7 Lentivirus packaging and infection	28
2.8 Electroporation	28
2.9 RNA extraction	29
2.10 Reverse transcription	29
2.11 Real-time quantitative polymerase chain reaction (Q-PCR)	30
2.12 Protein extraction	30
2.13 Protein concentration measurement	30
2.14 Sodium dodecyl sulfate polyacrylamide gel electrophoresis (SDS-PAGE)	31
2.15 Western Blot	31
2.16 Human primary B cell purification	32
2.17 Lymphoblastoid cell line (LCL) establishment	33
2.18 Indirect immunofluorescent assay	33



2.19 Subcellular fractionation	33
2.20 Co-immunoprecipitation (Co-IP)	34
2.21 Luciferase reporter assay	34
2.22 Cell proliferation rate determination	35
2.23 Chromatin immunoprecipitation assay (ChIP)	35
Results	38
1. EBV infection and reactivation increased the expression of IQGAP2.	38
2. Rta increased IQGAP2 expression with both of its DNA-binding and transactivation domains.	40
3. Rta increased IQGAP2 expression though direct binding to the promoter.	41
4. Rta recruited IQGAP2 to the nucleus.	41
5. IQGAP2 was required for lytic replication since it participated in Rp auto-activation.	43
6. IQGAP2 mediated cell-to-cell adhesion in LCLs through E-cadherin.	44
Discussion	45





1. Hypothesis	45
2. Direct transcription activation of Rta	45
3. Association of IQGAP2 with Rta in gene expression regulation	46
4. Nuclear function of IQGAP2	47
5. Diverse functions of IQGAP family in EBV infection	49
6. The role of IQGAP2 in EBV-associated disease progression	50
Figures	51
Figure 1. Schematic diagrams reveal binding factors on Epstein-Barr virus Zta and Rta promoters.	51
Figure 2. A diagram represents the structure of EBV Rta protein.	52
Figure 3. Schematic representation of human IQGAP family.	53
Figure 4. Expression kinetics of IQGAP2 mRNA and protein in human primary B cell along the course of EBV-induced LCL transformation were analyzed by Q-PCR.	54
Figure 5. mRNA and protein expression of IQGAP family in human primary B cells and paired EBV-transformed LCLs were revealed.	56
Figure 6. mRNA expression of IQGAP2 in EBV-infected, anti-CD40 / IL-4 stimulated, LPS-stimulated human or poly I:C-stimulated B	

cells was measured with Q-PCR.

Figure 7. Reactivation of EBV in Akata+ increased the expression of IQGAP2.

Figure 8. Reactivation of EBV in NA cells increased the expression of IQGAP2.

Figure 9. EBV Rta increased IQGAP2 protein expression.

Figure 10. Rta upregulated IQGAP2 promoter activity in 293T and TW01 cells.

Figure 11. Rta with C-terminal deletion or N terminal deletion could not induce IQGAP2 protein expression in TW01 cells.

Figure 12. IQGAP2 promoter luciferase reporter assay with different Rta-GFP proteins.

Figure 13. Luciferase activity assay with different 5'-deleted IQGAP2 reporter plasmids revealed the important promoter region.

Figure 14. Knockdown of Sp1 did not affect Rta-induced IQGAP2 promoter activation.

Figure 15. Rta binds to IQGAP2 promoter.

Figure 16. Nuclear expression of IQGAP2 was associated with Rta





expression.

Figure 17. Subcellular localization of transfected and induced IQGAP2 in relation with Rta was analyzed with confocal microscopy.

Figure 18. Subcellular localization of IQGAP2 in human CD19+ B lymphocytes and EBV-immortalized LCL was analyzed with confocal microscopy.

Figure 19. Interaction of IQGAP2 and Rta was analyzed with co-immuniprecipitation.

Figure 20. Knockdown of IQGAP2 affected spontaneous lytic progression in LCLs.

Figure 21. Knockdown of IQGAP2 impaired TPA/SB-induced lytic progression in NA cells.

Figure 22. Knockdown of IQGAP2 impacted Rta autoregulation in 293T cells.

Figure 23. Knockdown of IQGAP2 did not affect Rta-induced Zp or pBLLF1 activation in 293T cells.

Figure 24. Knockdown of IQGAP2 altered LCL clumping

morphology.

Figure 25. Knockdown of IQGAP2 did not affect LCL

proliferation.

Figure 26. Knockdown of IQGAP2 decreased E-cadherin in LCLs.

Figure 27. Hypothesis Model.

Figure 28. Rta activates lytic promoters through different pathways.

## Tables

Table 1. Primers used for plasmid constructs (pGL3-pIQGAP2 and

promoter serial deletion)

Table 2 Primers used for polymerase chain reactions

Table 3. shRNA sequence for gene knockdown lentiviruses

Table 4. Dilution fold for antibodies

## Appendixes

Appendix I. Expression of IQGAPs in B cells and EBV-infected B

cells was analyzed with cDNA microarray.

Appendix II. Expression of IQGAPs was analyzed when TW01

cells were transfected with EBV viral genes.

## References



# Introduction



## 1. Epstein-Barr Virus

### 1.1 Discovery

In 1958, British surgeon Denis Burkitt observed a child with abnormal swellings in the jaw area, which was then identified as Burkitt's lymphoma (Burkitt, 1958). Six years later, Michael Epstein and Yvonne Barr saw herpes-like particles under an electron microscope for the first time when observing cultured Burkitt's lymphoma cells (Epstein et al., 1964). In 1968, virologists Werner Henle and Gertrude Henle classified and named the virus Epstein-Barr virus (EBV) (Henle et al., 1968).

### 1.2 Classification and viral structure and genome


EBV belongs to *lymphocryptovirus* genus of gammaherpesvirus subfamily. The virus has a linear, double-stranded, 172-kilobase DNA genome, wrapped in a 100 nm-icosahedral nucleocapsid, inside of a lipid envelope with glycoprotein spikes such as gp350/220 and gp42. There are tegument proteins between the nucleocapsid and the envelope (Longnecker, 2013). Both ends of the EBV genome consist of 2 to 5 tandem, 500 basepair (bp) terminal repeats (TRs). Once EBV infects host cells, the termini of the viral genome ligate with each other to form an extra-chromosomal episome in the host nucleus. Other than TRs, EBV genome also contains 4 internal repeats (IRs) and 5 unique sequence domains (U) (Longnecker, 2013). The nomenclature of EBV open reading

frame (ORF) is according to the rank of length after B95.8 strain EBV genome is digested by restriction enzyme BamHI, from A (longest) to Z (shortest), as well as the reading orientation (Baer et al., 1984).



### **1.3 Life Cycle**

Like other herpesviruses, EBV life cycle consists of latency and lytic replication. The virus predominantly infects lymphocytes and epithelial cells and persists mostly in latency (Thompson and Kurzrock, 2004). In latent stage, EBV only expresses a small set of viral genes. In EBV-immortalized lymphoblastoid cell line (LCL), the latent gene products include EBV nuclear antigens (EBNA1, 2, 3A, 3B, 3C, LP), latent membrane proteins (LMP1, 2A, 2B) and viral RNAs (EBER1&2, BARTs) (Longnecker, 2013). A variety of stimuli can induce EBV lytic replication. For instance, treating EBV-carrying cell lines with phorbol ester 12-O-tetradecanoylphorbol-13-acetate (TPA), sodium butyrate (SB), anti-human immunoglobulin ( $\alpha$ -hIgG) or transforming growth factor  $\beta$  (TGF- $\beta$ ), as well as alternation of the intracellular calcium concentration can trigger EBV into lytic replication (Tovey et al., 1978; zur Hausen et al., 1978; Kallin et al., 1979; Chasserot-Golaz et al., 1988). Also, UV irradiation and hypoxia can initiate EBV lytic cycle (Liu et al., 1997; Jiang et al., 2006). Upon stimulation, the immediate-early (IE) transactivators, Zta (BZLF1, ZEBRA), Rta (BRLF1), and Mta (BMLF1, EB2, SM) are produced and cooperate with each other to initiate the transcription of downstream early



(E) and late (L) genes (Countryman and Miller, 1985; Hardwick et al., 1988). Most of the viral early gene products, including BALF5 (DNA polymerase), EA-D (BMRF1, DNA polymerase processivity factor), BGLF4 (protein kinase), and BALF2 (single-strand DNA binding protein), are associated with DNA replication, while late proteins such as gB (BALF4, gp110), gp350/220 (BLLF1) and LR2 (BLRF2, p23) are viral structure components (Lin et al., 1991; Tsurumi et al., 1996; Longnecker, 2013).

#### **1.4 Regulation of lytic reactivation**

Rta promoter (Rp) initiates transcription of Rta and Zta while Zta promoter (Zp) initiates transcription of Zta. The two lytic promoter orchestrate EBV lytic progression (Longnecker, 2013). The cellular regulatory elements that are reported to influence the expression of Zta and Rta and their corresponding binding sites are depicted in Figure 1. Other than chemical reagents and physical stimuli mentioned above, cellular factors contribute to activation of Zp and Rp as well. For example, cellular kinases, including mitogen-activated protein kinase (MAPK), protein kinase C (PKC), and phosphoinositide 3-kinase (PI3K) / protein kinase B (AKT) are required for lytic activation (Darr et al., 2001; Liang et al., 2002; Tsai et al., 2011; Goswami et al., 2012). Also, plasma cell differentiation factor, XBP-1, can bind and transactivate Zp (Sun and Thorley-Lawson, 2007). Moreover, early growth response protein 1 (EGR1) directly activates Rp, playing an important role in EBV reactivation when cells are treated with phorbol esters,  $\alpha$ -hIgG,

or UV irradiation (Zalani et al., 1995; Chang et al., 2006; Ye et al., 2010). A recent study found that cellular differentiation regulator BLIMP1 induces Epstein-Barr virus lytic reactivation in both epithelial and B cells by activating Rp and Zp (Reusch et al., 2015).

In contrast, many cellular factors contribute to latency by negatively regulating Zp and Rp. For example, B-cell-specific transcription factors PAX5 and Oct-2 can bind to Zta and prevent it from activating lytic promoters through Zta responsive elements (ZREs) (Robinson et al., 2012; Raver et al., 2013). Also, Ying Yang 1 (YY1) and Zinc finger E-box-binding homeobox proteins (ZEB) 1/2 have been reported to have negative effect upon Rp and Zp (Zalani et al., 1997; Kraus et al., 2003; Yu et al., 2007; Ellis et al., 2010).

### **1.5 EBV-associated diseases**

EBV infects over 90% of human population and mostly establishes life-long latent infection (Yao et al., 1985; Macsween and Crawford, 2003). However, in some cases, when the primary infection occurs in the teens, EBV can cause infection mononucleosis known as “kissing disease”, since EBV can be transmitted via saliva (Ebell, 2004). As the first defined oncogenic virus, EBV infection has been reported to associate with wide spectrums of lymphomas and epithelial cancers such as Burkitt’s lymphoma, Hodgkin lymphoma, NK/T-cell lymphoma, nasopharyngeal carcinoma and gastric cancer (Johansson et al., 1970; zur Hausen et al., 1970; Jones et al., 1988; Burke and Lee, 1990; Pallesen et al., 1991). EBV may lead to malignancies when the patients’ immune systems



are suppressed. For example, EBV may cause to post-transplant lymphoproliferative disease in organ transplant patients. In acquired immunodeficiency syndrome (AIDS) individuals, EBV is related to oral hairy leukoplakia and AIDS-associated lymphomas (Ziegler et al., 1982; Greenspan et al., 1985; Rea et al., 1994).


## **2. Rta**

### **2.1 Structure**

The immediate-early transactivator R (Rta) plays a crucial role in EBV lytic progression and DNA replication (Kenney and Mertz, 2014). Similar to Zta, Rta is a sequence-specific DNA binding protein that bind directly to the response element of its target promoter known as Rta response element (RRE). Rta protein is composed of 605 amino acids, its dimerization and DNA-binding domain locates on the N-terminal while the C-terminal is the transactivation domain (Manet et al., 1991; Hardwick et al., 1992) (Figure 2). TBP/TFIIB interacts with the C-terminal of Rta to promote transactivation activity. Also, amino acid 408-414 is the nuclear localization signal (NLS) of Rta (Hsu et al., 2005). Even if NLS of Rta is mutated and Rta retained in the cytosol, it can still activate Zp and Rp, resulting in induction of viral reactivation (Hsu et al., 2005).

### **2.2 Transactivator ability**

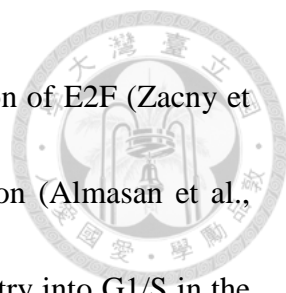
There are mainly two ways through which Rta activates gene expression: Rta either directly binds to the promoters of target genes or cooperates with other protein factors to



regulate gene expression. In some cases, Rta selectively binds to a GC-rich 17 base-paired DNA sequence (5'GNCCNNNNNNNNNGGNG3'), known as Rta responsive element (RRE). Promoters of viral genes like BLLF1, BMRF1 and BARF1, as well as cellular genes such as decoy receptor 3 (DcR3) (Quinlivan et al., 1993; Gruffat and Sergeant, 1994; Ho et al., 2007; Heilmann et al., 2012). In other scenario, when RRE is absent from target gene promoter, interaction with auxiliary cellular factors is needed for Rta to alter gene expression. For instance, association with Sp1 and methyl-CpG binding domain 1(MBD1)-containing chromatin-associated factor 1 (MCAF1) contributes largely to auto-simulation of Rp (Ragoczy and Miller, 2001; Chang et al., 2005). Also, Rta activates Zp by increasing phosphorylation of p38 and c-Jun N terminal kinase, resulting in activating transcription factor (ATF) 2 binding to ZII element of Zp (Adamson et al., 2000). Nonetheless, Rta transactivates BALF5 via DNA-bound transcription factors upstream stimulatory factor (USF) and E2F (Liu et al., 1996). In contrast, the early-lytic viral protein LF2 directly interacts with Rta, sequestering it in an inactive form in the cytoplasm (Heilmann et al., 2010).

### **2.3 Cellular effects**

Besides switching on EBV lytic replication, Rta also affects cellular functions. For instance, Rta can activate c-myc, a cellular gene important in proliferation (Gutsch et al., 1994). In BL cell lines, Rta is found to interact with an important tumor suppressor,

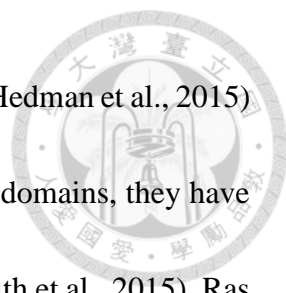


retinoblastoma protein (Rb), which alleviates Rb-mediated repression of E2F (Zacny et al., 1998). Since E2F activates genes important for DNA replication (Almasan et al., 1995), it is suggested that the binding of Rta to Rb facilitates the entry into G1/S in the cell cycle (Zacny et al., 1998). On the contrary, in epithelial cells, Rta induces G1 phase arrest and thereafter cellular senescence by increasing the expression of cyclin-dependent kinase regulators p21, p27 and cyclin E, while decreasing the expression of cyclin D, cyclin-dependent kinases (CDK) 4, CDK6, and phosphorylation level of tumor suppressor Rb (Chen et al., 2009). Furthermore, a recent study demonstrates that Rta elicits cell autophagy via the extracellular signal-regulated kinase (ERK) pathway in order to promote viral lytic development (Hung et al., 2014).

### **3. IQGAP**

#### **3.1 IQGAP family**

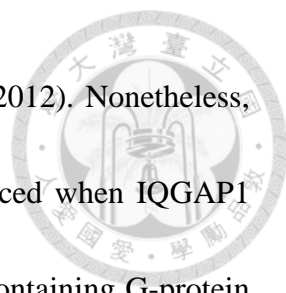
IQGAPs are an evolutionarily conserved proteins that interact with many partners to regulate diverse cellular processes, including cytokinesis, cell migration, cell proliferation, intracellular signaling, vesicle trafficking, and cytoskeletal dynamics (Hedman et al., 2015). The human IQGAPs are comprised of three members, namely IQGAP1, IQGAP2, and IQGAP3, all of which contain the CHD (calponin homology domain), the WW (tryptophan-tryptophan, poly-leucine binding) domain, the IQ (isoleucine-glutamine) domains, the GRD (GAP-related domain), and the RGCT (Ras-GAP C terminus) that



mediate protein-protein interactions and carry out various functions (Hedman et al., 2015) (Figure 3). Although human IQGAPs harbor similar protein binding domains, they have diverse functions, tissue expression, and subcellular localization (Smith et al., 2015). Ras GTPase activating proteins (GAPs) are thought to catalyze the transition from Ras-GTP to Ras-GDP, however, IQGAP1 and IQGAP2 can only stabilize GTP-bound active form of Ras-related C3 botulinum toxin substrate (Rac) 1 and cell division cycle (Cdc) 42 when associated with them via GRDs (Weissbach et al., 1994; Brill et al., 1996). Thus, IQGAPs are deemed scaffold proteins that participate in multiple cellular activities.

### 3.2 IQGAP1

Among the IQGAPs, IQGAP1 has been most extensively studied and well characterized since it was characterized in 1994 (Weissbach et al., 1994). Ubiquitously expressed IQGAP1 is encoded by *IQGAP1* on chromosome 15. Over 100 unique interacting proteins have been identified, implying that IQGAP1 is a critical mediator of many receptor signaling pathways (Brown and Sacks, 2006). IQGAP1 associates with endothelial growth factor receptors (EGFRs) and CD44 through second messengers (protein kinase C,  $\text{Ca}^{2+}$ , and Ras) or directly. In the downstream, IQGAP1 binds to extracellular signal-regulated kinases (ERKs), MAPK–ERK kinases (MEKs), and Raf kinases and help activation of the signal transduction pathway (Roy et al., 2005; Ren et al., 2007; Sbroggio et al., 2011). Also, IQGAP1 is involved PI3K–Akt pathways by

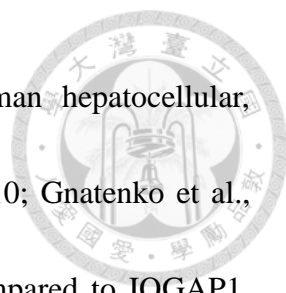


interacting with Akt kinase. (Chen et al., 2010; Tekletsadik et al., 2012). Nonetheless, both canonical and noncanonical Wnt pathways signaling is enhanced when IQGAP1 associates with components such as  $\beta$ -catenin, leucine-rich repeat-containing G-protein coupled receptor (LGCR) 4, importin- $\beta$ 5, and disheveled (Dvl) (Briggs et al., 2002; Goto et al., 2013a; Goto et al., 2013b; Carmon et al., 2014).

The association of F-actin with the IQGAP1 CHD indicates that IQGAP1 modulates cell cytoskeleton and that IQGAP1 links signaling components to cytoskeletal regulators (Abel et al., 2015). For instance, in Wnt signaling, the association of IQGAP1 with the actin polymerization proteins Diaphanous-related formin-1 (mDia1) and neuronal Wiskott–Aldrich syndrome protein (N-WASP) promotes cell polarity (Carmon et al., 2014). In addition, IQGAP1 participates in focal adhesion assembly and turnover and promote proper cell motility by interacting with integrins, cadherins, as well as focal adhesion proteins paxillin and vinculin (Kohno et al., 2013). IQGAP1 can stabilize microtubules through the microtubule-binding protein CLIP-170 near the cell margins, leading to establishment of cell polarity and subsequently cell migration (Noritake et al., 2005).

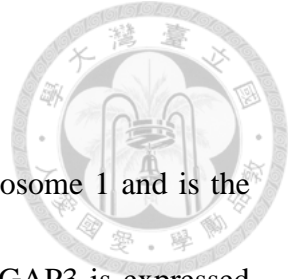
### **3.3 IQGAP2**

*IQGAP2* gene is located on chromosome 5 and IQGA2 protein is predominantly expressed in the liver (Brill et al., 1996; Wang et al., 2007). Decreased expression of



IQGAP2 protein is associated with malignancies including human hepatocellular, prostate, and gastric carcinomas (Jin et al., 2008; White et al., 2010; Gnatenko et al., 2013). Therefore, despite IQGAP2 has 62% sequence identity compared to IQGAP1, IQGAP2 is considered as a tumor suppressor while IQGAP1 is hinted as an oncoprotein (Brill et al., 1996; White et al., 2009). This is supported by the findings in hepatocellular carcinoma progression, where *iqgap2*-deficient mice require IQGAP1 for tumorigenesis (Schmidt et al., 2008). Another report also demonstrates that ablation of *IQGAP2* impairs hepatic long-chain fatty acids (LCFA) uptakes. Additionally, IQGAP2 overexpression inhibits Akt activation in prostate cancer cells while IQGAP1 expression promotes Akt signaling in hepatocellular carcinoma (Chen et al., 2010; Xie et al., 2012).

Nevertheless, IQGAP1 and IQGAP2 share several cellular functions. For example, similar subsequent effects of IQGAP1 and IQGAP2 are observed when associated with A-kinase anchoring protein (AKAP) 220. AKAP-bound IQGAP2 is phosphorylated by protein kinase A and promotes membrane ruffling while AKAP-bound IQGAP1 is recruited to the leading edge of migrating cells, promoting cell migration through microtubule interaction (Logue et al., 2011a; Logue et al., 2011b). Comparable to IQGAP1, IQGAP2 interacts with E-cadherin to regulate cell-to-cell adhesion (Yamashiro et al., 2007; Xie et al., 2012). Also, IQGAP2 can also modulate cytoskeletal reorganization in thrombin-activated platelets (Schmidt et al., 2003).



### **3.4 IQGAP3**

IQGAP3 was identified in 2007, the gene is located on chromosome 1 and is the least characterized gene among the family (Wang et al., 2007). IQGAP3 is expressed mainly in the brain, lung and testis of mice (Wang et al., 2007). Unlike IQGAP2, the findings on IQGAP3 are quiet similar to IQGAP1. IQGAP3 promotes proliferation and regulate cytokinesis through the Ras/ERK signaling cascade in mammary epithelial cells (Nojima et al., 2008; Adachi et al., 2014). Recently, a study found that both IQGAP1 and IQGAP3 are required for keratinocyte proliferation, and their high expression can result in tumorigenesis (Monteleon et al., 2015).

### **3.5 Interaction of IQGAP1 with viruses**

Microbes interact with host cells often through manipulating cellular factor. As a key factor in cytoskeletal regulation, IQGAP1 is at times altered in infections. For instance, upon viral entry or replication, Moloney murine leukemia virus (M-MuLV) uses matrix protein, classical swine fever virus (CSFV) uses core protein, Ebola virus uses matrix protein VP40 to interact with IQGAP1 (Leung et al., 2006; Gladue et al., 2011; Lu et al., 2013). Furthermore, in a study on Marburg virus, IQGAP1 is found to associate with tumor susceptibility gene 101 (TSG101) to mediate virion release (Dolnik et al., 2014).

## **4. Study Aim**

Previous studies found that IQGAP2 expression was elevated in EBV-infected B

cells via cDNA microarray. We attempted to further investigate the regulation mechanism of IQGAP2 and elucidate its biological significance in EBV-infected cells.





## Materials and Methods



### 1. Materials

#### 1.1 Cell Lines

##### **Akata-EBV+ / Akata-EBV-**

The Akata cell line was derived from an EBV-positive BL from a Japanese patient. EBV-negative Akata cell line is Akata cell line with EBV DNA loss (Takada et al., 1991; Shimizu et al., 1994).

##### **BJAB**

The BJAB cell line was derived from EBV-negative BL from an African patient (Menezes et al., 1975).

##### **HEK 293T (293T)**

293T cell line was derived from adenovirus type 5 E1 antigen and Simian virus 40 (SV40) large T antigen-transformed human embryonic kidney cells (ATCC No. CRL-1573).

##### **Lymphoblastoid Cell Line (LCL)**

LCLs were established by infecting CD19+ purified human primary B cells with B95.8 strain EBV for 28 days.

##### **NPC-TW01 (TW01)**

The TW01 cell line was derived from an EBV-positive NPC from a Taiwanese

patient with EBV DNA loss during cultivation (Lin et al., 1993).

## **NA**

The NA cell line was established by co-culturing TW01 cells with EBV-positive Akata cells. EBV latently-infected NA cells contain G418 selection marker and may undergo lytic cycle under TPA/SB treatment. (Chang et al., 1999)

## **1.2 Competent cells**

### **DH5 $\alpha$**

DH5 $\alpha$  is a recombinase A-deficient (RecA-) *Escherichia coli*. strain that maintains integrities of plasmids.

## **1.3 DNA plasmids**

### **pSG5**

pSG5 is a eukaryotic cell expression vector with SV40 promoter.

### **pSG5-Rta, pSG5-Zta**

pSG5-Zta is a B95.8 strain Zta-expressing plasmid. pSG5-Rta is a B95.8 strain Rta-expressing plasmid. Both of them use pSG5 as vector.

### **pEGFP-C1**

pEGFP-C1 is a CMV promoter-driven green fluorescent protein (GFP)-expressing



plasmid with multiple cloning sites (MCS) located upstream of GFP.

### **pEGFP-Rta, pEGFP-Rta 1-441, pEGFP-Rta 401-605**

Rta and truncated form of Rta plasmids are provided by Dr. Tuey-Ying Hsu.

Plasmids express B95.8 strain full-length Rta, amino acid 1 to amino acid 441 Rta (C terminal deletion), or amino acid 401 to amino acid 605 Rta (N terminal deletion).

Expressed proteins are fused with GFP at C terminus.

### **pCDNA3**

pCDNA3 is an eukaryotic cell expression vector with CMV promoter.

### **pCDNA3-IQGAP2-HA**

pCDNA3-IQGAP2-HA is a HA-tagged IQGAP2 expression plasmid using pCDNA3 as vector.

### **pGL2, pGL3**

pGL2 and pGL3 (Promega) are luciferase reporter vector lack eukaryotic promoter sequences. Their MCS locate upstream of luciferase for promoter insert.

### **pGL2-Zp, pGL2-Rp**

pGL2 luciferase reporter plasmids that use either -221 /+21 Zta promoter or -711/+256 Rta promoter.

### **pGL2-pBLLF1**

This pGL2 luciferase reporter plasmid that uses EBV BLLF1 (gp350/220) promoter,



provided by Dr. Mei-Ru Chen



### **pGL3-pIQGAP2 -853/+291, -642/+291, -523/+291, -167/+291, and -41/+291**

These pGL3 luciferase reporter plasmids use indicated part of IQGAP2 promoter to drive transcription of luciferase.

### **pLKO.1-shLuciferase, pLKO.1-shIQGAP2-2, and pLKO.1-shIQGAP2-3**

These are small hairpin RNA (shRNA)-producing plasmids containing sequences targeting luciferase or IQGAP2. (Table 3)

### **pCMVΔR8.91**

pCMV-ΔR8.91 is the packaging plasmid containing gag, pol and rev genes for lentiviruses. (Purchased from Academia Sinica RNAi core)

### **pMD.G**

pMD.G is the envelope plasmid that expresses G glycoprotein of vesicular stomatitis virus (VSV-G). (Purchased from Academia Sinica RNAi core)


## **1.4 Primers**

Table 1, 2

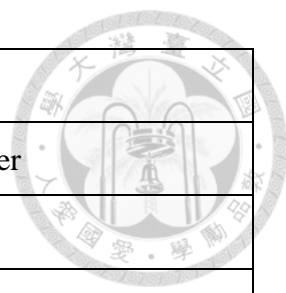
## **1.5 Antibodies**

Table 4


## 1.6 Chemicals and Reagents



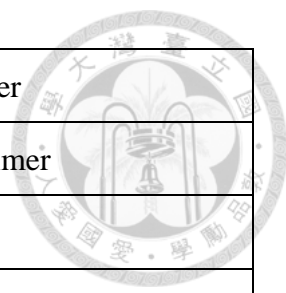
Chemicals and Reagents	Manufacturer
2-mercaptoethanol (2-ME)	Sigma
2-propanol	J.T. Baker
Acetic acid	J.T. Baker
Acrylamide	Bio-rad
AlamarBlue®	AbD Serotec
Agar A	Bionovas
Agarose	Invitrogen
Ammonium persulfate (APS)	Sigma
Ampicillin	Sigma
Bovine serum albumin (BSA)	Roche
Bromophenol blue	Sigma
Chloroform	Merck
Calf intestinal alkaline phosphatase (CIP)	New England Biolabs
Diethyl pyrocarbonate (DEPC)	Sigma
Dimethyl sulfoxide (DMSO)	Merck
Dipotassium phosphate ( $K_2HPO_4$ )	Merck
Disodium phosphate ( $Na_2HPO_4$ )	Merck
Deoxyribonucleotide triphosphate (dNTP)	Protech
Dithiothreitol (DTT)	Promega
Dulbecco's modified Eagle's medium (DMEM)	Hyclone
Dual-Glo® Luciferase Substrate	Promega
Ethanol	Burnett



Ethidium bromide (EtBr)	Sigma
Ethylenediaminetetraacetic acid (EDTA)	J.T. Baker
Fast green	Sigma
Fat-free skim milk	Anchor
Fetal bovine serum (FBS)	Hyclone
Ficoll-Paque	GE Healthcare
G418 sulfate	Merck
Glycerol	J.T. Baker
Glycine	Bio Basic
Hydrochloric acid (HCl)	J.T. Baker
IGEPAL	Sigma
Imidazole	Usb
Kanamycin	Sigma
Lipofectamine™ 2000	Invitrogen
L-glutamine	Sigma
Methanol	J.T. Baker
M-MLV Reverse transcriptase	Promega
Non-liposome transfection reagent II (NTR II)	T-pro
Opti-MEM®	Invitrogen
Penicillin:streptomycin solution	Gemini
Peptone	Usb
Phusion™ Hot Start High-Fidelity DNA Polymerase	Finnzymes
Protein assay dye	Biorad
ProZyme DNA polymerase	Protech



Random primers	Bionovas
RNase A	Sigma
Rnasin RNase inhibitor	Promega
Roswell Park Memorial Institute medium (RPMI)	Hyclone
Potassium chloride (KCl)	J.T. Baker
Potassium dihydrogen phosphate (KH <sub>2</sub> PO <sub>4</sub> )	Merck
Propidium iodide	Sigma
Cømplete Protease inhibitor cocktail tablets	Roche
Puromycin	Sigma
Sodium acetate (NaOAc)	Merck
Sodium azide	Sigma
Sodium chloride (NaCl)	J.T. Baker
Sodium deoxycholate	Sigma
Sodium dodecyl sulfate (SDS)	Merck
Sodium fluoride (NaF)	Merck
Sodium hydroxide (NaOH)	J.T. Baker
Sodium orthovanadate (Na <sub>3</sub> VO <sub>4</sub> )	Sigma
T4 DNA ligase	New England Biolabs
N,N,N',N'-Tetramethylethylenediamine (TEMED)	Sigma
Tris	Bio Basic
Triton X-100	Merck
TRIzol® reagent	Invitrogen
Trypan blue	Sigma
Trypsin	Biological Industries



Tween 20	J.T. Baker
Western Lightning™ chemiluminescence reagent plus	PerkinElmer
Xylene cyanol FF	BDH
Yeast extract	BD

### 1.7 Kits

Kit	Manufacturer
Gel/PCR DNA fragments extraction kit	Geneaid
Presto™ High-speed plasmid mini kit	Geneaid
Neon® Transfection System 10 µL Kit	Invitrogen
Plasmid maxi kit	Qiagen
RNeasy Mini Kit	Qiagen

### 1.8 Buffers

#### Phosphate-buffered saline (PBS) -EDTA (per liter)

EDTA 0.2 g, KCl 0.2 g, KH<sub>2</sub>PO<sub>4</sub> 0.2 g, NaCl 8.0 g, Na<sub>2</sub>HPO<sub>4</sub> 1.15 g, add ddH<sub>2</sub>O to 1 L, autoclaved.

#### 0.5% Trypan blue (per 100 ml)

Trypan blue 0.5 g, add PBS to 100 ml.

#### 10X Phosphate-buffered saline (PBS) (per liter)

KCl 2.0 g, KH<sub>2</sub>PO<sub>4</sub> 2.4 g, NaCl 80.0 g, Na<sub>2</sub>HPO<sub>4</sub> 14.4 g, adjust to pH 7.4 with NaOH,





mix and add ddH<sub>2</sub>O to 1 L.

**Lysogeny broth (LB) medium (per liter)**

NaCl 10.0 g, Peptone 10.0 g, Yeast extract 5.0 g, adjust to pH 7.0 with NaOH, mix

and add ddH<sub>2</sub>O to 1 L, autoclaved.

**Terrific broth (TB) medium (per liter)**

Glycerol 4 ml, KH<sub>2</sub>PO<sub>4</sub> 2.31 g, K<sub>2</sub>HPO<sub>4</sub> 12.54 g, Peptone 12.0 g, Yeast extract 24.0

g, mix and add ddH<sub>2</sub>O to 1 L, autoclaved.

**50X Tris-acetate-EDTA (TAE) buffer (per liter)**

Acetic acid 57.1 ml, pH 8.0 0.5M EDTA 100 ml, Tris 242.0 g, mix and add ddH<sub>2</sub>O

to 1 L.

**6X DNA loading dye (per 100 ml)**

Glycerol 30 ml, Xylene cyanol FF 0.25 g, mix and add ddH<sub>2</sub>O to 100 ml.

**4X Sample loading buffer (per 100 ml)**

Bromophenol blue 0.4 g, Glycerol 40 ml, SDS 8.0 g, pH 6.8 1M Tris 20 ml, mix and

add ddH<sub>2</sub>O to 100 ml, store at -20°C, supplemented with 2-ME 14.3 µl/ml freshly before

use.

**DEPC ddH<sub>2</sub>O (per liter)**

DEPC 1.0 g, add ddH<sub>2</sub>O to 1 L, autoclaved.

**Radioimmunoprecipitation assay (RIPA) buffer (per liter)**

pH 8.0 0.5M EDTA 4 ml, NaCl 87.0 g, NaF 2.1 g, Na<sub>3</sub>VO<sub>4</sub> 0.018 g, 10% SDS 10 ml,  
Sodium deoxycholate 5.0 g, pH 7.4 1M Tris 50 ml, mix and add ddH<sub>2</sub>O to 1 L,  
supplemented with 50X Ccomplete protease inhibitor 40 µl/ml freshly before use.

**10X Western blot running buffer (per liter)**

Glycine 188.0 g, SDS 10.0 g, Tris 30.0 g, adjust to pH 8.3 with NaOH, mix and add  
ddH<sub>2</sub>O to 1 L.

**10X Western blot transfer buffer (per liter)**

Glycine 188.0 g, Tris 30.0 g, mix and add ddH<sub>2</sub>O to 1 l, supplemented with methanol  
200 ml 1X transfer buffer freshly before use.

**Western blot blocking buffer (per 100 ml)**

Fat-free skim milk powder 4.0 g, add western blot washing buffer to 100 ml.

**10X Western blot washing buffer (per liter)**

NaCl 90.0 g, pH 7.4 1M Tris 100 ml, Tween 20 20 ml, mix and add ddH<sub>2</sub>O to 1 L.

**Antibody dilution buffer (per 50 ml)**

Skim milk 0.25 g, 20% Sodium azide 0.5 ml, add western blot washing buffer to  
50 ml

**Stripping buffer (per 100 ml)**

10% SDS 20 ml, pH 6.8 1M Tris 6.68 ml, add ddH<sub>2</sub>O to 100 ml, supplemented with  
2-ME 8.2 µl/ml freshly before use.



### **0.1% TritonX-100 (per 100 ml)**

100  $\mu$ l TritonX-100, add 1X PBS to 100ml.

### **Fractionation buffers**

#### **Buffer A**

pH 7.9 10 mM HEPES, 10 mM KCl, 0.1 mM EDTA, 1 % IGEPAL, supplemented with 1X protease inhibitor freshly before use.

#### **Buffer B**

pH 7.9 20 mM HEPES, 0.4 mM NaCl, 1 mM EDTA, 10% glycerol, supplemented with 1X protease inhibitor freshly before use.

### **Chromatin immunoprecipitation (ChIP) buffers**

#### **Cell lysis buffer**

pH 8.0 5 mM HEPES, 85 mM KCl, 0.5% IGEPAL, supplemented with 1 mM DTT, 1X protease inhibitor, 0.1 mM PMSF freshly before use.

#### **Nuclei lysis buffer**

pH 8.0 50 mM Tris, 10 mM EDTA, 1% SDS, supplemented with 1 mM DTT, 1X protease inhibitor, 0.1 mM PMSF, 0.1 M NaF, 1 mM  $\text{Na}_3\text{VO}_4$  freshly before use.

#### **IP dilution buffer**

pH 8.0 16.7 mM Tris, 167 mM NaCl, 1 mM EDTA, 1% Triton X-100, supplemented with 1 mM DTT, 1X protease inhibitor, 0.1 mM PMSF, 0.1 M NaF, 1



mM  $\text{Na}_3\text{VO}_4$  freshly before use.

#### **Low salt wash buffer**

pH 8.0 50 mM Tris, 150 mM NaCl, 5 mM EDTA, 1% IGEPAL, 0.1% SDS, 1%

deoxycholic acid

#### **High salt wash buffer**

pH 8.0 50 mM Tris, 300 mM NaCl, 5 mM EDTA, 1% IGEPAL, 0.1% SDS, 1%

deoxycholic acid

#### **LiCl wash buffer**

pH 8.0 50 mM Tris, 150 mM NaCl, 5 mM EDTA, 300 mM LiCl, 1% IGEPAL,

0.1% SDS, 1% deoxycholic acid

#### **Tris-EDTA buffer (TE buffer)**

1 mM EDTA, pH 8.0 10 mM Tris

#### **Elution buffer**

Fresh prepared with 50 mM  $\text{NaHCO}_3$ , 1% SDS

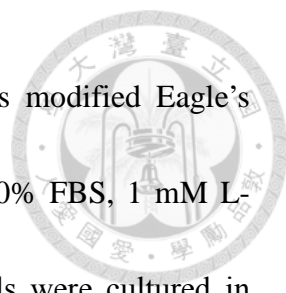
#### **Proteinase K buffer**

pH 7.5 50 mM Tris, 25 mM EDTA, 1.25% SDS

## **2. Methods**

### **2.1 Cell culture**

Akata, BJAB, and LCLs were cultured in Roswell Park Memorial Institute medium



(RPMI) while 293T, TW01, and NA were cultured in Dulbecco's modified Eagle's medium (DMEM). Cell culture medium was supplemented with 10% FBS, 1 mM L-glutamine, 100 U/ml penicillin, and 100 µg/ml streptomycin. Cells were cultured in humid incubators with 5% CO<sub>2</sub> at 37 °C.

## **2.2 Polymerase chain reaction (PCR)**

ProZyme DNA polymerase and Phusion<sup>TM</sup> Hot Start High-Fidelity DNA Polymerase were used for mRNA detection and plasmid construct respectively. PCRs were conducted as in users' manual provided by DNA polymerase manufactures. In brief, primers, template DNA, 10X reaction buffer, and DNA polymerase were mixed in a 200 µl PCR tube. Using T3 Thermocycler (Biometra), DNA templates were denature at 94 °C, primers were annealed at 60 °C, and then underwent elongation at 72 °C. This cycle was repeated for 24-34 times to make adequate DNA products for proceeding agarose gel electrophoresis. The elongation step of the final cycle was extended for extra 10 minutes.

## **2.3 Plasmid construct**

Insert genes were prepared by PCR with Phusion<sup>TM</sup> Hot Start High-Fidelity DNA Polymerase with specialized primers and LCL genomic DNA template. PCR products were digested with restriction enzymes at 37 °C O/N (overnight) and processed through gel extraction. Vectors were prepared by restriction enzyme digestion, CIP digestion, and gel extraction. Insert genes and vectors were ligated with T4 DNA ligase at 16 °C O/N.

Resulting plasmids were then transformed into competent cells, amplified, extracted, and sequenced.



## **2.4 Transformation**

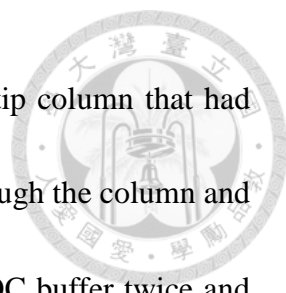
Plasmids were mixed with competent cells and cooled on ice for 30 minutes. The mixture was transferred to 42 °C for a 90 second-heat shock. Afterwards, the mixture is cooled on ice immediately for another 30 minutes and recovered in antibiotic-free LB medium for 1-2 hours. Selection is performed by spreading the cells on antibiotic-containing LB agar plate with silicon beads and cultured O/N at 37 °C.

## **2.5 Plasmid preparation**

DNA plasmids were prepared with QIAGEN Plasmid midi kit or Presto™ Mini Plasmid Kit according to instructions from user manuals.

### **2.5.1 QIAGEN Plasmid midi kit**

Five-hundred ml of target plasmid-containing bacterial culture was prepared in antibiotic-containing TB buffer O/N at 37 °C with 160 rpm constant shaking (LM-530D). Bacterial culture was centrifuged at 12000 x g for 15 minutes at 4 °C. Medium was discarded and resulting bacterial pellet was resuspended with 7 ml P1 buffer. Bacterial cells were lysed with 7 ml P2 buffer at room temperature for 15 minutes with gentle stir. Afterwards, the mixture was neutralized with 7 ml P3 buffer for 20 minutes on ice with gentle stir. Unwanted clumps were removed by centrifugation at 12000 x g for 30 minutes



at 4 °C. Supernatant was transferred to a DNA-binding QIAGEN-tip column that had been equilibrated with 5 ml QBT buffer. The supernatant passed through the column and flow-through was discarded. The column was washed with 10 ml QC buffer twice and the plasmid was eluted with 10 ml QF buffer. DNA was precipitated by adding 7 ml isopropanol and stored the mixture O/N at -20 °C. Precipitated DNA pellets were wash with 1 ml ethanol twice after centrifugation at 12000 x g for 30 minutes at 4 °C. DNA was dissolved in adequate amount of ddH<sub>2</sub>O.

### **2.5.2 Presto™ Mini Plasmid Kit**

5 ml of target plasmid-containing bacterial culture was prepared in antibiotic-containing LB buffer O/N at 37 °C with 160 rpm constant shaking (LM-530D). Bacterial culture was centrifuged at 12000 x g for 5 minutes at 4 °C. Medium was discarded and resulting bacterial pellet was resuspended with 200µl PD1 buffer. Bacteria were then lysed with 200 µl PD2 buffer at room temperature for 5 minutes with gentle inverts. Afterwards, the mixture was neutralized with 300 µl PD3 buffer for 5 minutes on ice with gentle inverts. Unwanted clumps were removed by centrifugation at 12000 x g for 5 minutes at 4 °C. Supernatant was transferred to a DNA-binding PDH column. The column was centrifuged at 12000 x g for 30 seconds at 4 °C and the flow-through was removed. The column was washed with 600 ml wash buffer twice. One additional centrifugation was applied to get rid of excess washing buffer. Finally, DNA was

dissolved in adequate amount of ddH<sub>2</sub>O.

## **2.6 NTRII Transfection**

Two µl of NTRII transfection reagent is added for every µg of DNA transfectant in 160 µl OPTI-MEM and incubated for 15 min at room temperature, along with the DNA transfectant. Then, the mixture is added dropwise to 3 X 10<sup>5</sup> cell seeded in a 6-well plate well. Seventy-two hours post-transfection, cells were harvest for further analysis

## **2.7 Lentivirus packaging and infection**

293T cells were seeded in antibiotics-free DMEM in 75T flasks with 70 to 80% confluence and co-transfected with 13.5 µg of p8.91, 1.5 µg of pMD.G and 15 µg of shRNA-expressing plasmid using lipofectamine<sup>TM</sup> 2000. Sixteen hours post-transfection, the medium was replaced with 20 ml of fresh DMEM containing 20% FBS and incubated for 48 hours to collect the supernatants containing infectious shRNA lentiviruses. Supernatants were filtered through 0.22 µm filters and stored at -80°C until use. One MOI was used for infection. Cells were seeded in 6 well with lentiviruse and centrifuged at 2250 rpm at room temperature for 30 minutes. 5 days post-infection, infected cells underwent 2 µg / ml puromycin selection before further analysis.

## **2.8 Electroporation**

Cells were electroporated using a Neon kit (Invitrogen) according to the manufacturer's instructions. Briefly, cells were washed with EDTA-free PBS for three





times and then resuspended in 10  $\mu$ l of R buffer (provided in the Neon kit) and mixed with the relevant plasmids before electroporation. After pulse induction, the samples were transferred into fresh medium and then incubated for the indicated time before being subjected to further assays. In general,  $2 \times 10^5$  cells were electroporated with 0.5  $\mu$ g of plasmids with a pulse of 1250 V for 30 ms.

## **2.9 RNA extraction**

Extraction of total cellular RNA was performed with TRIzol reagent according to the manufacturer's instructions. In brief, cells were lysed by 1 ml of TRIzol reagent, pipetted for homogenization, incubated for 5 minutes at room temperature. Then, 0.2 ml of chloroform was added, followed by vigorous shakes for 10 times and incubation for 2 minutes at room temperature. The samples were then centrifuged at 12000 x g for 15 minutes at 4 °C. After centrifugation, the aqueous phase was transferred to a fresh eppendorf and mixed with 0.5 ml of isopropanol to precipitate RNA, along with 1  $\mu$ g glycogen to help RNA precipitation at -20 °C O/N. On the next day, the samples were centrifuged at 12000 x g for 10 minutes at 4 °C. The supernatant was discarded and the RNA pellets were washed with 1 ml of 75% DEPC-ethanol. Finally, the RNA was dissolved in adequate amount of DEPC-treated ddH<sub>2</sub>O.

## **2.10 Reverse transcription**

For reverse transcription, 2  $\mu$ g of RNA with 1  $\mu$ g of random hexamers was denatured

at 70 °C for 10 minutes in a 12 µl reaction, and then supplemented with 4 µl of M-MLV RT 5X Reaction buffer, 2 µl of 100 mM DTT, 1 µl of 2.5 mM dNTP mix, and 1 µl (20 units) of M-MLV reverse transcriptase. The reaction was carried out at 25°C for 10 minutes, 42 °C for 50 minutes and 70 °C for 15 minutes.

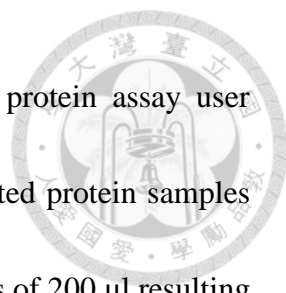
### **2.11 Real-time quantitative Polymerase chain reaction (Q-PCR)**

Q-PCR was performed with Bioline SensiFAST™ SYBR® No-ROX Kit accordingly to user manual. In brief, 8.4 µl of ddH<sub>2</sub>O-diluted DNA sample was mixed with 0.8 µl 10 µM forward primer, 0.8 µl 10 µM reverse primer, and 10 µl 2X SensiFAST SYBR No-ROX Mix. The mixture was loaded in a 96-well plate and subjected to Biorad CFX Connect for reactions. Polymerase was first activated at 95 °C for 2 minutes. Thirty-nine-time-repeated cycles were performed at 95 °C for 5 seconds, 60 °C for 10 seconds, and 72 °C for 15 seconds to amplify target sequence. Threshold cycles (Ct) were acquired and compared to determine gene expression.

### **2.12 Protein extraction**

Cells were harvested and washed with PBS. 50 µl RIPA was added for every 1X10<sup>5</sup> collected cells, followed by brief pipetting. Samples were then homogenized on ice with sonication (UP400A Sonicor) and centrifuged at 12000 x g for 5 minutes at 4 °C to obtain soluble protein extracts.

### **2.13 Protein concentration measurement**



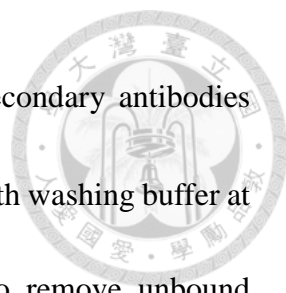
Protein concentration was determined according to Bio-Rad protein assay user manual. In brief, 400  $\mu$ l of protein standards and 500X ddH<sub>2</sub>O-diluted protein samples were mixed with 100  $\mu$ l protein assay dye. After 5 minutes, replicates of 200  $\mu$ l resulting mixtures were loaded into a 96-well plate and absorbance at 595 nm was measured. A standard curve can be produced by graphing absorbance of proteins standards. Absorbance of protein samples was induced to calculate protein concentration.

#### **2.14 Sodium dodecyl sulfate polyacrylamide gel electrophoresis (SDS-PAGE)**

Twenty  $\mu$ g of protein lysates were mixed 4X protein loading dye and RIPA to produce 20  $\mu$ l of loading samples, followed by heat denature at 95 °C for 10 minutes. SDS-gel was prepared by pouring 8% - 12% resolving acrylamide gel mix and 5% stacking acrylamide gel mix between two glass plates on a cast (Sambrook, 2001). Combs were inserted to stacking gels to make loading wells. Electrophoresis was performed under 80 V in running buffer until proteins were separated as indicated by protein marker.

#### **2.15 Western Blot Analysis**

Transfer apparatus was assembled with SDS-PAGE gel adjacent to polyvinylidene (PVDF) fluoride membrane. Separated proteins were then transferred from gel to PVDF in 1X transfer buffer at 4 °C or on ice using 350 mA electricity for 90 minutes. Resulting membranes were blocked with blocking buffer at room temperature for an hour and sliced into strips accordingly after a brief wash with washing buffer. Indicated primary



antibodies, respective horseradish peroxidase (HRP)-conjugated secondary antibodies were incubated with the membranes at 4 °C O/N. Repeated wash with washing buffer at room temperature was required after each antibody incubation to remove unbound antibodies. Visualization was performed by adding western Lightning™ chemiluminescence reagent to the membrane and pressing an X-ray film (Fuji) on the transparent slide-covered membrane to detect luminescence.

## **2.16 Human primary B cell purification**

Peripheral blood mononuclear cells (PBMCs) were isolated from healthy donors' whole blood by Ficoll-hypaque density gradient centrifugation. Two units of human pack white blood cells (WBC) were diluted with 120 ml of PBS buffer and then loaded onto Ficoll-hypaque™ Plus. The samples were centrifuged at 1500 x g for 30 minutes at room temperature, and then the PBMCs in the interface were transferred to a fresh tube, followed by two washes with PBS. CD19<sup>+</sup> B cells were purified from PBMCs using Dynabeads according to the manufacturer's instructions. Briefly, purified PBMCs were incubated with 25 µl Dynabeads for every 5×10<sup>7</sup> purified PBMCs to capture CD19<sup>+</sup> B cells at room temperature for 40 min with constant rotating. After three PBS washes, for every 1X10<sup>7</sup> estimated CD19<sup>+</sup> B cells, 10 µl of DETACHaBEAD was added and incubated with the beads at room temperature for 60 min with constant rotating to release purified CD19<sup>+</sup> B cells

## 2.17 LCL establishment

CD19<sup>+</sup> B cells were seeded at the density of  $1 \times 10^6$  cells per  $\mu\text{l}$  per well in a 12-well plate with 1 ml RPMI medium containing 20% FBS and infected with the EBV stock with a 100-fold dilution. The EBV-infected B cells were kept in a 37 °C incubator containing 5 % CO<sub>2</sub> without any disturbance until day 14 post-infection. On day 14, 21 and 28 post-infection, cells were divided into two wells. Cell RNA and protein lysates were collected at indicated time points.

## 2.18 Indirect immunofluorescence assay

Ten-thousand epithelial cells were seeded on a sterile 22-mm<sup>2</sup> glass coverslip in a 6-well plate one night before transfection. Seventy-two hours post-transfection, the coverslip was collected and briefly washed with PBS. For suspension cells, PBS-diluted cells were air-dried to be fixed on a glass slide. Cells were cross-linked with 4% formaldehyde at room temperature for 20 minutes. Cell membranes were permeabilized with 0.1% Triton X-100 at room temperature for 10 minutes. Cells were then incubated with indicated primary antibodies at 4 °C O/N. Afterwards, fluorophore-conjugated secondary antibodies were added to the cells and the nucleuses were stained with Hoechst 33342. PBS washes were performed between each step. Fluorescence was detected by fluorescent microscopy or confocal microscopy.

## 2.19 Subcellular fractionation

Transfected TW01 cells were treated with membrane lysis buffer on ice for 15 minutes and underwent rigorous vortex for 1 min. After centrifugation at 1200 x g for 5 minutes, the supernatant was harvested as the cytosolic fraction. Pellets were washed with membrane lysis buffer twice, treated with nuclei lysis buffer, homogenized, centrifuged to obtain nuclear fraction.

## **2.20 Co-immunoprecipitation**

293T cells were transfected with pEGFP-Rta and pcDNA3-IQGAP2-HA plasmids for 72 hours. Lysates of 293T cells harvested with RIPA buffer. For immunoprecipitation, 20% protein A-Sepharose beads-precleared cell lysates were incubated with GFP antibody or HA antibody at 4 °C O/N on a rotating rocker. 20% protein A-Sepharose beads were added to pull down the immunocomplexes at 4 °C for 2 hours. After PBS wash, the immunoprecipitated complexes were added to 25 µl of 2X protein loading dye and heated to 95 °C for 5 minutes to detach the complexes from the beads. Immunocomplexes were then analyzed with SDS-PAGE and Western Blot.

## **2.21 Luciferase reporter assay**

293T cells were seeded at a density of  $2 \times 10^5$  cells/well in a 12-well plate and then transfected with 0.5 µg of the promoter luciferase reporter plasmid combined with 0.05 µg of GFP-expressing plasmids (pEGFP-C1, Promega) and 0.5 µg effector plasmid using NTRIL. Seventy-two hours post-transfection, the cells were lysed and the luciferase

activities and GFP fluorescent intensities were detected using the Bright-Glo Luciferase Assay System kit (Promega, Madison, WI, USA), Orion II Microplate Luminometer (Titertek-Berthold), and SpectraMax M5 (Molecular Devices). The relative fold of luciferase activity from each transfectant was normalized to its GFP intensity.

## 2.22 Cell proliferation rate determination


Triplicates of 100  $\mu$ l  $1 \times 10^4$  cells were seeded in a 96-well plate and mixed with 10  $\mu$ l AlamarBlue<sup>®</sup> reagent. Four hours after incubation in a 37 °C incubator containing 5 % CO<sub>2</sub>, absorbance at 570 nm and 600 nm were measured to obtain reagent reduction percentage using the equation below:

$$\text{Reduction percentage of AlamarBlue}^{\circledR} = \frac{(117216 \times A1) - (80586 \times A2)}{(155677 \times N2) - (14652 \times N1)}$$

Where A1, A2 stands for absorbance at 570nm and 600nm respectively, while N1, N2 are absorbance at 570 nm and 600 nm measure with medium-AlamarBlue<sup>®</sup> mix as negative control. Reduction percentage from cells collected at different time points were compared and graph with Microsoft Excel to obtain cell proliferation rate.

## 2.23 Chromatin immunoprecipitation assay (ChIP)

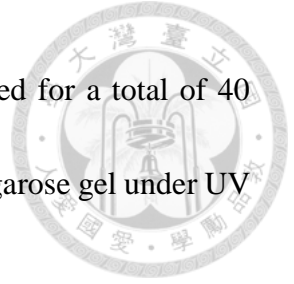
Five-million 293T cells were transfected with pEGFP-Rta using NTRII. Seventy-two hours post-transfection, the cells were cross-linked by addition of 1% formaldehyde



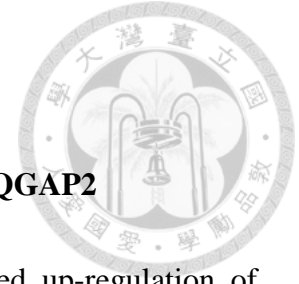
directly to the culture medium and incubation for 10 minutes at room temperature. To neutralize formaldehyde, glycine was added until the final concentration reached 0.125M. Then, the mixtures were incubated at room temperature for 5 minutes with gentle rotation. Afterwards, cells were lysed by nuclei lysis buffer and sonicated to fragment DNA into 500 to 1000 bps in length. The cells were centrifuged at highest speed to remove insoluble pellet, and the supernatants were determined for its protein concentration. Two-hundred  $\mu\text{g}$  of protein was used to immunoprecipitate DNA-protein complex by using anti-GFP antibody or control mouse IgG at 4 °C O/N with gently rotation, then protein A beads were added to capture the antibody-protein complexes for additional 2 hours. The beads were washed twice with 1 ml of low salt buffer, high salt buffer, and LiCl buffer orderly at 4 °C for 5 minutes gently rotation. To de-crosslink the DNA-protein complexes, 500  $\mu\text{l}$  of elution buffer was added to the beads and incubated at 65 °C overnight. The reaction mixtures were centrifuged at 2000 rpm for 2 min to collect the supernatant, and then treated the supernatant with 10 mg/ml of proteinase K at 45 °C for 1 to 2 hours. The DNA was extracted with equal volume of phenol/chloroform/ isoamyl alcohol and then precipitated with 2.5-fold volume of absolute ethanol containing 20  $\mu\text{g}$  of glycogen at -80°C for at least 2 hours. The DNA pellet was washed with 70% ethanol and dissolved in 20  $\mu\text{l}$  ddH<sub>2</sub>O. 2  $\mu\text{l}$  of DNA was taken as template for PCR to detect the fragment containing IQGAP2 promoter region -232 to +65. The amplification program was 95 °C



for 1 minute, 55 °C for 30 seconds, 72 °C for 30 seconds, repeated for a total of 40 cycles. Finally, PCR products were detected in an EtBr stained-2% agarose gel under UV irradiation.



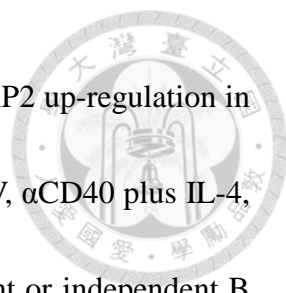
## Results



### 1. EBV infection and reactivation increased the expression of IQGAP2

Previous cDNA microarray data from our lab have identified up-regulation of IQGAP2 and IQGAP3 in EBV-immortalized LCLs (Appendix I). To validate the results on IQGAP2, human CD19<sup>+</sup> B lymphocytes were purified from whole blood of healthy donors and infected with B95.8 strain EBV. RNA and protein were isolated from EBV-infected B cells at day 3, 7, 14, 21, and 28. RNA extracts were reverse-transcribed into cDNA, followed by PCR to detect expression of, IQGAP2. The mRNA expression of IQGAPs in EBV-infected cells, comparing with the expression in uninfected B cells, indicated that EBV infection increased IQGAP2 expression (Figure 4A). Western blotting confirmed the increased expression of IQGAP2 in B lymphocytes along the course of EBV infection (Figure 4B). mRNA extracts and protein lysates from more LCLs and their counterpart uninfected B lymphocytes were collected and analyzed. These results confirmed that when EBV immortalized B lymphocytes into LCLs, expression of IQGAP2 and IQGAP3 increased at mRNA level (Figure 5A). Increased IQGAP2 expression was further validated at protein level (Figure 5B). However, there was no significant change in IQGAP1 expression (Figure 4B). This hinted that IQGAPs may have different roles in EBV infected cells (Figure 5).

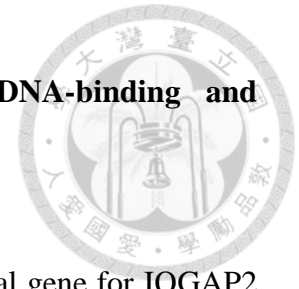
B cells alters cellular gene expression in response to different stimuli (Wakatsuki et



al., 1994). In order to elucidate the underlying mechanisms of IQGAP2 up-regulation in B lymphocytes, purified CD19<sup>+</sup> B cells were treated with B95.8 EBV,  $\alpha$ CD40 plus IL-4, or lipopolysaccharides (LPS). The chemicals mimic T cell dependent or independent B cell activation respectively. The resulting cells were extracted on day 1, 2, and 3 post-treatment for RNA. Results of Q-PCR revealed that only EBV infection could increase IQGAP2 expression. Therefore, IQGAP2 upregulation seemed specific to EBV infection (Figure 6A). On the contrary, not only EBV infection but also treatment with B cells stimuli can induce IQGAP3 expression (Figure 6B).

As a main biological feature, EBV persists in latent and lytic stages in hosts (Longnecker, 2013). Since IQGAP2 up-regulation was found associated with EBV infection, we would like to explore if this up-regulation were relevant to EBV lytic progression. Thus, Akata<sup>-</sup> and Akata<sup>+</sup> cells were treated with 0.5% of goat anti-human immunoglobulin G ( $\alpha$ -hIgG) or mock dimethyl sulfoxide (DMSO) for 48 hours. The resulting RNA was extracted for analysis. RT-PCR results showed that there were more IQGAP2 transcripts when Akata<sup>+</sup> cells entered lytic cycle (Figure 7). To verify, EBV-bearing NA cells were used as an epithelial cell model in lytic cycle. NA cells were treated with 12-O-tetradecanoylphorbol-13-acetate (TPA) and sodium butyrate (SB). 72 hours post-treatment, cells were harvested for protein lysates. Western blotting data indicated that IQGAP2 increased as NA entered lytic progression (Figure 8).


## **2. Rta increased IQGAP2 expression with both of its DNA-binding and transactivation domains**



In our previous studies, in order to identify the responsible viral gene for IQGAP2 upregulation, TW01 cells were transfected with several important viral genes namely EBNA<sub>s</sub>, LMP1, LMP2A, EBER<sub>s</sub>, BARF0, Rta, Zta, and BGLF4 for 72 h. RT-PCR result identified Rta as the EBV viral gene that could increase IQGAP2 expression (Appendix II). A. Protein lysates of Rta-transfected TW01 cells and BJAB cells were analyzed. Western blotting results confirmed the upregulation of IQGAP2 at translation level (Figure 9). Additionally, IQGAP2 promoter reporter plasmid was constructed to conducted reporter assays in 293T and TW01 cells. Both assays implied that Rta can activate IQGAP2 promoter (Figure 10).

Rta possesses two distinguished functional domains, namely DNA-binding N-terminal and transactivating C-terminal (Figure 2) (Hsu et al., 2005). TW01 cells were transfected with truncated N- or C-terminal Rta to see how each domain contributed to IQGAP2 upregulation. In addition, the results of western blotting demonstrated that Rta required both N and C terminal to induce IQGAP2 expression (Figure 11). A follow-up reporter assay also revealed that only full-length Rta can activated IQGAP2 promoter (Figure 12). Altogether, the results showed that Rta required both DNA binding and transactivation domains to induce IQGAP2 expression.


### **3. Rta increased IQGAP2 expression through direct binding to the promoter**



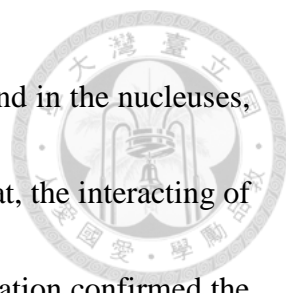
As has mentioned before, Rta required DNA-binding domain and transactivation domain to induce IQGAP2 expression. With that in mind, we would like to explore the underlying mechanism. Considering Rta can directly or indirectly induce gene expression, IQGAP2 promoter was scanned for several Rta-related transcription factor binding sites with two online softwares (Figure 13A). Accordingly, serial deletions of the promoter were constructed for reporter assay. The reporter assay recognized the importance of a Rta response element (RRE) on the promoter region -121 / -41 in transcription activation (Figure 13B). The softwares also found that there are many putative Sp1 binding sites on IQGAP2 promoter (Figure 13A). However, when Sp1 was downregulated with shRNA, Rta could still activate IQGAP2 promoter (Figure 14). This implied that Sp1 had no effect on Rta-induced IQGAP2 up-regulation. To confirm the direct binding of Rta on IQGAP2 promoter, chromatin immunoprecipitation (ChIP) was performed with GFP antibody and Rta-GFP transfected 293T cells. Rta-GFP-binding DNA was analyzed using primers targeting part of IQGAP2 promoter spanning the putative RRE. The ChIP revealed that Rta directly associated with IQGAP2 promoter (Figure 15).

### **4. Rta recruited IQGAP2 to the nucleus**

IQGAP2 is thought to interact with different protein factors to perform cellular functions (Hedman et al., 2015). In order to elucidate the biological roles of IQGAP2 in



Rta induction, cellular distribution of IQGAP2 was investigated. TW01 cells were transfected with Rta alone, IQGAP2 alone, or both Rta and IQGAP2. 72 hours post-transfection, cells were fractionated and subjected to western blotting. When only IQGAP2 was expressed, IQGAP2 was found in the cytoplasmic fraction (Figure 16A), which is consistent with other reports (Jin et al., 2008; Xie et al., 2012). In contrast, when both Rta and IQGAP2 was expressed, IQGAP2 was found in the nuclear fraction as well as the cytoplasmic (Figure 16B & C). The phenomenon could result from the nuclear expression of Rta. Further studies with IFA and confocal microscopy discovered that IQGAP2 located at the cortex of TW01 cells in the absence of Rta while Rta-induced IQGAP2 colocalized with Rta in the nuclear region. Likewise, IQGAP2 was found both in the cytoplasm and the nucleus when cells were cotransfected with Rta and IQGAP2 (Figure 17). For the purpose of exploring the distribution of IQGAP2 when EBV infects B cells, LCLs and their uninfected B cells counterpart were analyzed with IQGAP2 and Rta antibodies through IFA and observe under a confocal microscope. The results revealed different patterns in B lymphocytes. Consistent with earlier experiments (Figure 5), basal expression IQGAP2 could be detected in uninfected B cells. In these cells, IQGAP2 distributed thoroughly in the cells, with aggregation around plasma membrane region (Figure 18 first row and fourth row). This pattern was similar to what was observed in LCLs that maintained in latency (Figure 18 second row and fifth row). Conversely, in



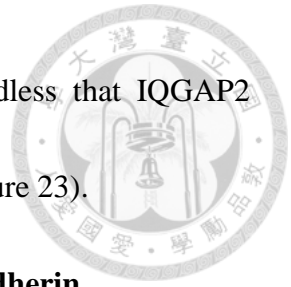
LCLs that entered lytic cycle and expressed Rta, IQGAP2 could found in the nucleuses, colocalizing with Rta (Figure 18 third row and sixth row). Seeing that, the interacting of Rta and IQGAP2 was investigated. As the result, co-immunoprecipitation confirmed the interaction between IQGAP2 and Rta (Figure 19). On the whole, these results implied that Rta recruited IQGAP2 to the nuclear region of the cell.

### **5. IQGAP2 was required for lytic replication since it participated in Rp auto-activation**

The functions of IQGAPs are highly related to its binding partners (Hedman et al., 2015). Therefore, it can be speculated that IQGAP2 helped Rta to carry out viral functions. As a transactivator, Rta is best known for its lytic replication initiation. So, we would like to know whether IQGAP2 participated in EBV lytic cycle. To do that, LCLs were infected with lentiviruses containing shRNA-expressing plasmids that targeted IQGAP2. Surprisingly, repression of IQGAP2 resulted in regression of spontaneous lytic replication in LCLs as less lytic proteins were observed (Figure 20). Furthermore, when IQGAP2 expression could not be induced in TPA/SB-treated NA cells, less lytic protein was observed (Figure 21). These indicated that IQGAP2 participated in lytic replication.

It was intriguing that whether IQGAP2 could affect the two important lytic promoters, Rp and Zp. Thus, 293T cells with IQGAP2 knockdown were used in auto-activation reporter assays. When there was not sufficient IQGAP2 in 293T, auto-

stimulation of Rp was dramatically decreased (Figure 22), regardless that IQGAP2 depletion did not affect Rta-induced Zp and pBLLF1 activation (Figure 23).



## **6. IQGAP2 mediated cell-to-cell adhesion in LCLs through E-cadherin**

In IQGAP2 depleted LCLs, we found that clumping morphology of IQGAP2 had changed. LCL clumps were scattered rather than spherical (Figure 24). Alternation of LCL clumping could be a result of decreased cell proliferation or growth. Thus, Alamar Blue assay was performed to determine cell proliferation rate when IQGAP2 was knocked-down. The results showed that LCLs with suppressed expression of IQGAP2 had comparable proliferation rate with negative control (Figure 25). Further western blotting indicated that IQGAP2 knockdown led to less adhesion molecule E-cadherin in cells (Figure 26). These results implied that IQGAP2 might mediated LCL cell-to-cell adhesion by regulating E-cadherin expression.




## Discussion

### 1. Hypothesis

According to the results mentioned before, we hypothesized that EBV lytic immediate-early protein Rta binds to scaffold protein IQGAP2 promoter and directly activates IQGAP2 transcription during EBV infection and lytic activation. The translated IQGAP2 protein may be recruited into the nucleus. The association between Rta and IQGAP2 may regulate lytic promoter Rp in auto-stimulation. Consequently, IQGAP2 is required in EBV lytic activation. Besides, IQGAP2 may mediate clumping pattern of LCLs through regulation of cell-to-cell adhesion molecule E-cadherin. (Figure 27)

### 2. Direct transcription activation of Rta

The immediate-early transactivator Rta is critical for EBV lytic progression (Kenney and Mertz, 2014). It is well documented that Rta activates transcription of lytic genes (Quinlivan et al., 1993; Gruffat and Sergeant, 1994; Ho et al., 2007; Heilmann et al., 2012). However, growing evidence points out that Rta may regulate cellular factors (Li et al., 2004; Chang et al., 2005; Ho et al., 2007; Chen et al., 2009; Huang et al., 2012). Here, we demonstrated a novel finding that Rta can regulate another cellular factor, IQGAP2. Rta bound to IQGAP2 promoter and directly activated IQGAP2 transcription via Rta responsive element (RRE). The GC-rich RRE was firstly defined on EBV viral promoters (Gruffat and Sergeant, 1994). Throughout years, the binding sequence of Rta on EBV genome has been extensively studied (Heilmann et al., 2012), however, the




binding on cellular genes is seldom discussed. In 2007, Rta was shown to increase DcR3, a soluble decoy receptor that belongs to the tumor necrosis factor receptor superfamily, by direct binding to its promoter. In our case, in addition to the direct interaction between Rta and IQGAP2 promoter (Figure 15), the RRE on -157/-140 of pIQGAP2 was important to Rta-induced IQGAP2 up-regulation as deletion of this sequence failed to be activated by Rta (Figure 13).

### **3. Association of IQGAP2 with Rta in gene expression regulation**

In this study, we demonstrated that IQGAP2 associated with Rta to activate Rp (Figure 22). However, IQGAP2 did not involve in Rta-induced Zp and pBLLF1 activation (Figure 23). The reason behind this phenomenon could be that Rta activates these promoters through different pathways (Figure 28). Rta activates pBLLF1 by direct binding through RRE (Gruffat and Sergeant, 1994). On the contrary, Rta regulates the other two genes through indirect, non-DNA binding fashion as RRE is absent from their promoters. Rta mediates Rp activation via Sp1 (Ragoczy and Miller, 2001), while transcription factor ATF2 is required for Rta to activate Zp (Adamson et al., 2000). It has been reported that through Sp1, Rta can up-regulate cellular genes including tumor suppressor p16, cyclin-dependent kinase inhibitor p21, and small nuclear ribonucleoprotein polypeptide N (SNRPN) (Chang et al., 2005). Therefore, it can be speculated that IQGAP2, along with Rta, has the ability to alter cellular gene expression


and affects cell activities such as cell cycle.



It has been reported that Rta interacts with cellular factors for lytic progression. For example, Rta interacts with an Sp1-interacting protein, methyl-CpG-binding domain protein 1 (MBD1) -containing chromatin-associated factor 1 (MCAF1), forming an Sp1-MCAF1-Rta complex that enhances Sp1-mediated transcription (Chang et al., 2005). Rta also interacts with cellular transcription factor Oct-1 to enhance transactivation activation of EBV lytic genes such as SM, EA-D, BHLF1, BHRF1, and Zta (Robinson et al., 2011). Similarly, in our lab we previously found that Rta interacts with TSG101 to activate the expression of EBV late genes, including BcLF1, BDLF3, BILF2, BLLF1, and BLRF2 (Chua et al., 2007). What is more, Rta is reported to increase fatty acid synthase (FAS) expression through mitogen-activated protein kinase (MAPK) pathway. This report shows that FAS participates in EBV lytic progression (Li et al., 2004). Comparatively, our work demonstrated that IQGAP2 was required for EBV to enter lytic cycle (Figure 20 & 21), and this prerequisite is correlated to Rta-induced Rp activation (Figure 22).

#### **4. Nuclear function of IQGAP2**

So far, the cellular distribution of IQGAP family is mostly found cytoplasmic. They have been reported to be involved in the modulation of cytoskeleton and cell adhesion through binding to various effectors (Sokol et al., 2001; Swart-Mataraza et al., 2002; Noritake et al., 2004; Wang et al., 2007; Yamashiro et al., 2007; Schmidt et al., 2008).



Few studies have focus on the subcellular localization of IQGAP2. In prostate cancer cell lines, LNCaP and DU145, IQGAP2 was observed in the cytosol (Xie et al., 2012). However, IQGAP2 protein is limited to the membrane of gastric cancer cell lines, HSC-59, NUGC4, MKN45 and TGBC11TKB (Jin et al., 2008). Also, IQGAP2 was found in the leading rim filopodia of activated platelets (Schmidt et al., 2003).

Although the findings regrading IQGAP1 and IQGAP2 are mainly cytoplasmic, several studies indicate that they may have nuclear effects. IQGAP1 interacts with several nuclear proteins, including estrogen receptor (ER)  $\alpha$ , ER $\beta$ , nuclear factor of activated T cells 1 (NFAT1), and nuclear factor-erythroid-related factor 2 (Nrf2) (Sharma et al., 2011; Cheung et al., 2013; Kim et al., 2013; Erdemir et al., 2014). IQGAP1 serves as a coregulator with ER $\alpha$  or Nrf2, enhancing steroid signal transduction or MEK–ERK pathway signal transduction respectively (Cheung et al., 2013; Erdemir et al., 2014). Comparatively, mass spectrometry and bioinformatics have identified that IQGAP2 may participate in TNF- $\alpha$ -stimulated NF- $\kappa$ B pathway (Bouwmeester et al., 2004; Hoesel and Schmid, 2013). The biological roles of IQGAPs largely depend on the binding partner in the cellular actions. As a transactivator, Rta often expresses in the nucleus to affect gene transfection. We showed that Rta-induced IQGAP2 colocalized with Rta in the nucleus (Figure 17&18). Even though nuclear expression of IQGAP2 had not been reported, we demonstrated Rta could recruit IQGAP2 to the nucleus, where IGAP2 possibly

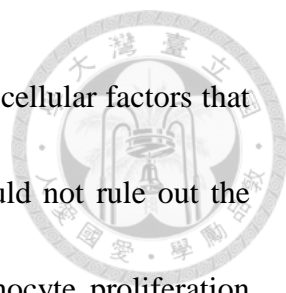
participated in Rta-related gene regulation.

## **5. Diverse functions of IQGAP family in EBV infection**

Members of IQGAP family act differently in cellular events (Smith et al., 2015). Our findings indicated that IQGAP2 was involved in EBV replication, specifically, IQGAP2 cooperated with Rta to activate one of the important lytic promoters, Rp. In other words, IQGAP2 was required in EBV lytic activation and thus crucial for new virion production. However, in an unpublished research, knockdown of IQGAP1 enhanced EBV DNA replication and virion maturation. This study also found that EBV kinase BGLF4 phosphorylates IQGAP1 to induce a compact Golgi structure by reorganizing the microtubule-organizing center (MTOC) (Yang, 2013). In 2007, the association of BGLF4 and IQGAP2 was identified using yeast two-hybrid systems (Calderwood et al., 2007). Nevertheless, whether BGLF4 associates with IQGAP2 in Rp auto-stimulation remains unclear.

EBV often manipulates cellular factors to benefit its own infection and pathogenesis. Abnormal expression of cellular factors in EBV infection may be a sign for viral regulation (Young and Rickinson, 2004). In this study, we found that IQGAP2 and IQGAP3 expression increased when purified human CD19<sup>+</sup> B lymphocytes were immortalized into LCLs. However, when these B cells were treated with B cells stimuli other than EBV, the expression of IQGAP3 still increased (Figure 6B). Since IQGAP3





correlates with proliferation and cytokinesis, IQGAP3 be one of the cellular factors that EBV manipulates to promote B cell proliferation. Even so, we could not rule out the possibility that IQGAP3 up-regulation was resulted from B lymphocyte proliferation rather than resulted in. In conclusion, despite our findings revealed some roles IQGAP2 played in EBV infection, yet more effort is needed to fully understand the interaction between IQGAPs and EBV.

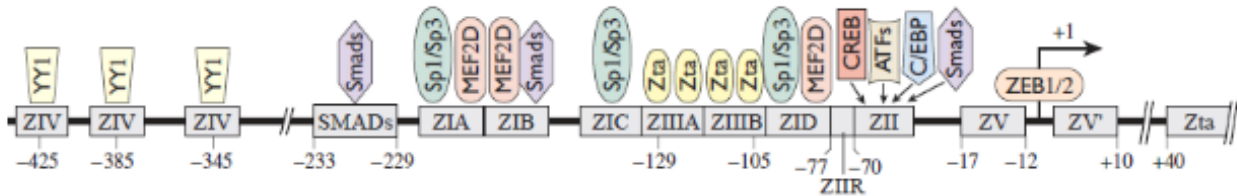
## **6. The role of IQGAP2 in EBV-associated disease progression**

Elevated antibodies against EBV lytic proteins and increased EBV DNA copy number in the serum have been reported in patients suffering from Burkitt's lymphoma, Hodgkin's lymphoma, PTLN, or NPC (Cohen, 2000; Lin et al., 2004; Besson et al., 2006), indicating that EBV lytic progression may play an important role in EBV pathogenesis. Even though our ex vivo EBV infection LCL model identified the correlation of IQGAP2, along with Rta, and EBV lytic progression, we could not be fully confident on how IQGAP2 affect EBV-associated diseases. Examining patient specimen is required to reassure the impact of IQGAP2 on diseases. Since LCL resembles tissue specimen of PTLN patients, for starters, immunohistochemistry can be conducted on PTLN samples. We can look for increased expression of IQGAP2 and nuclear distribution of IQGAP2 to verify our results.

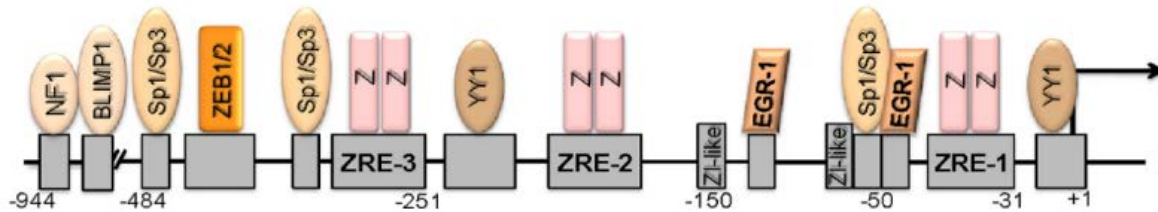
## Figures



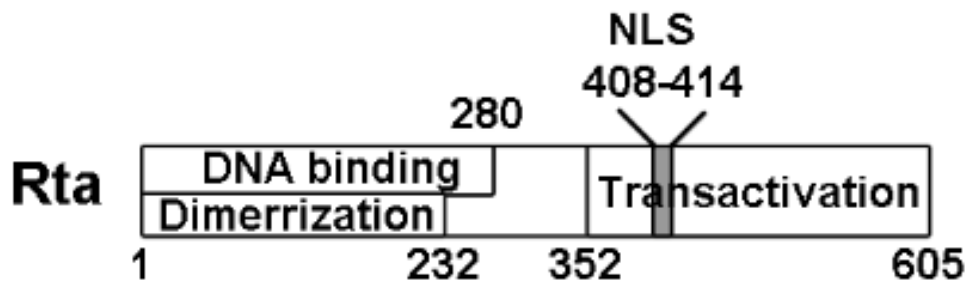
(A) Zta promoter (Zp)



(B) Rta Promoter (Rp)

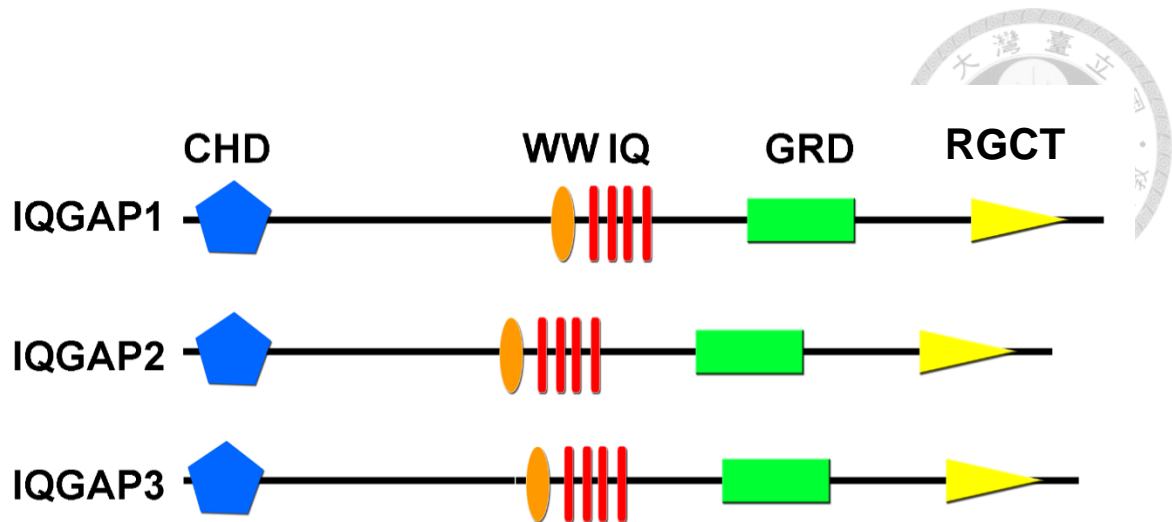


**Figure 1. Schematic diagrams reveal binding factors on Epstein-Barr virus Zta and Rta promoters.** (A) Binding sites for transcriptional regulators on EBV Zp. Zta cis-acting elements are termed ZIA, ZIB, ZIC, ZID, ZII, ZIIIA, ZIIIB, ZIV, ZV, and ZV'. Trans-acting elements includes Sp1, Sp3, myocyte enhancer factor 2D (MEF2D), (cAMP)-response element (CRE)-binding protein (CREB), ATF family members (C/EBPs), activating transcription factors (ATFs), mothers against decapentaplegic homologs (SMADs), and Ying Yang 1 (YY1). There is also a SMAD binding site on Zp. (Longnecker, 2013) (B) Binding sites for transcriptional regulators on EBV Rp. Cis -acting elements are indicated by gray rectangles, with their corresponding trans -acting factors shown directly above or below them. ZRE stands for Zta-responsive element. Trans-acting elements includes Zta (Z), early growth response protein 1 (EGR1), Sp1, Sp3, cellular differentiation regulator BLIMP1, neurofibromin 1, (NF1), Ying Yang 1 (YY1) and Zinc finger E-box-binding homeobox proteins (ZEB) 1/2. (Kenney and Mertz, 2014)

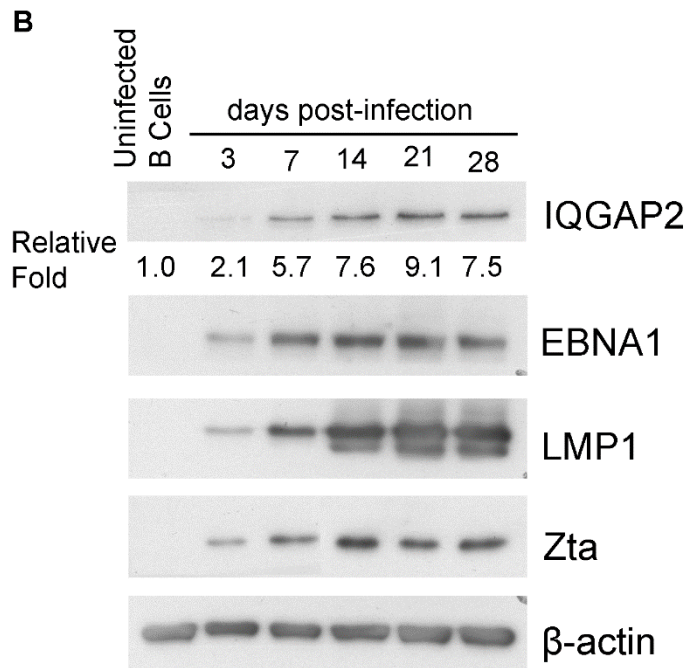
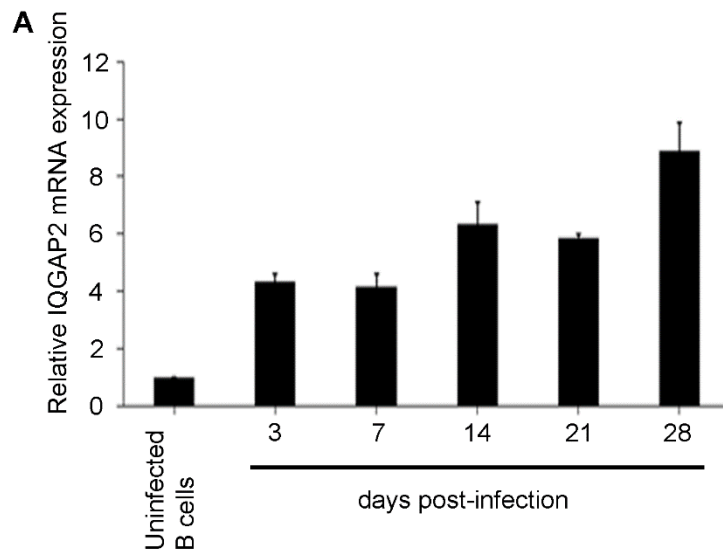


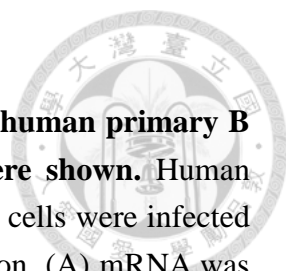
**Figure 2. A diagram represents the structure of EBV Rta protein.** Rta consists of three main domains. The DNA binding and dimerization domain locate on the N terminus, while transactivation domain locates on the C terminus. A nuclear localization signal (NLS) is found in the proline-rich region of transactivation domain. (Hsu et al., 2005; Chua et al., 2007)



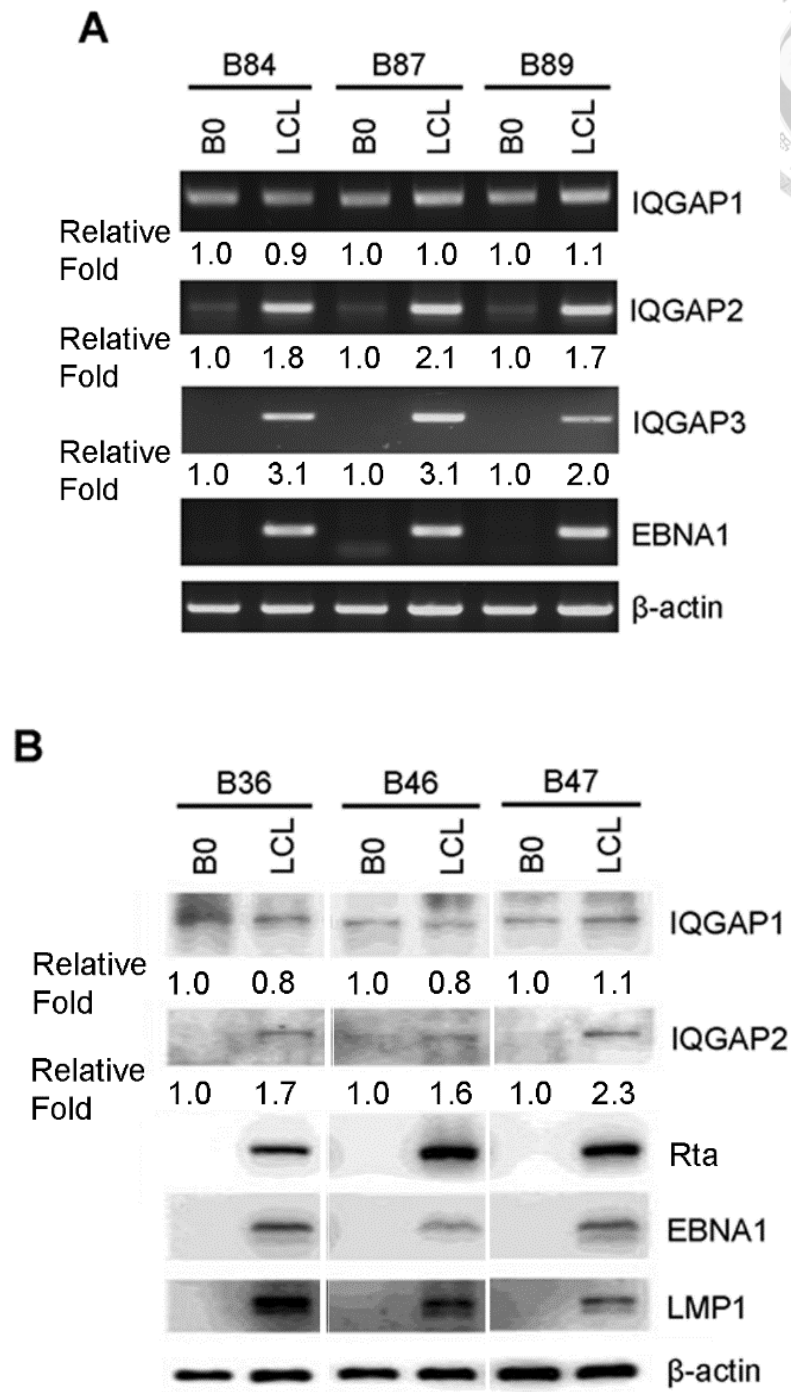


**Figure 3. Schematic representation of human IQGAP family.** All three human IQGAP proteins possess five homologous domains as indicated. CHD, calponin homology domain; WW, tryptophan-tryptophan poly leucine binding domain; IQ motif, calmodulin binding motif; GRD, RasGAP-related domain; RGCT, common C terminus of RasGAP.





**Figure 4. Expression kinetics of IQGAP2 mRNA and protein in human primary B cell along the course of EBV-induced LCL transformation were shown.** Human primary B cells were purified with CD19 Dynabeads®. The isolated cells were infected with B95.8 strain EBV and harvested on indicated days post infection. (A) mRNA was reverse-transcribed and subjected to Q-PCR for analysis. Expression of IQGAP2 was detected and its relation with  $\beta$ -actin expression was calculated and graphed. (B) Protein lysates were analyzed through western blotting with IQGAP2 antibody whereas EBNA1 served as EBV infection marker, Zta served as lytic progression marker and  $\beta$ -actin served as internal loading control. This experiment was performed twice with B cells originated from two different healthy donors.



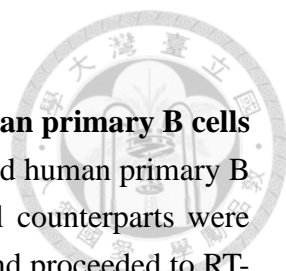


**Figure 5. mRNA and protein expression of IQGAP family in human primary B cells and their paired EBV-immortalized LCLs were revealed.** Purified human primary B cells and B95.8 EBV-immortalized LCL and its uninfected B cell counterparts were harvested for mRNA and protein analysis. (A) RNA was extracted and proceeded to RT-PCR, in which IQGAP1, IQGAP2, IQGAP3 expression level was compared. EBNA1 was used EBV infection indicator and  $\beta$ -actin was served as loading control. (B) Protein lysates were analyzed by western blotting. Protein expression was determined by IQGAP1, IQGAP2, Rta, EBNA1, LMP1, and  $\beta$ -actin antibodies.

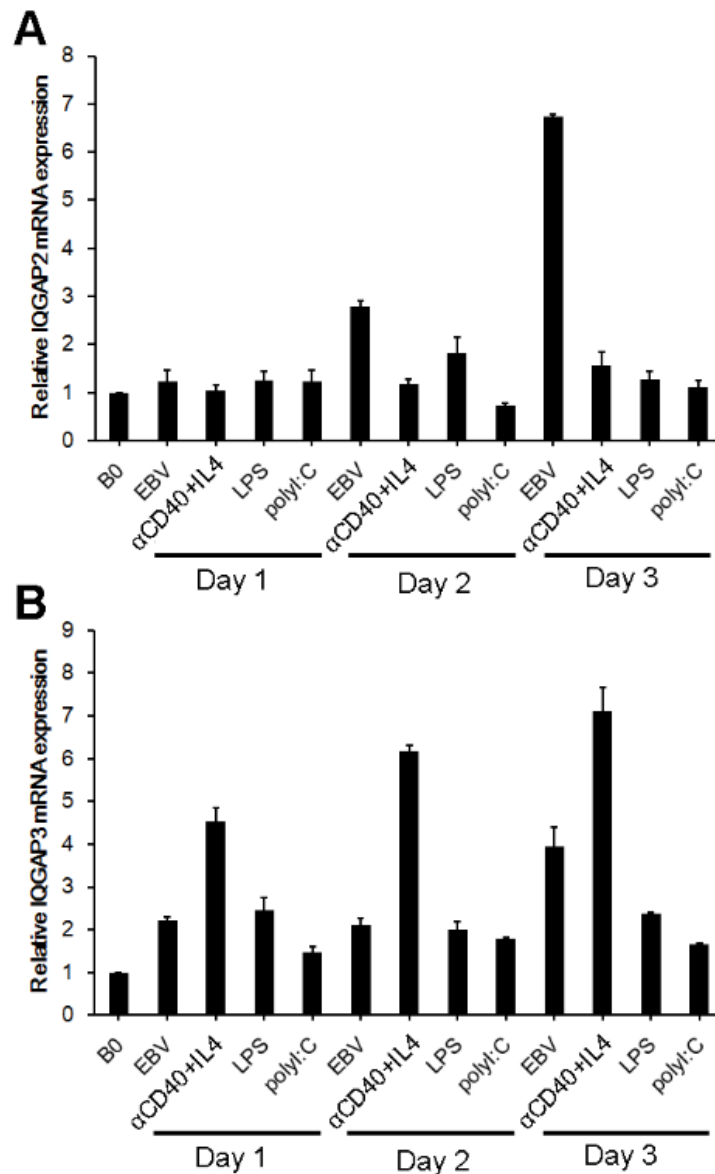


**Figure 6. mRNA expression of IQGAP2 in EBV-infected, anti-CD40 / IL-4 stimulated, LPS-stimulated human or poly I:C-stimulated B cells was measured with Q-PCR.** Purified human primary B cells was infected with EBV, stimulated with anti-CD40 / IL-4, triggered with lipopolysaccharides (LPS) or agitate with poly I:C. Cells were collected at day 1, 2, or 3 post treatment for total RNA extraction, followed by reverse transcription. Resulting cDNA was subjected to Q-PCR. IQGAP2 expression were normalized with  $\beta$ -actin transcripts. Relative expression fold was acquired by comparing normalized expression levels of treated B cells to those from untreated B cells. This experiment was performed twice with B cells originated from two different healthy donors

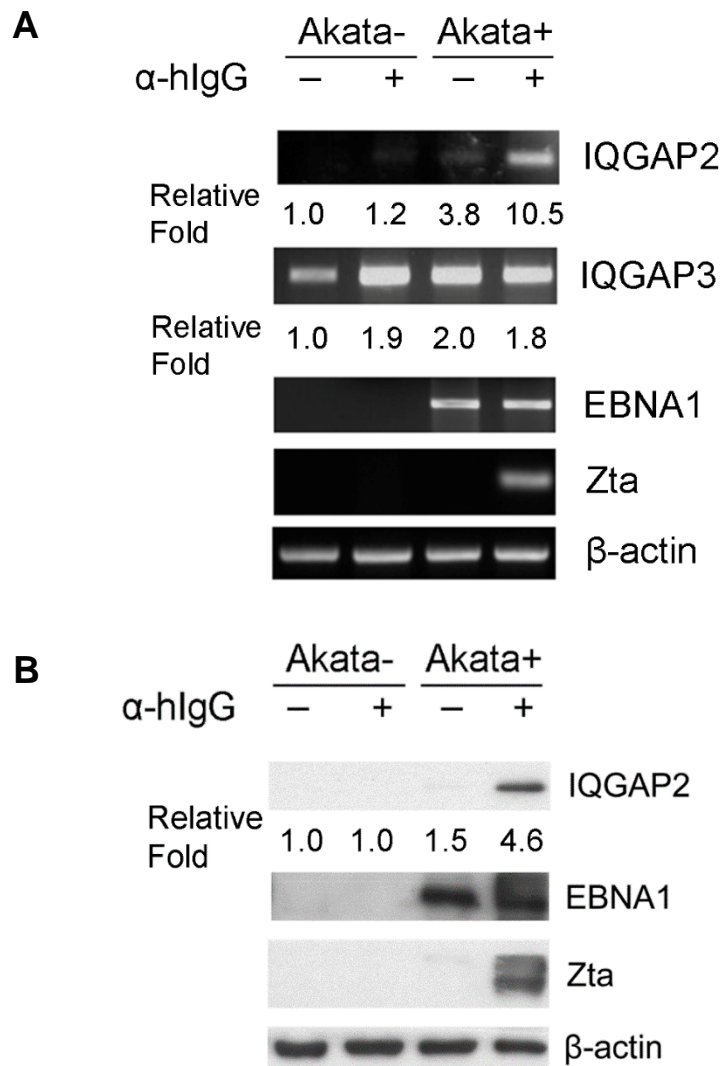


**Figure 7. Reactivation of EBV in Akata+ increased the expression of IQGAP2.** Akata+ cells were treated with DMSO (control) or 0.5% (vol/vol) goat anti-human IgG to trigger EBV lytic cycle. RNA and protein were extracted and proceeded to (A) RT-PCR or (B) western blotting, in which expression of IQGAP2, EBNA1, Zta, and  $\beta$ -actin (loading control) was detected. mRNA expression of IQGAP3 was also detected in RT-PCR. This experiment was performed for three times independently.

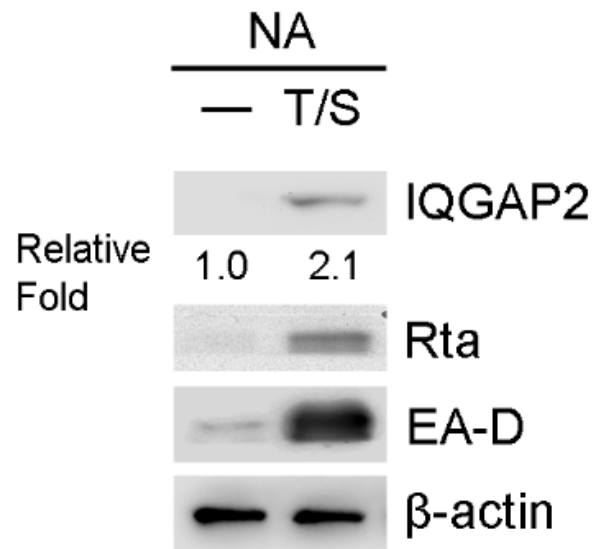


**Figure 8. Reactivation of EBV in NA cells increased the expression of IQGAP2.** NA cells were treated with DMSO (negative control) or TPA and SB for 72 h. Protein lysates were prepared and subjected to SDS-PAGE and western blotting in order to detect IQGAP2, lytic proteins Rta and EA-D, and internal loading control  $\beta$ -actin. This experiment was performed twice independently.



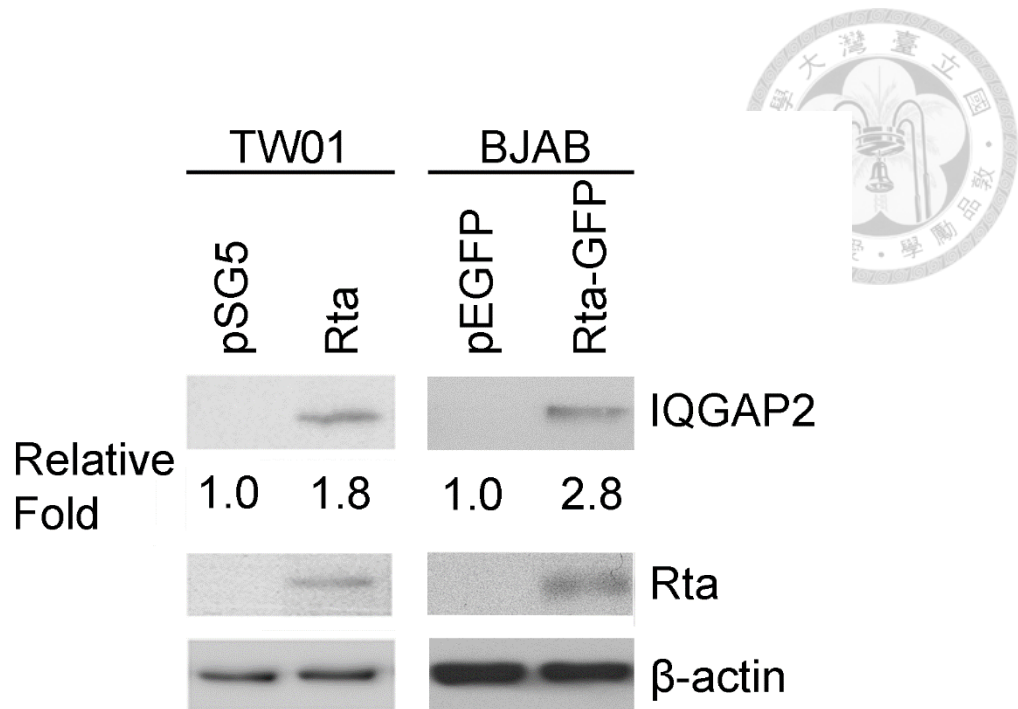


**Figure 9. EBV Rta increased IQGAP2 protein expression.** TW01 cells was transfected with pSG5 and pSG5-Rta using NTRII, cells were lysed for protein 72 hours later (Left panels). BJAB transient Rta expression was achieved by electroporation (Right panels). Whole cell lysate was prepared 48 hours later. Protein lysates were subjected to SDS-PAGE and western blotting for IQGAP2 and Rta protein detection.  $\beta$ -actin served as internal loading control. This experiment was performed twice independently.

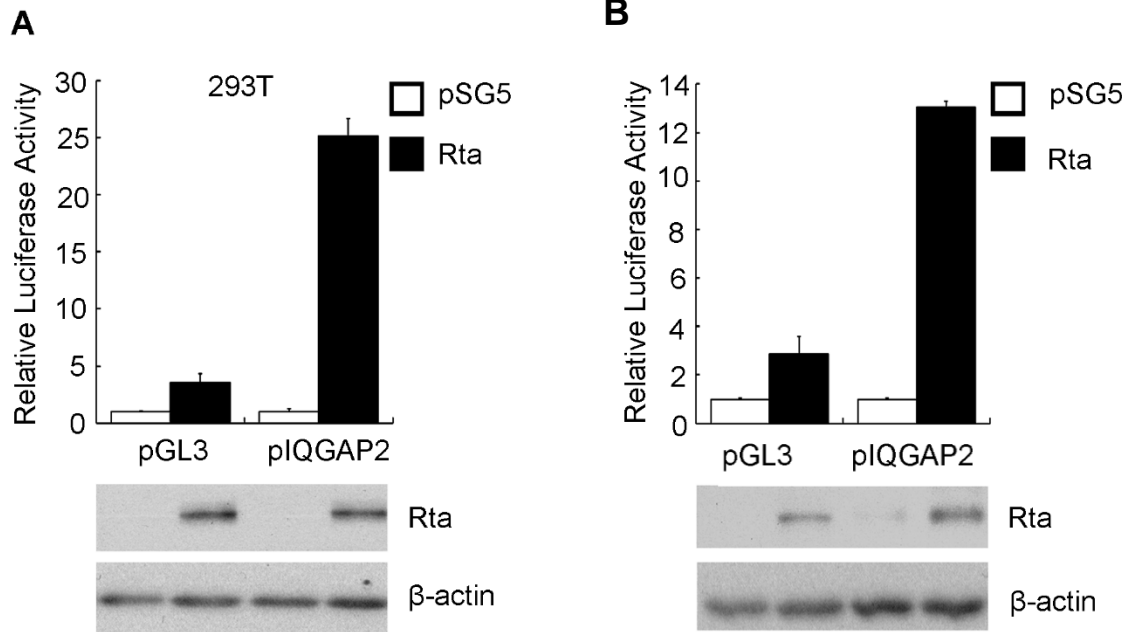


**Figure 10. Rta upregulated IQGAP2 promoter activity in 293T and TW01 cells.** (A) 293T and (B) TW01 cells were transfected with pGL3 or pGL3-pIQGAP2, pSG5 or pSG5-Rta, and pEGFP (transfection efficiency indicator). Luciferase activities were measured and relative activities were calculated according to GFP fluorescence. (higher panels). Portion of transfected cells were subjected to cell lysis for protein analysis. The results verified Rta expression (lower panels). This experiment was performed for three times independently.

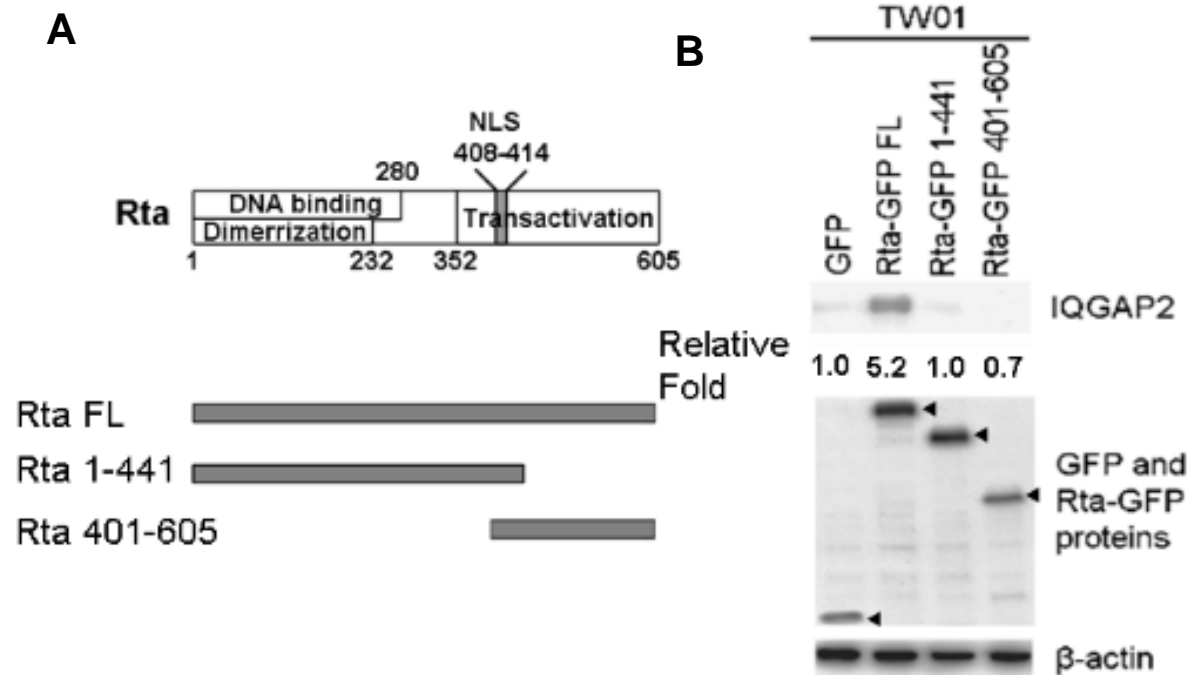


**Figure 11. Rta with C-terminal deletion or N terminal deletion could not induce IQGAP2 protein expression in TW01 cells.** (A) Structural diagram of full-length Rta, Rta transactivation domain mutation, and Rta DNA-binding domain deletion. (B) TW01 cells were transfected with pEGFP-C1, pEGFP-Rta, pEGFP-Rta NLSm, pEGFP-Rta 1-441, pEGFP-Rta 1-333, pEGFP 401-605 using NTRII. 72 h post infection, cells were lysed and protein lysates were subjected to SDS-PAGE and western blotting. IQGAP2, GFP, and  $\beta$ -actin antibodies were used for protein detection. This experiment was performed for three times independently.

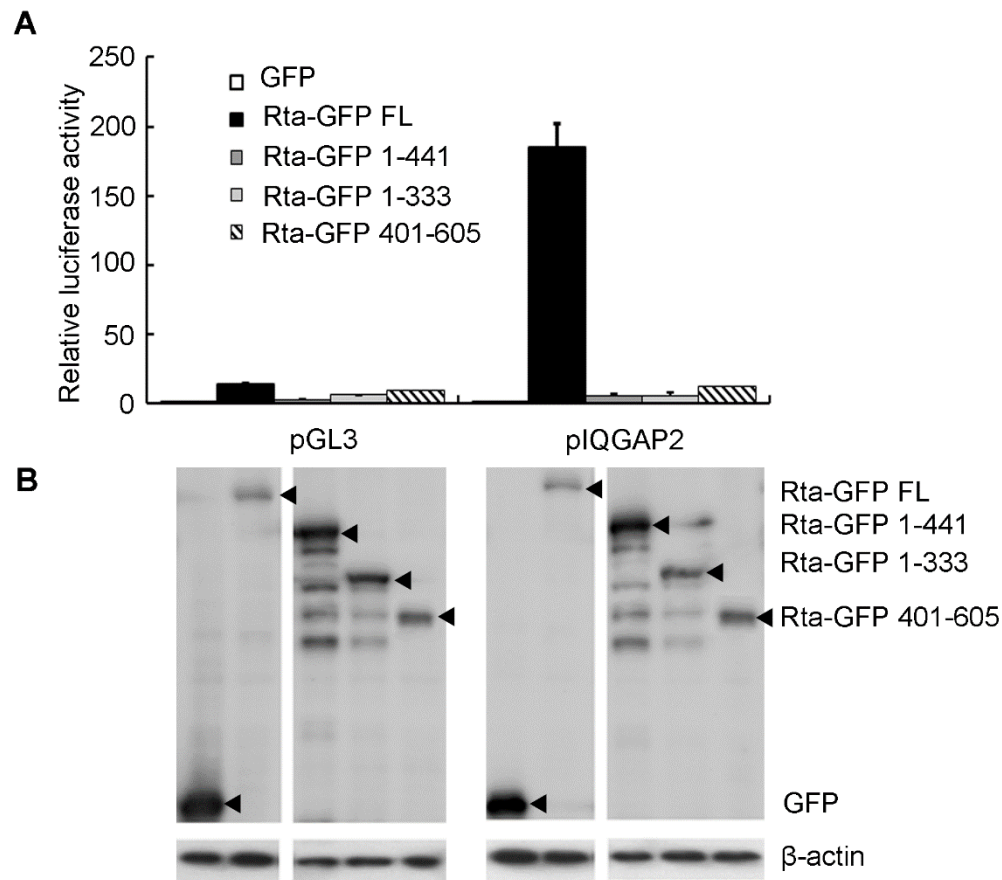
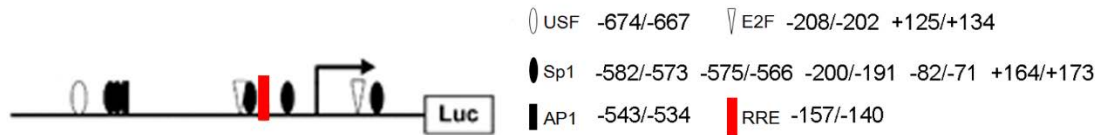


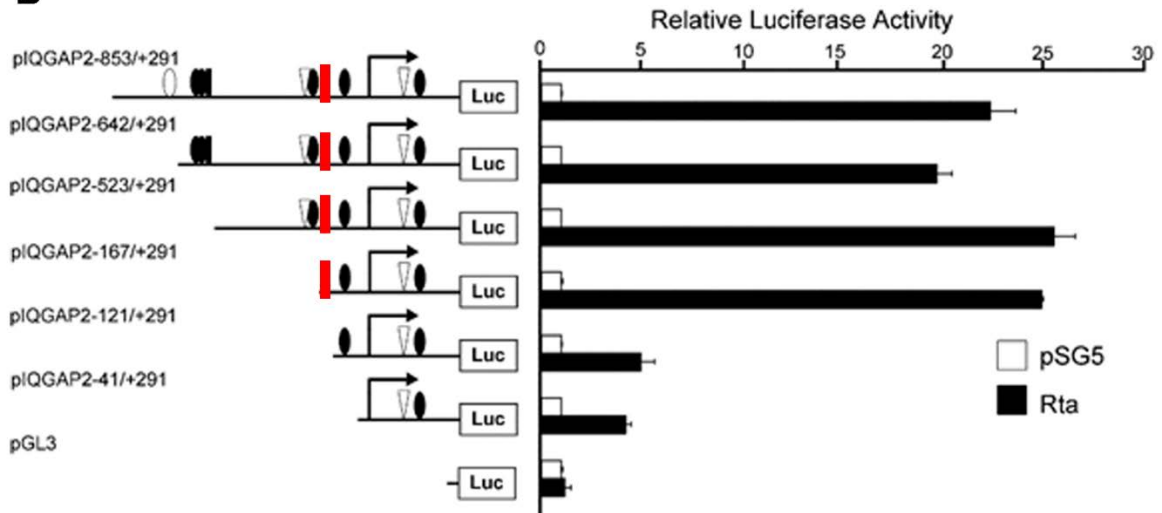
**Figure 12. IQGAP2 promoter luciferase reporter assay with different Rta-GFP proteins.** (A) 293T cells were transfected with pGL3 or pIQGAP2; pEGFP, pEGFP-Rta FL, pEGFP-Rta 1-441, pEGFP-Rta 1-333, or pEGFP-Rta 401-605. Luciferase activities were measured and relative activities were calculated according to GFP fluorescence. Graph was made using Microsoft Excel. (B) Portion of transfected cells were subjected to cell lysis for protein analysis. The results verified GFP, Rta-GFP, and truncated Rta-GFP protein expression. This experiment was performed twice independently.



**A**

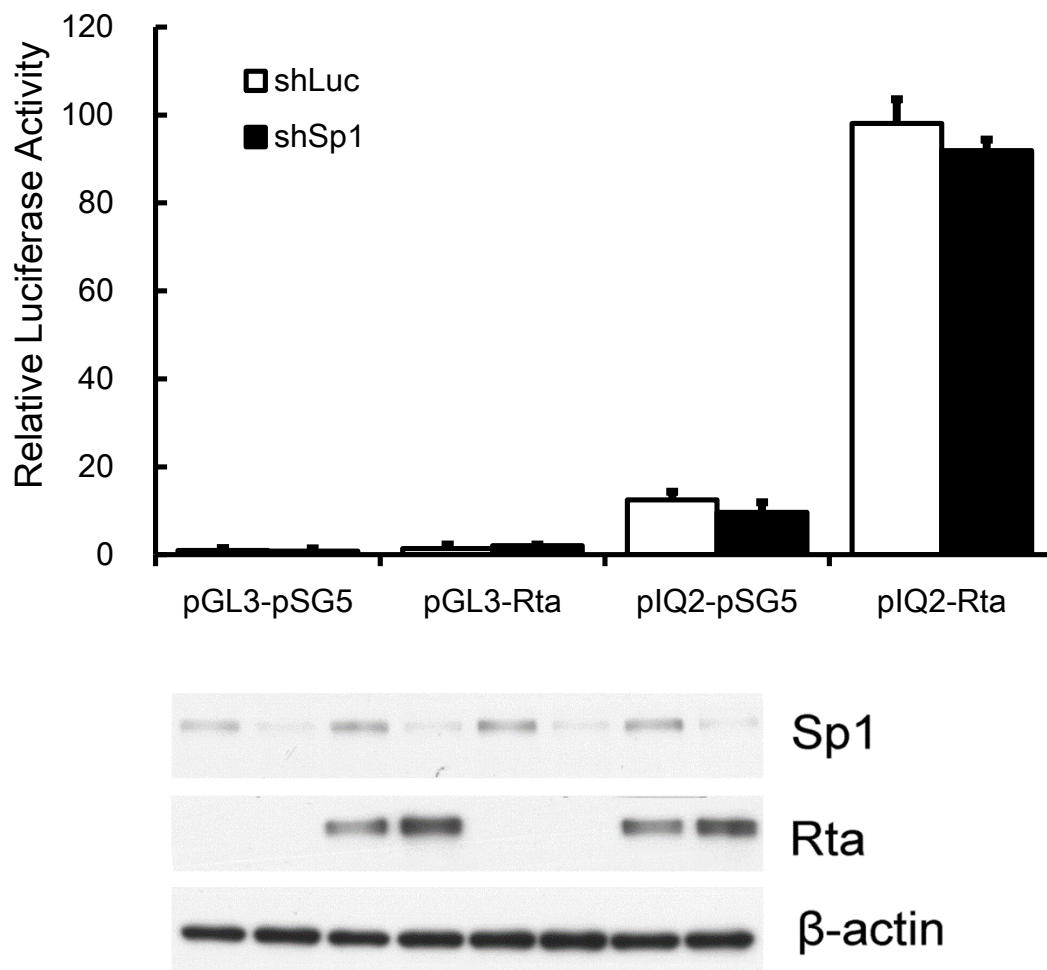


**B**

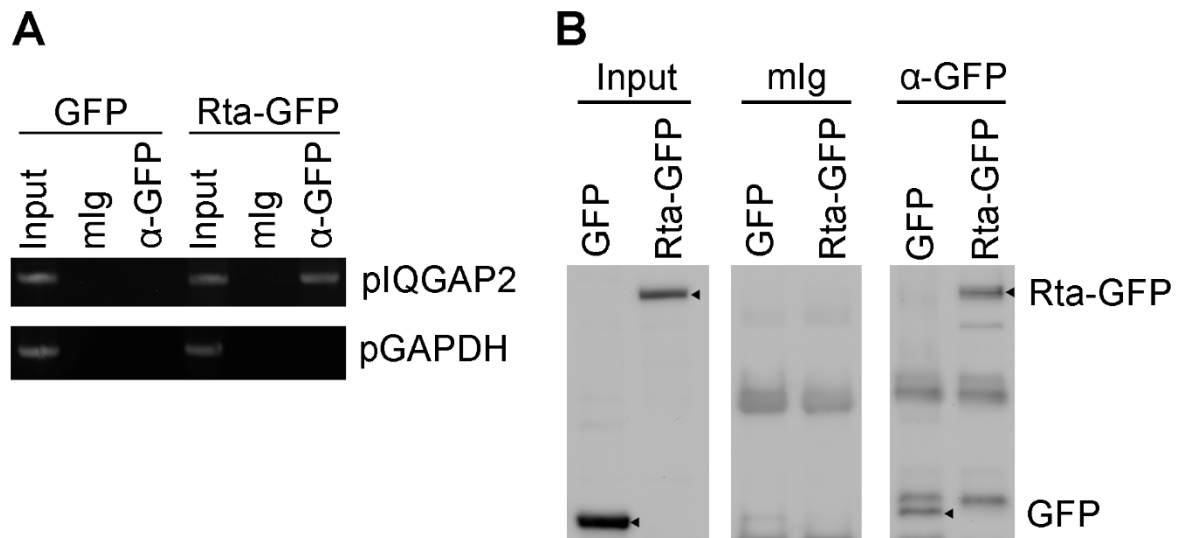


**Figure 13. Luciferase activity assay with different 5'-deleted IQGAP2 reporter plasmids revealed the important promoter region.**

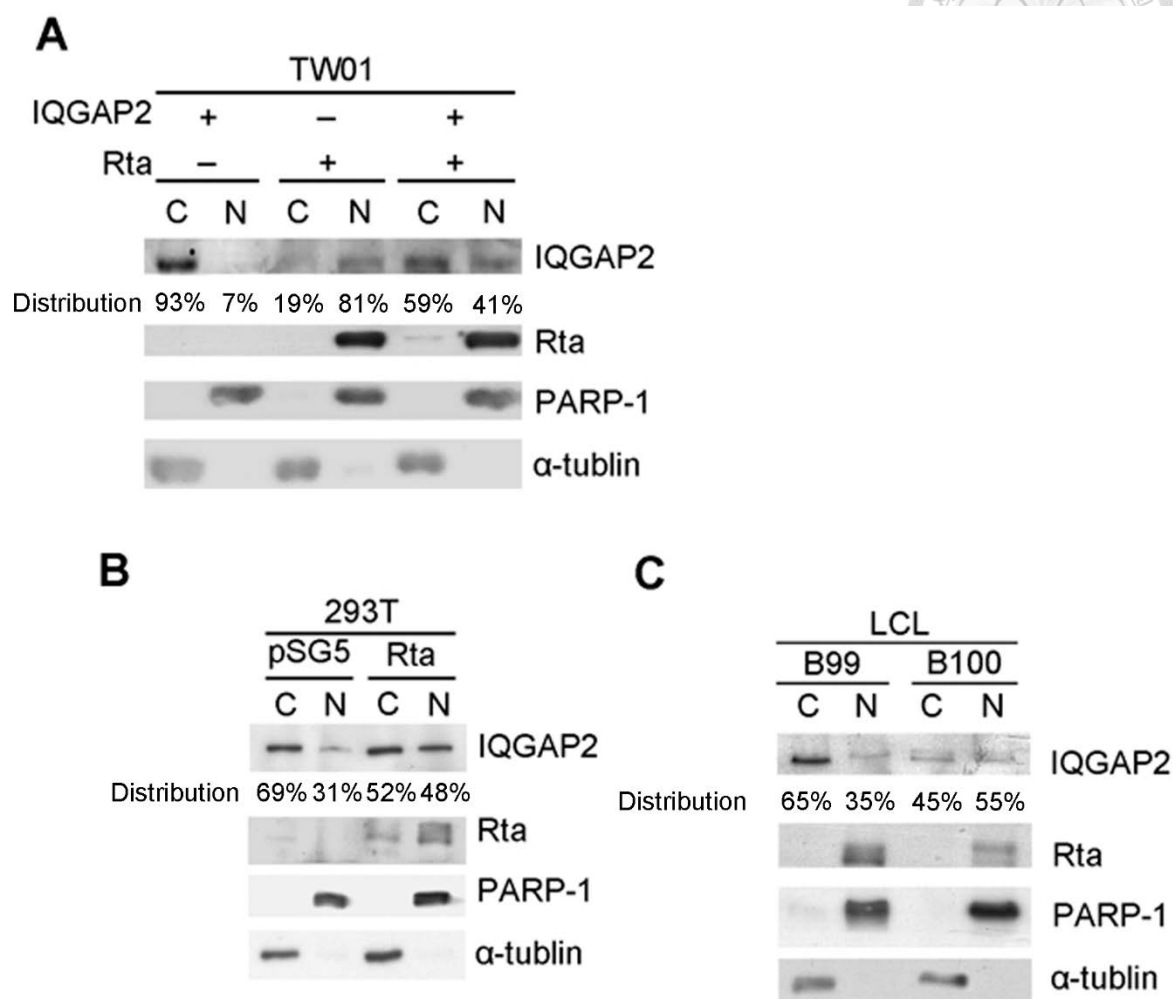
(A) Predicted Rta-related DNA binding sites on IQGAP2 promoter. Schematic illustration of the reporter plasmids of the IQGAP2 promoter. Algen Promo ([http://algen.lsi.upc.es/cgi-bin/promo\\_v3/promo/promoinit.cgi?dirDB=TF\\_8.3](http://algen.lsi.upc.es/cgi-bin/promo_v3/promo/promoinit.cgi?dirDB=TF_8.3)) and TFSEARCH (Parallel Application TRC Laboratory, RWCP, Japan) were used in this prediction. (B) 293T cells were transfected with Rta-expressing plasmids, 5'-deleted IQGAP2 reporter plasmids and pEGFP-C1 as a transfection control. After 72 hours, the relative luciferase activity of each transfectant was normalized to its GFP intensity and standardized to the vector control cells. This experiment was performed twice independently.



**Figure 14. Knockdown of Sp1 did not affect Rta-induced IQGAP2 promoter activation.** 293T cells were infected with shSp1-expression lentivirus and underwent 48h puromycin selection. Sp1-repressed 293T cells were transfected with pIQGAP2 and Rta. After 72 hours, the relative luciferase activity of each transfectant was normalized to its GFP intensity and standardized to the vector control cells

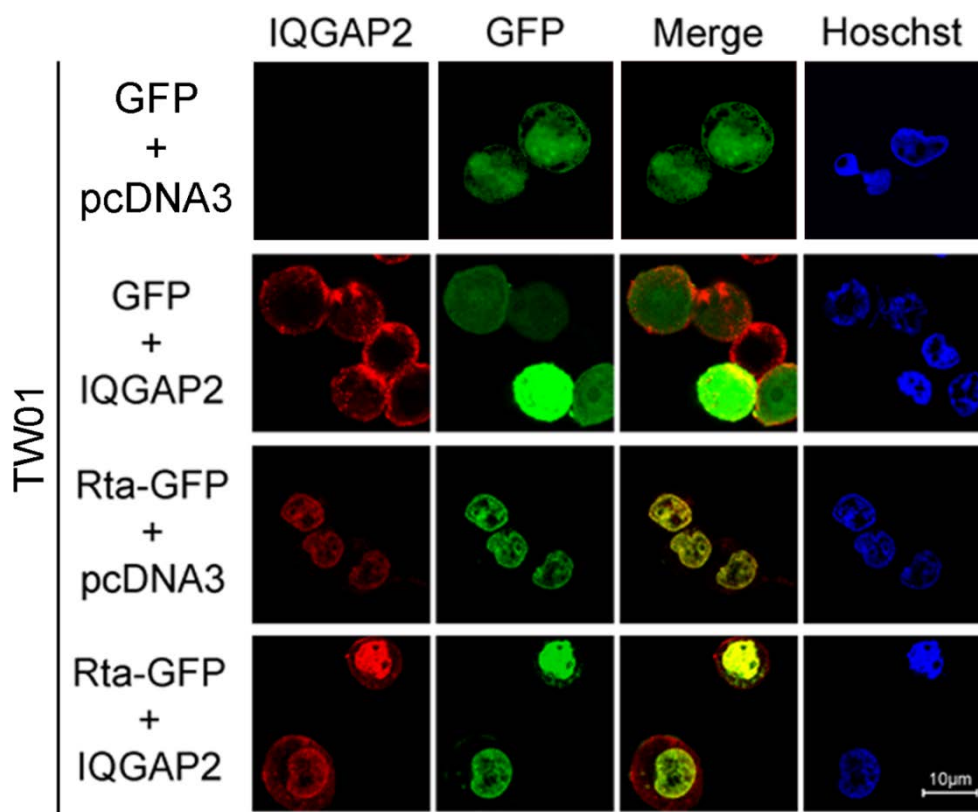


**Figure 15. Rta binds to IQGAP2 promoter.** 293T cells were transfected with Rta-GFP for 72 hours and lysed. Complexes of DNA and Rta-GFP were immunoprecipitated from the cells using anti-GFP antibody or mouse IgG. (A) DNA of IQGAP2 promoter (pIQGAP2) and GAPDH promoters (pGAPDH) were detected in the immunoprecipitates by PCR. Total DNA was harvested from GFP or GFP-Rta- expressing cells and used as the input control. (B) Partial immunoprecipitates were subjected to western blotting to verified the efficiency of immunoprecipitation. Portion of protein extracts from GFP or GFP-Rta-transfected cells were adapted as input. This experiment was performed twice independently.

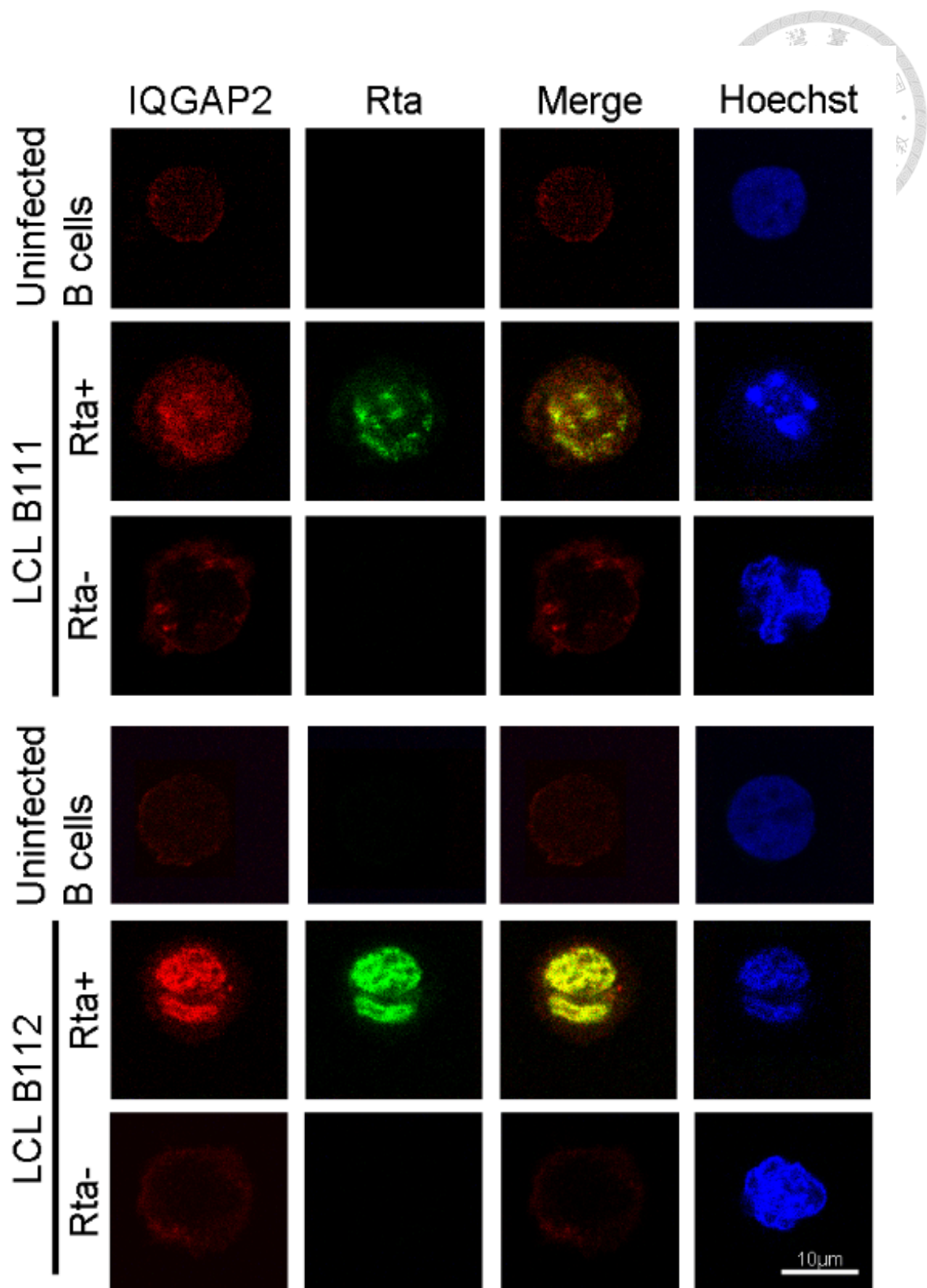


**Figure 16. Nuclear expression of IQGAP2 was associated with Rta expression.** C stands for cytosol and N stands for nucleus. (A) TW01 cells were transfected with IQGAP2, Rta or both IQGAP2 and Rta. 72h post-transfection, cells were harvested for subcellular fractionation. The resulting protein lysates were subjected to SDS-PAGE and western blotting for IQGAP2 and Rta expression. poly-ADP-ribose polymerase-1 (PARP-1) and  $\alpha$ -tubulin were cytoplasmic and nuclear marker, respectively. (B) 293 cells were transfected with Rta and subjected to subcellular fractionation 72h post-transfection. (C) Cytoplasm and nucleus of LCLs were separated was subjected to SDS-PAGE and western blotting. These experiments were performed twice independently.





**Figure 17. Subcellular localization of transfected and induced IQGAP2 in relation with Rta was analyzed with confocal microscopy.** TW01 cells were seeded on coverslips and transfected with plasmids indicated on the left. 72 hours later, cells were fixed with 2% formaldehyde, and permeabilized with 0.1% Triton X-100. IQGAP2 antibody was used for detection. Confocal microscopy was utilized to observed related expression of IQGAP2 and Rta in a cell, whereas Hoeschst indicated nucleuses of cells. This experiments was performed for three times independently.



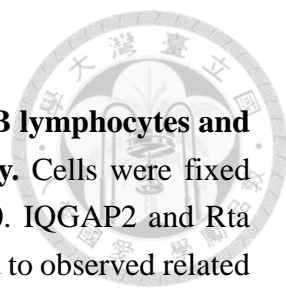


**Figure 18. Subcellular localization of IQGAP2 in human CD19+ B lymphocytes and EBV-immortalized LCL was analyzed with confocal microscopy.** Cells were fixed with 2% formaldehyde, and permeabilized with 0.1% Triton X-100. IQGAP2 and Rta antibodies were used for detection. Confocal microscopy was utilized to observed related expression of IQGAP2 and Rta in a cell, whereas Hoechst indicated nucleuses of cells.

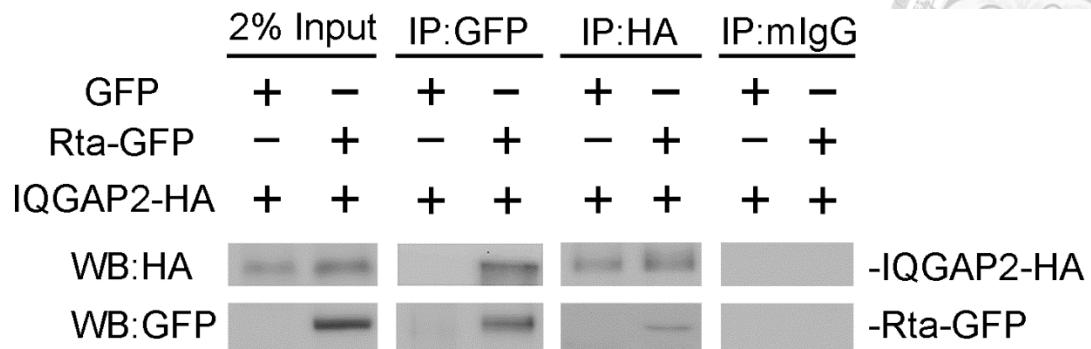


**Figure 19. Interaction of IQGAP2 and Rta was analyzed with co-immunoprecipitation.** 293T cells were transfected with both IQGAP2-HA and Rta-GFP. 72 hours later, cell were lysed with cell lysis buffer and precleared with 20% protein A beads. GFP antibody was used for Rta-GFP binding while HA antibody was used for IQGAP2-HA binding. Protein-antibody complexes were then precipitated with protein A beads. After 2X protein sample dye was added, the precipitates were denatured at 95°C, and subjected to SDS-PAGE as well as western blotting. This experiment was performed twice independently.

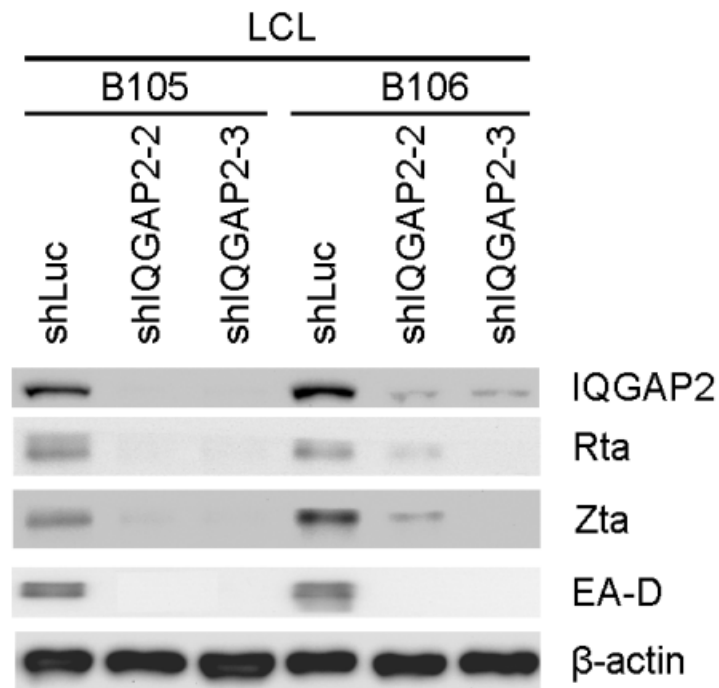


**Figure 20. Knockdown of IQGAP2 affected spontaneous lytic progression in LCLs.** LCLs were infected with shIQGAP2-expressing lentivirus for 5 days and then underwent 48 h of puromycin selection. Cells were then harvested for protein analysis with SDS-PAGE and western blotting. IQGAP2 antibody was used to verify knockdown efficiency. Rta, Zta and EA-D antibodies was used to observe lytic progression.  $\beta$ -actin served as internal loading control. This experiment was performed twice independently.

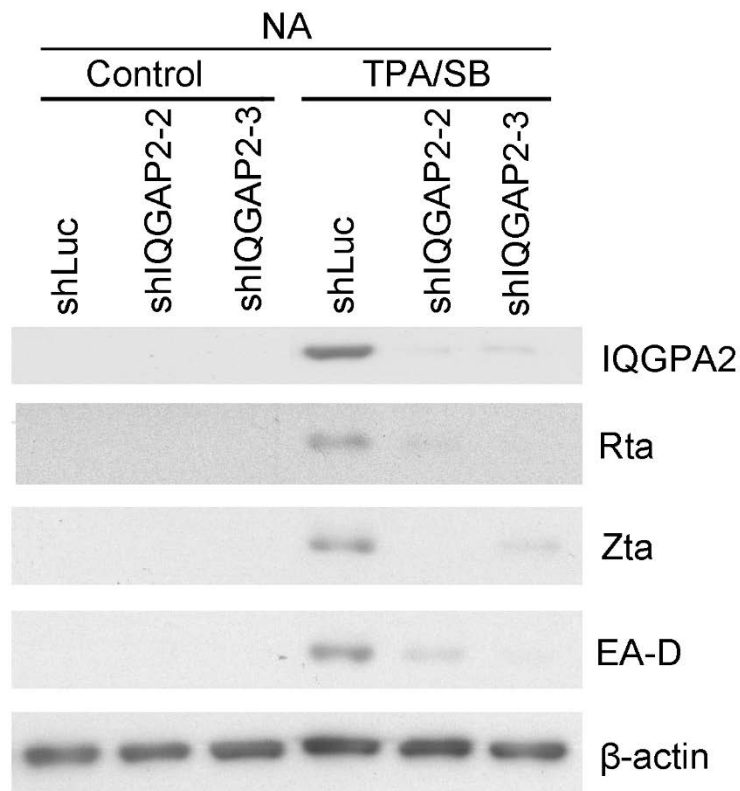


**Figure 21. Knockdown of IQGAP2 impaired TPA/SB-induced lytic progression in NA cells.** NA cells were transfected with shIQGAP2-expression plasmids for 72 hours and then underwent 48 h of puromycin selection. The selected cells were then treated with TPA and SB for 72 hours and harvested for protein analysis. Western blotting was performed with IQGAP2, Rta, EA-D, and  $\beta$ -actin antibodies. This experiment was performed for three times independently.

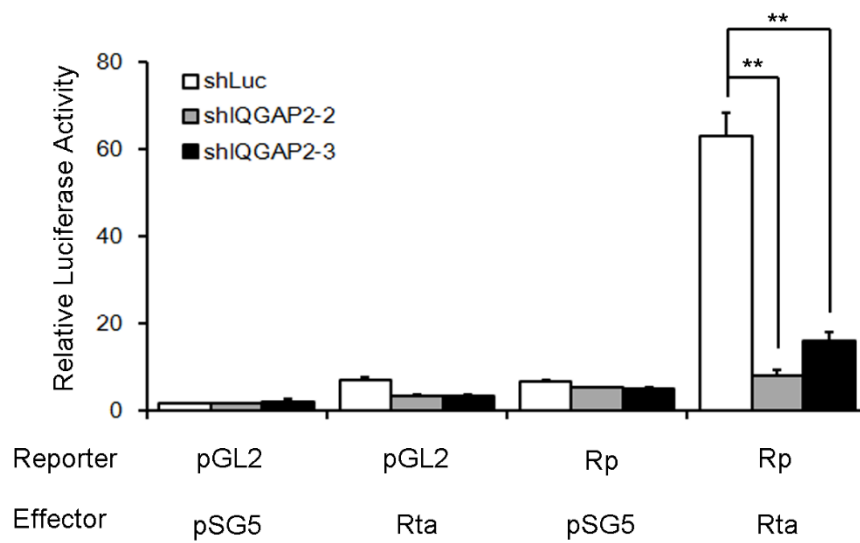


**Figure 22. Knockdown of IQGAP2 impacted Rta autoregulation in 293T cells.** 293T cells were transfected with shIQGAP2-expression plasmids for 72 hours and then underwent 48 h of puromycin selection. The selected cells were further transfected with Rp, Rta, and pEGFP for reporter assay. 72 hours later, cells were lysed and measured for luciferase activity. Relative luciferase activity was obtained in accordance with GFP fluorescence, and the relative luciferase activity of cells transfected with pGL2 and pSG5 was set as 1. This experiment was performed twice independently. \*\* indicates  $p < 0.01$ .

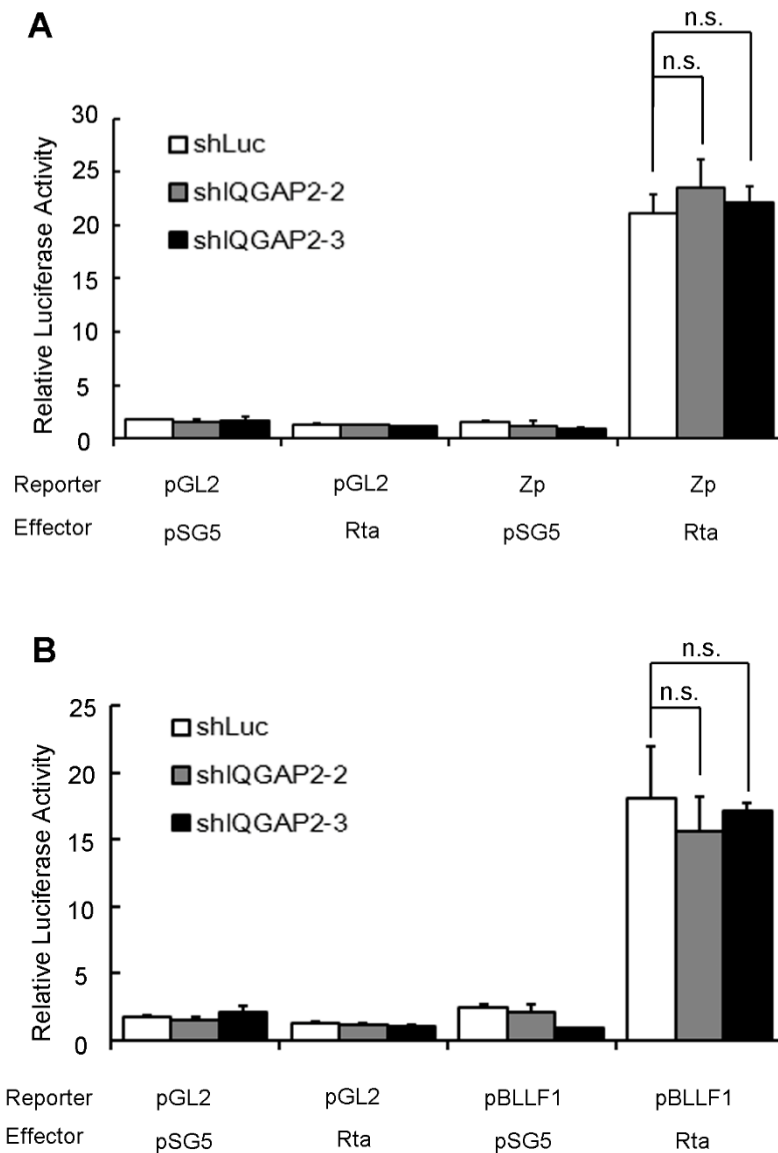


**Figure 23. Knockdown of IQGAP2 did not affect Rta-induced Zp or pBLLF1 activation in 293T cells.** 293T cells were transfected with shIQGAP2-expression plasmids for 72 hours and then underwent 48 h of puromycin selection. The selected cells were further transfected with (A) Zp, Zta, and pEGFP; (B) Zp, Rta, and pEGFP; (C) pBLLF1, Rta, and pEGFP for reporter assay. 72 hours later, cells were lysed and measured for luciferase activity. Relative luciferase activity was obtained in accordance with GFP fluorescence, and the relative luciferase activity of cells transfected with pGL2 and pSG5 was set as 1. This experiment was performed twice independently. n.s. indicates no significance,  $p > 0.05$ .



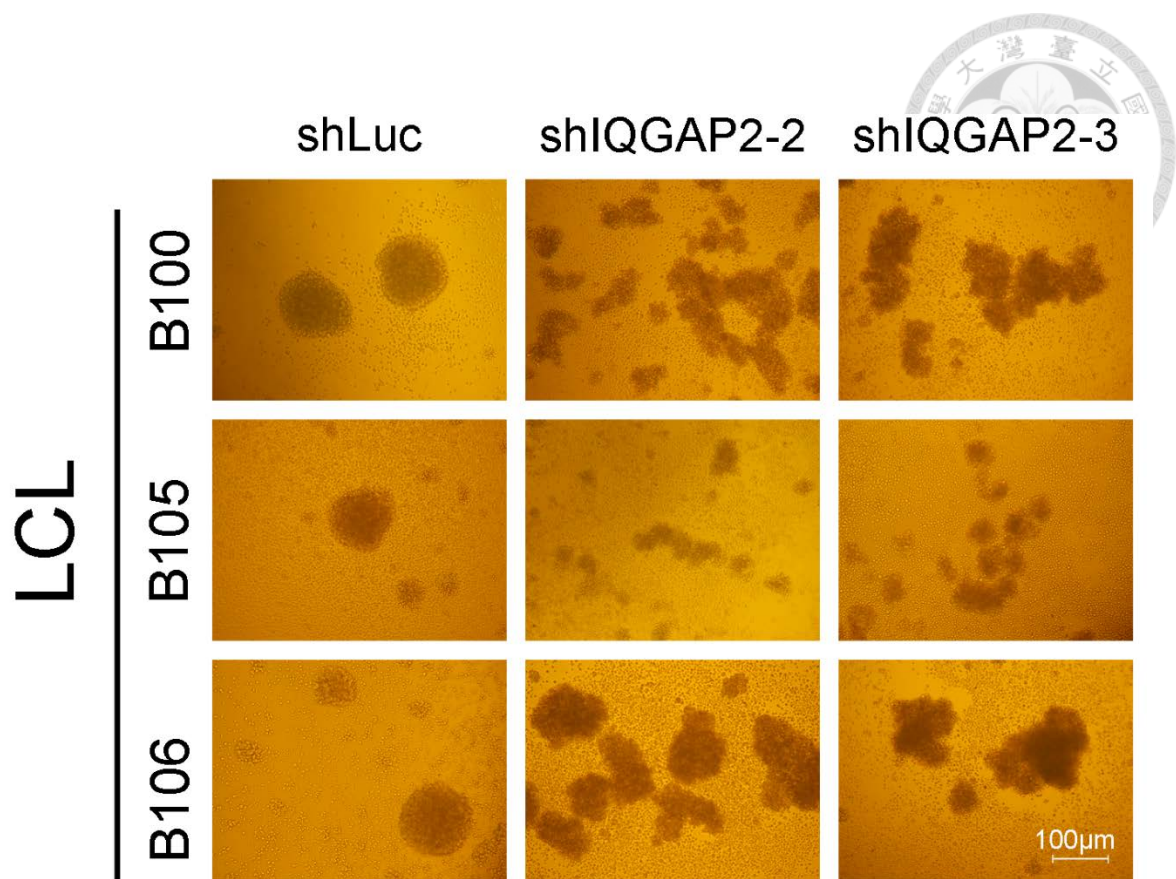


**Figure 24. Knockdown of IQGAP2 altered LCL clumping morphology.** LCLs were infected with shIQGAP2-expressing lentivirus for 5 days and then underwent 48 h of puromycin selection. Cells were seeded in 96-well plates and incubated for 24 h. Photos were taken under a bright-field microscope. This experiment was performed twice independently.

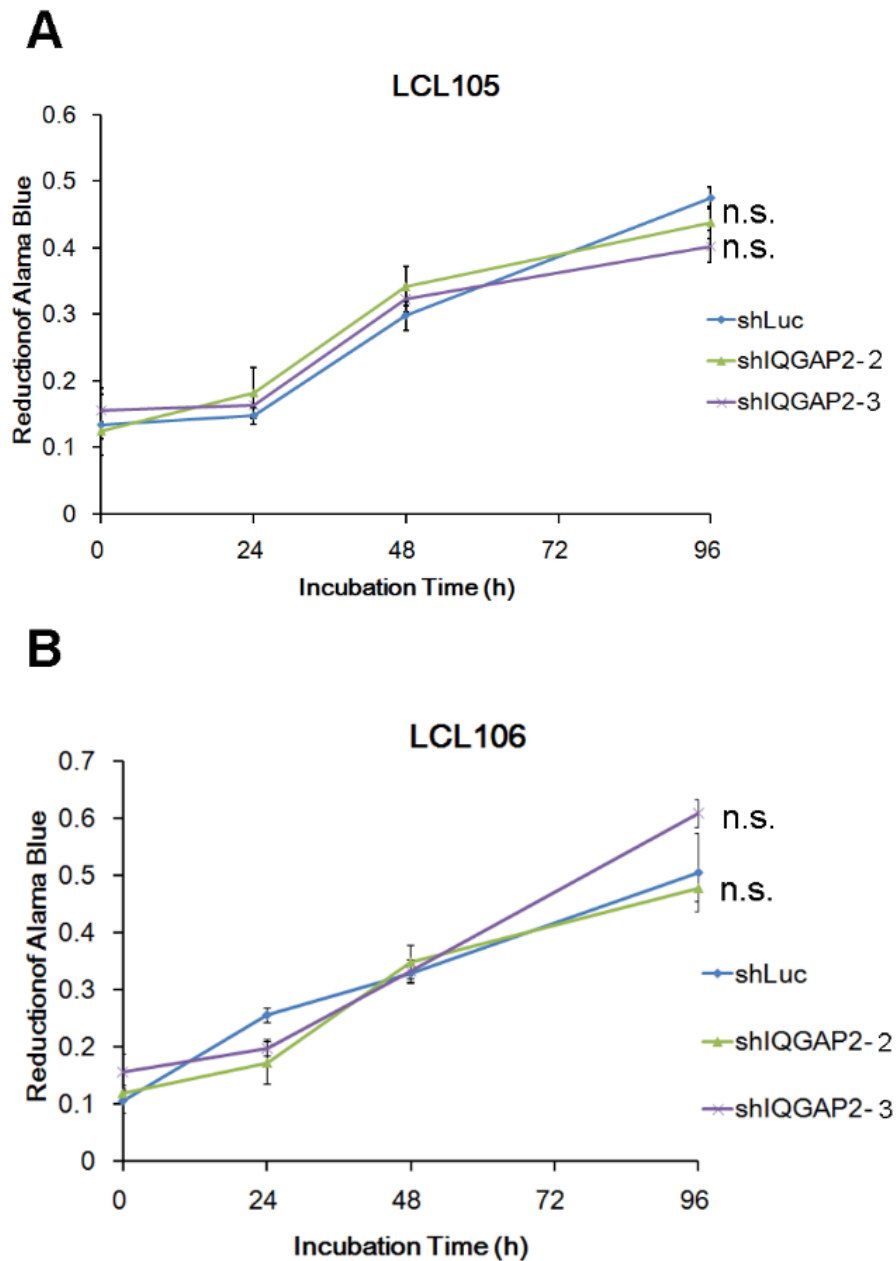


**Figure 25. Knockdown of IQGAP2 did not affect LCL proliferation.** LCLs were infected with shIQGAP2-expressing lentivirus for 5 days and then underwent 48 h of puromycin selection. Cells were seeded in 96-well plates and viable cell number was measured with Alamar blue assay kit. Cell proliferation rate was obtained by comparing viable cell numbers at indicated time. This experiment was performed twice independently. n.s. indicates no significance,  $p > 0.05$ .

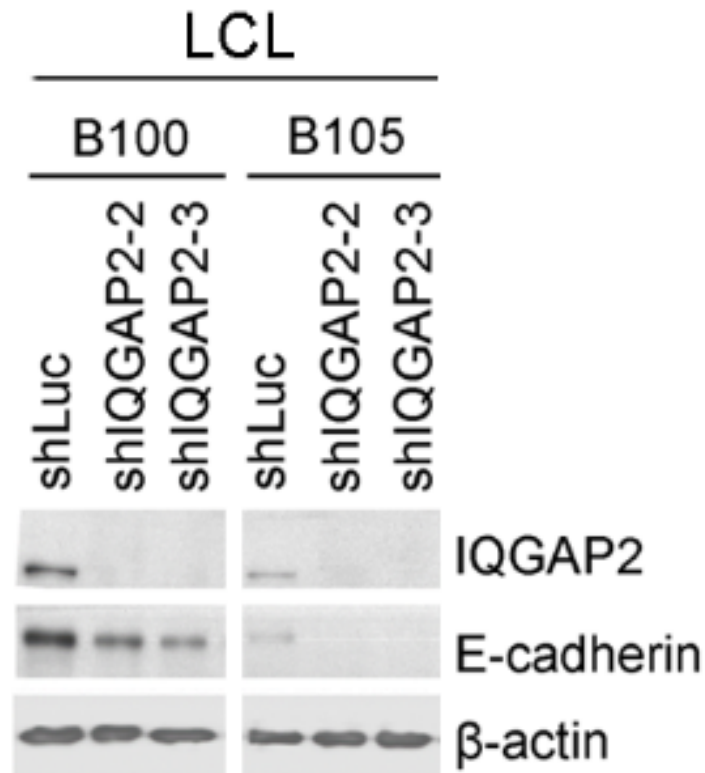


**Figure 26. Knockdown of IQGAP2 decreased E-cadherin in LCLs.** LCLs were infected with shIQGAP2-expressing lentivirus for 5 days and then underwent 48 h of puromycin selection. Cells were then harvested for protein analysis with western blotting to detect E-cadherin expression. IQGAP2 antibody was used to verify knockdown efficiency.  $\beta$ -actin served as internal loading control. This experiment was performed twice independently.

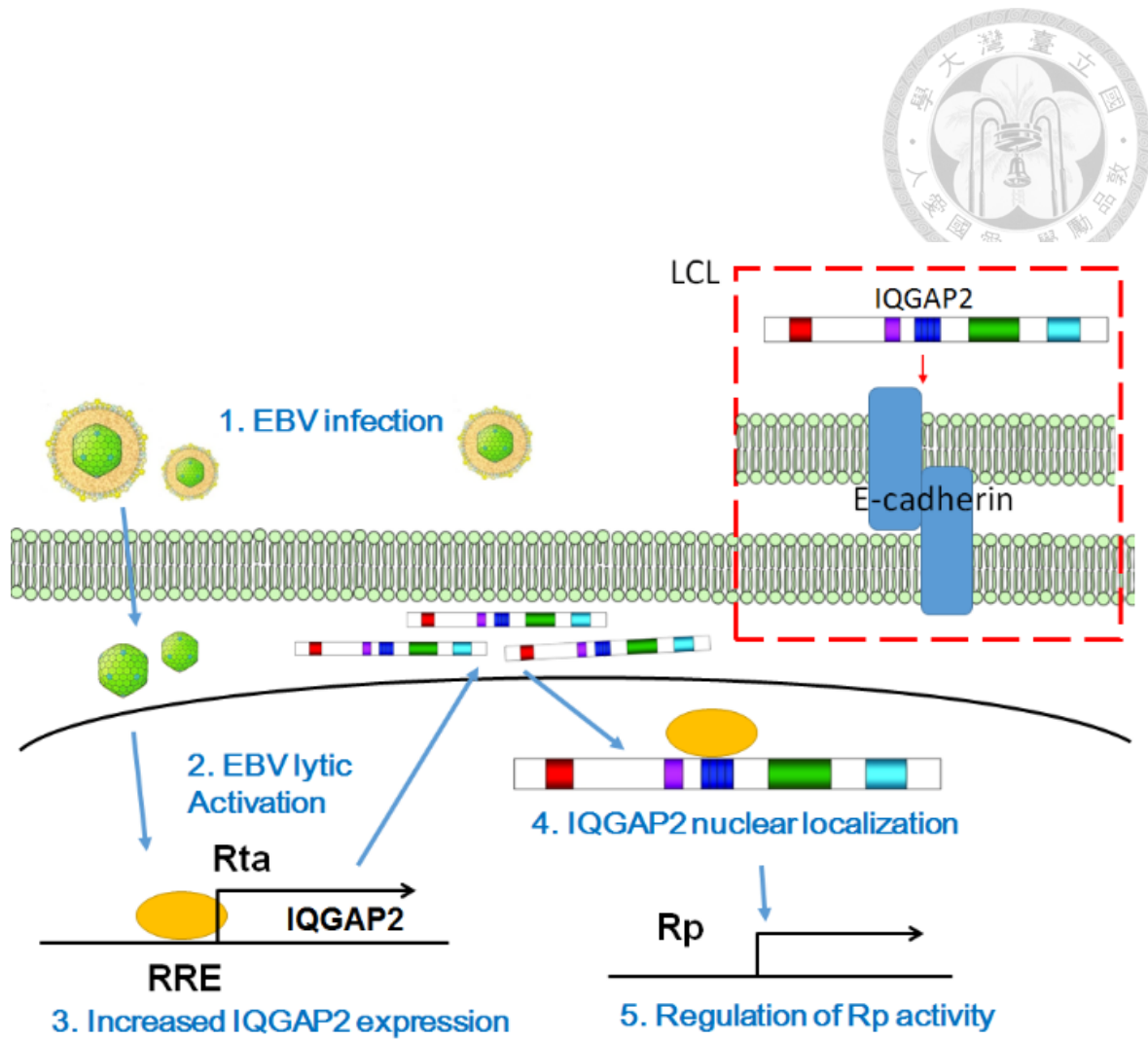


**Figure 27. Hypothesis Model.** EBV infection and reactivation express lytic protein Rta in host cells. Rta binds to RRE on IQGAP2 promoter and upregulation IQGAP2 transcription. Rta recruits translated IQGAP2 protein in to the nucleus. Rta-IQGAP2 complex facilitate activation of Rp, promoting lytic progression. Furthermore, in LCLs, IQGAP2 may mediate cell-to-cell adhesion through E-cadherin.

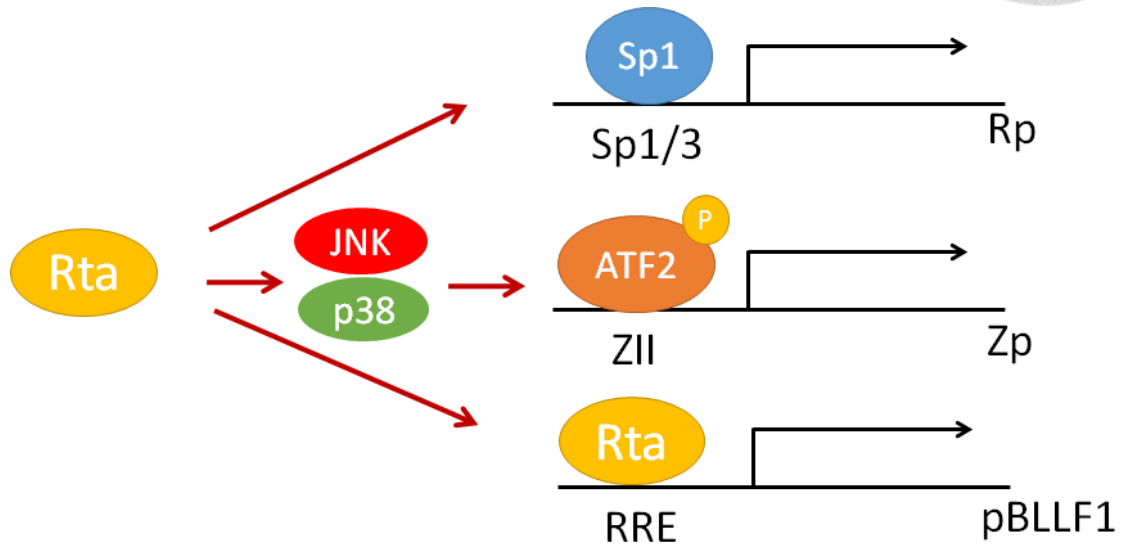


**Figure 28. Rta activates lytic promoters through different pathways.** Rta activates Rp through Sp1. Rta modulates the phosphorylation of the p38 and JNK signaling pathways, resulting in binding of phosphorylated ATF2 to the ZII element in Zp to activate Zta expression. Rta binds to a RRE in pBLLF1 to activates transcription.

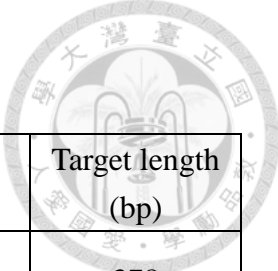
## Tables



**Table 1. Primers used for plasmid constructs (pGL3-pIQGAP2 and promoter serial deletion)**

Primer	Sequence (5' to 3')
Xho I-pIQGAP2-R	CTAGCTAGCTAGTATCGCCCTCCCTCAGTTTG
Nhe I-pIQGAP2-F -853	CCGCTCGAGCGGCTCGCCGATTTCCCCTAGC
Nhe I-pIQGAP2-F -642	CTAGCTAGCTAGCCAAGCTTAGCCGGAAAAGGT
Nhe I-pIQGAP2-F -523	CTAGCTAGCTAGAGTGGTTGCCTTGGGTTATCTTG
Nhe I-pIQGAP2-F -164	CTAGCTAGCTAGGAAAAGGAACCGCGCTGTTT
Nhe I-pIQGAP2-F -121	CTAGCTAGCTAGCCACCAGCTGTGCGGG
Nhe I-pIQGAP2-F -41	CTAGCTAGCTAGGGTAGGGGTCGCTGCGTCT

**Table 2 Primers used for polymerase chain reactions**



Gene	Sequence (5' to 3')	Target length (bp)
IQGAP1	F: GCCAGACAGCACTGTGTTG	378
	R: TCACGGATAGCACGTCTCTG	
IQGAP2	F: CCTTGTGAAGGCAAAAGAGC	399
	R: CCGCCTGTGTGCATATACTCCT	
IQGAP3	F: ATGACTCCAACACCCGTAGC	317
	R: ACTAGCCCCTGGTAGCCATT	
$\beta$ -actin	F: TTCTACAATGAGCTGCGTGT	636
	R: GCCAGACAGCACTGTGTTGG	
Rta	F: CGGGATCCAAATAGACAGCCCAGTTGAAA	612
	R: CGGGATCCCAAGAGAGCGATGAGAGAC	
Zta	F: TTCCACAGCCTGCACCAGTG	182
	R: GGCAGCAGCCACCTCACGGT	
EBNA1	F: ATGAGCGTTTGGGAGAGCTGATTC	273
	R: TCCTCGTCCATGGTTATCAC	
pIQGAP2	F: TTCCACCCTCGAAACTCTCC	315
	R: CGCGCTGACACTGAAGTAAA	

Remarks:

F: forward

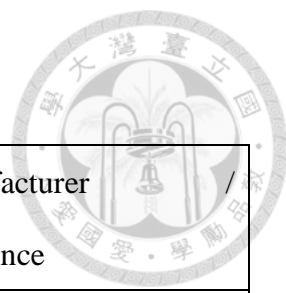
R: reverse

**Table 3. shRNA sequence for gene knockdown lentiviruses**


shRNA	Targeting sequence (5' to 3')
shLuciferase (shLuc)	CTTCGAAATGTCCGTTTCGGTT
shIQGAP2-2	GCCTCTAATCAGCGAGAAGAA
shIQGAP2-3	GCCATGTATCAGAACGAACTT



**Table 4. Dilution fold for antibodies**



Antibody	Dilution fold	Clone	Manufacturer / Reference
Mouse anti-IQGAP1 mAb	WB: 1/1000	05-504	Millipore
Mouse anti-IQGAP2 mAb	WB: 1/1000 IFA: 1/100	BB9	Millipore
Rabbit anti-IQGAP2 mAb	WB: 1/1000 IFA: 1/100	H-209	Santa Cruz
Human anti-EBNA1 pAb	WB: 1/1000		NPC47 (Tsai et al., 2009)
Mouse anti-LMP1 mAb	WB: 1/1000	S12	(Chang et al., 2004)
Mouse anti-Zta mAb	WB: 1/25	1B4	(Tsai et al., 1997)
Mouse anti-Rta mAb	WB: 1/50	467	(Hsu et al., 2005)
Mouse anti-EA-D mAb	WB: 1/50	88	(Chen et al., 2000)
Mouse anti-BGLF4 mAb	WB: 1/50	2616	(Wang et al., 2005)
Mouse anti-GFP mAb	WB: 1/1000 IP: 1 $\mu$ g / 400 $\mu$ g sample	M2	Sigma
Mouse anti-HA mAb	WB: 1/1000 IP: 1 $\mu$ g / 400 $\mu$ g	.11	Babco



	sample		
Mouse anti- $\beta$ -actin mAb	WB: 1/5000	AC-15	Sigma
Mouse anti-PARP-1 mAb	WB: 1/500	F-2	Santa cruz
Mouse anti- $\alpha$ -tubulin mAb	WB: 1/500	DM1A	CALBIOCHEM
Mouse anti-E-Cadherin mAb	WB: 1/1000	34	BD Bioscience
HRP-conjugated anti-mouse IgG	WB: 1/5000		Jackson
HRP-conjugated anti-rabbit IgG	WB: 1/5000		Jackson
Rhodamine-anti-mouse IgG	IFA: 1/500		cappel
Rhodamine-anti-rabbit IgG	IFA: 1/500		cappel
FITC-anti-mouse IgG	IFA: 1/500		cappel
FITC-anti-rabbit IgG	IFA: 1/500		cappel

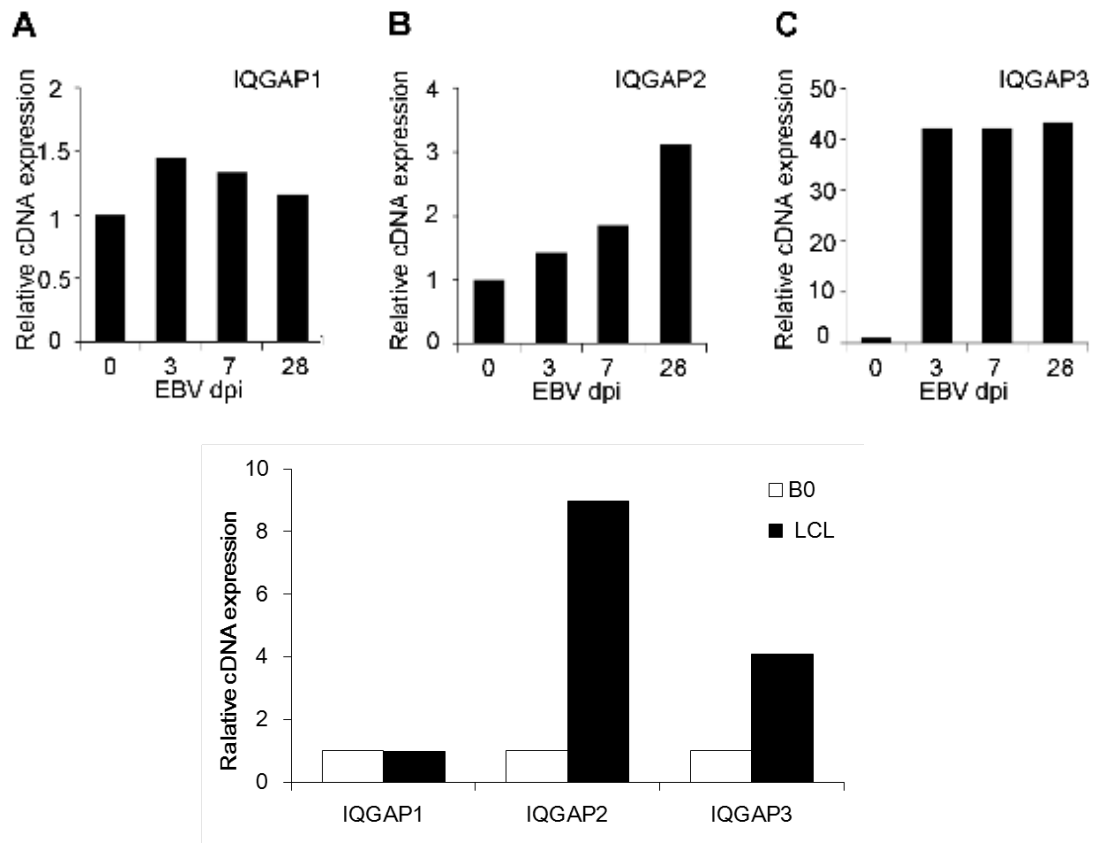
Remarks:

mAb: monoclonal antibody    pAb: polyclonal antibody    WB: Western Blotting

IFA: immunofluorescent assay    IP: immunoprecipitation

HRP: horseradish peroxidase    FITC: fluorescein isothiocyanate

## Appendixes



### Appendix I. Expression of IQGAPs in B cells and EBV-infected B cells was analyzed with cDNA microarray.

Purified human CD19<sup>+</sup> B lymphocytes from healthy donor were infected with B95.8 strain EBV for 3, 7, and 28 days. Infected and uninfected cells were collected. Expression of (A) IQGAP1, (B) IQGAP2, and (C) IQGAP3 was quantified with cDNA microarray. (D) Expression of IQGAP family in EBV-immortalized lymphoblastoid cell line (LCL) was compared in relation with its uninfected B cells counterpart. This experiment was performed by Dr. Shu-Chuin Tsai.



## TW01



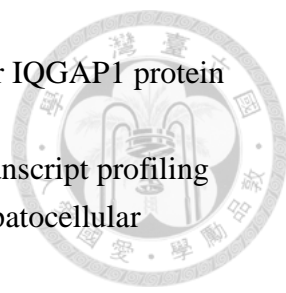
**Appendix II. Expression of IQGAPs was analyzed when TW01 cells were transfected with EBV viral genes.** TW01 cells were transfected with some of the important EBV viral genes. 72 h post transfection, cells were subjected to RT-PCR for IQGAPs mRNA expression analysis. This experiment was performed by Dr. Juin-Han Lin.

## References

1. Abel, A.M., Schuldt, K.M., Rajasekaran, K., Hwang, D., Riese, M.J., Rao, S., Thakar, M.S., and Malarkannan, S. (2015). IQGAP1: insights into the function of a molecular puppeteer. *Molecular immunology* 65, 336-349.
2. Adachi, M., Kawasaki, A., Nojima, H., Nishida, E., and Tsukita, S. (2014). Involvement of IQGAP family proteins in the regulation of mammalian cell cytokinesis. *Genes to cells : devoted to molecular & cellular mechanisms* 19, 803-820.
3. Adamson, A.L., Darr, D., Holley-Guthrie, E., Johnson, R.A., Mauser, A., Swenson, J., and Kenney, S. (2000). Epstein-Barr virus immediate-early proteins BZLF1 and BRLF1 activate the ATF2 transcription factor by increasing the levels of phosphorylated p38 and c-Jun N-terminal kinases. *Journal of virology* 74, 1224-1233.
4. Almasan, A., Yin, Y., Kelly, R.E., Lee, E.Y., Bradley, A., Li, W., Bertino, J.R., and Wahl, G.M. (1995). Deficiency of retinoblastoma protein leads to inappropriate S-phase entry, activation of E2F-responsive genes, and apoptosis. *Proceedings of the National Academy of Sciences of the United States of America* 92, 5436-5440.
5. Baer, R., Bankier, A.T., Biggin, M.D., Deininger, P.L., Farrell, P.J., Gibson, T.J., Hatfull, G., Hudson, G.S., Satchwell, S.C., Seguin, C., *et al.* (1984). DNA sequence and expression of the B95-8 Epstein-Barr virus genome. *Nature* 310, 207-211.
6. Besson, C., Amiel, C., Le-Pendeven, C., Brice, P., Ferme, C., Carde, P., Hermine, O., Raphael, M., Abel, L., and Nicolas, J.C. (2006). Positive correlation between Epstein-Barr virus viral load and anti-viral capsid immunoglobulin G titers determined for Hodgkin's lymphoma patients and their relatives. *Journal of clinical microbiology* 44, 47-50.
7. Bouwmeester, T., Bauch, A., Ruffner, H., Angrand, P.O., Bergamini, G., Croughton, K., Cruciat, C., Eberhard, D., Gagneur, J., Ghidelli, S., *et al.* (2004). A physical and functional map of the human TNF-alpha/NF-kappa B signal transduction pathway. *Nature cell biology* 6, 97-105.
8. Briggs, M.W., Li, Z., and Sacks, D.B. (2002). IQGAP1-mediated stimulation of transcriptional co-activation by beta-catenin is modulated by calmodulin. *The Journal of biological chemistry* 277, 7453-7465.
9. Brill, S., Li, S., Lyman, C.W., Church, D.M., Wasmuth, J.J., Weissbach, L., Bernards, A., and Snijders, A.J. (1996). The Ras GTPase-activating-protein-related human protein IQGAP2 harbors a potential actin binding domain and interacts with

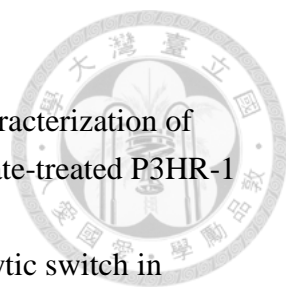
- 
- calmodulin and Rho family GTPases. *Molecular and cellular biology* *16*, 4869-4878.
10. Brown, M.D., and Sacks, D.B. (2006). IQGAP1 in cellular signaling: bridging the GAP. *Trends in cell biology* *16*, 242-249.
  11. Burke, A., and Lee, Y.K. (1990). Adenocarcinoid (goblet cell carcinoid) of the duodenum presenting as gastric outlet obstruction. *Human pathology* *21*, 238-239.
  12. Burkitt, D. (1958). A sarcoma involving the jaws in African children. *The British journal of surgery* *46*, 218-223.
  13. Calderwood, M.A., Venkatesan, K., Xing, L., Chase, M.R., Vazquez, A., Holthaus, A.M., Ewence, A.E., Li, N., Hirozane-Kishikawa, T., Hill, D.E., *et al.* (2007). Epstein-Barr virus and virus human protein interaction maps. *Proceedings of the National Academy of Sciences of the United States of America* *104*, 7606-7611.
  14. Carmon, K.S., Gong, X., Yi, J., Thomas, A., and Liu, Q. (2014). RSPO-LGR4 functions via IQGAP1 to potentiate Wnt signaling. *Proceedings of the National Academy of Sciences of the United States of America* *111*, E1221-1229.
  15. Chang, L.K., Chung, J.Y., Hong, Y.R., Ichimura, T., Nakao, M., and Liu, S.T. (2005). Activation of Sp1-mediated transcription by Rta of Epstein-Barr virus via an interaction with MCAF1. *Nucleic acids research* *33*, 6528-6539.
  16. Chang, Y., Lee, H.H., Chang, S.S., Hsu, T.Y., Wang, P.W., Chang, Y.S., Takada, K., and Tsai, C.H. (2004). Induction of Epstein-Barr virus latent membrane protein 1 by a lytic transactivator Rta. *Journal of virology* *78*, 13028-13036.
  17. Chang, Y., Lee, H.H., Chen, Y.T., Lu, J., Wu, S.Y., Chen, C.W., Takada, K., and Tsai, C.H. (2006). Induction of the early growth response 1 gene by Epstein-Barr virus lytic transactivator Zta. *Journal of virology* *80*, 7748-7755.
  18. Chang, Y., Tung, C.H., Huang, Y.T., Lu, J., Chen, J.Y., and Tsai, C.H. (1999). Requirement for cell-to-cell contact in Epstein-Barr virus infection of nasopharyngeal carcinoma cells and keratinocytes. *Journal of virology* *73*, 8857-8866.
  19. Chasserot-Golaz, S., Schuster, C., Dietrich, J.B., Beck, G., and Lawrence, D.A. (1988). Antagonistic action of RU38486 on the activity of transforming growth factor-beta in fibroblasts and lymphoma cells. *Journal of steroid biochemistry* *30*, 381-385.
  20. Chen, F., Zhu, H.H., Zhou, L.F., Wu, S.S., Wang, J., and Chen, Z. (2010). IQGAP1 is overexpressed in hepatocellular carcinoma and promotes cell proliferation by Akt activation. *Experimental & molecular medicine* *42*, 477-483.
  21. Chen, M.R., Chang, S.J., Huang, H., and Chen, J.Y. (2000). A protein kinase activity associated with Epstein-Barr virus BGLF4 phosphorylates the viral early

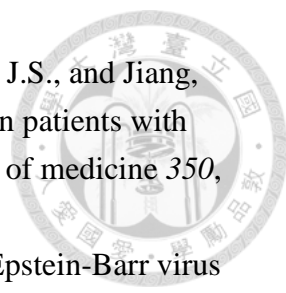
- antigen EA-D in vitro. *Journal of virology* 74, 3093-3104.
22. Chen, Y.L., Chen, Y.J., Tsai, W.H., Ko, Y.C., Chen, J.Y., and Lin, S.F. (2009). The Epstein-Barr virus replication and transcription activator, Rta/BRLF1, induces cellular senescence in epithelial cells. *Cell cycle (Georgetown, Tex)* 8, 58-65.
23. Cheung, K.L., Lee, J.H., Shu, L., Kim, J.H., Sacks, D.B., and Kong, A.N. (2013). The Ras GTPase-activating-like protein IQGAP1 mediates Nrf2 protein activation via the mitogen-activated protein kinase/extracellular signal-regulated kinase (ERK) kinase (MEK)-ERK pathway. *The Journal of biological chemistry* 288, 22378-22386.
24. Chua, H.H., Lee, H.H., Chang, S.S., Lu, C.C., Yeh, T.H., Hsu, T.Y., Cheng, T.H., Cheng, J.T., Chen, M.R., and Tsai, C.H. (2007). Role of the TSG101 gene in Epstein-Barr virus late gene transcription. *Journal of virology* 81, 2459-2471.
25. Cohen, J.I. (2000). Epstein-Barr virus infection. *The New England journal of medicine* 343, 481-492.
26. Countryman, J., and Miller, G. (1985). Activation of expression of latent Epstein-Barr herpesvirus after gene transfer with a small cloned subfragment of heterogeneous viral DNA. *Proceedings of the National Academy of Sciences of the United States of America* 82, 4085-4089.
27. Darr, C.D., Mauser, A., and Kenney, S. (2001). Epstein-Barr virus immediate-early protein BRLF1 induces the lytic form of viral replication through a mechanism involving phosphatidylinositol-3 kinase activation. *Journal of virology* 75, 6135-6142.
28. Dolnik, O., Kolesnikova, L., Welsch, S., Strecker, T., Schudt, G., and Becker, S. (2014). Interaction with Tsg101 is necessary for the efficient transport and release of nucleocapsids in marburg virus-infected cells. *PLoS pathogens* 10, e1004463.
29. Ebell, M.H. (2004). Epstein-Barr virus infectious mononucleosis. *American family physician* 70, 1279-1287.
30. Ellis, A.L., Wang, Z., Yu, X., and Mertz, J.E. (2010). Either ZEB1 or ZEB2/SIP1 can play a central role in regulating the Epstein-Barr virus latent-lytic switch in a cell-type-specific manner. *Journal of virology* 84, 6139-6152.
31. Epstein, M.A., Achong, B.G., and Barr, Y.M. (1964). Virus Particles In Cultured Lymphoblast From Burkitt's Lymphoma. *Lancet* 1, 702-703.
32. Erdemir, H.H., Li, Z., and Sacks, D.B. (2014). IQGAP1 binds to estrogen receptor-alpha and modulates its function. *The Journal of biological chemistry* 289, 9100-9112.
33. Gladue, D.P., Holinka, L.G., Fernandez-Sainz, I.J., Prarat, M.V., O'Donnell, V., Vepkhvadze, N.G., Lu, Z., Risatti, G.R., and Borca, M.V. (2011). Interaction

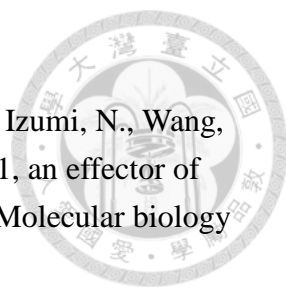
- 
- between Core protein of classical swine fever virus with cellular IQGAP1 protein appears essential for virulence in swine. *Virology* 412, 68-74.
34. Gnatenko, D.V., Xu, X., Zhu, W., and Schmidt, V.A. (2013). Transcript profiling identifies *iqgap2*(-/-) mouse as a model for advanced human hepatocellular carcinoma. *PloS one* 8, e71826.
  35. Goswami, R., Gershburg, S., Satorius, A., and Gershburg, E. (2012). Protein kinase inhibitors that inhibit induction of lytic program and replication of Epstein-Barr virus. *Antiviral research* 96, 296-304.
  36. Goto, T., Sato, A., Adachi, S., Iemura, S., Natsume, T., and Shibuya, H. (2013a). IQGAP1 protein regulates nuclear localization of beta-catenin via importin-beta5 protein in Wnt signaling. *The Journal of biological chemistry* 288, 36351-36360.
  37. Goto, T., Sato, A., Shimizu, M., Adachi, S., Satoh, K., Iemura, S., Natsume, T., and Shibuya, H. (2013b). IQGAP1 functions as a modulator of dishevelled nuclear localization in Wnt signaling. *PloS one* 8, e60865.
  38. Greenspan, J.S., Greenspan, D., Lennette, E.T., Abrams, D.I., Conant, M.A., Petersen, V., and Freese, U.K. (1985). Replication of Epstein-Barr virus within the epithelial cells of oral "hairy" leukoplakia, an AIDS-associated lesion. *The New England journal of medicine* 313, 1564-1571.
  39. Gruffat, H., and Sergeant, A. (1994). Characterization of the DNA-binding site repertoire for the Epstein-Barr virus transcription factor R. *Nucleic acids research* 22, 1172-1178.
  40. Gutsch, D.E., Marcu, K.B., and Kenney, S.C. (1994). The Epstein-Barr virus BRLF1 gene product transactivates the murine and human c-myc promoters. *Cellular and molecular biology (Noisy-le-Grand, France)* 40, 747-760.
  41. Hardwick, J.M., Lieberman, P.M., and Hayward, S.D. (1988). A new Epstein-Barr virus transactivator, R, induces expression of a cytoplasmic early antigen. *Journal of virology* 62, 2274-2284.
  42. Hardwick, J.M., Tse, L., Applegren, N., Nicholas, J., and Veluona, M.A. (1992). The Epstein-Barr virus R transactivator (Rta) contains a complex, potent activation domain with properties different from those of VP16. *Journal of virology* 66, 5500-5508.
  43. Hedman, A.C., Smith, J.M., and Sacks, D.B. (2015). The biology of IQGAP proteins: beyond the cytoskeleton. *EMBO reports* 16, 427-446.
  44. Heilmann, A.M., Calderwood, M.A., and Johannsen, E. (2010). Epstein-Barr virus LF2 protein regulates viral replication by altering Rta subcellular localization. *Journal of virology* 84, 9920-9931.
  45. Heilmann, A.M., Calderwood, M.A., Portal, D., Lu, Y., and Johannsen, E. (2012).

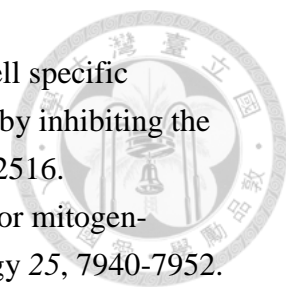


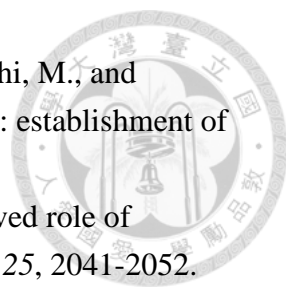
- Genome-wide analysis of Epstein-Barr virus Rta DNA binding. *Journal of virology* 86, 5151-5164.
46. Henle, G., Henle, W., and Diehl, V. (1968). Relation of Burkitt's tumor-associated herpes-yppe virus to infectious mononucleosis. *Proceedings of the National Academy of Sciences of the United States of America* 59, 94-101.
  47. Ho, C.H., Hsu, C.F., Fong, P.F., Tai, S.K., Hsieh, S.L., and Chen, C.J. (2007). Epstein-Barr virus transcription activator Rta upregulates decoy receptor 3 expression by binding to its promoter. *Journal of virology* 81, 4837-4847.
  48. Hoesel, B., and Schmid, J.A. (2013). The complexity of NF-kappaB signaling in inflammation and cancer. *Molecular cancer* 12, 86.
  49. Hsu, T.Y., Chang, Y., Wang, P.W., Liu, M.Y., Chen, M.R., Chen, J.Y., and Tsai, C.H. (2005). Reactivation of Epstein-Barr virus can be triggered by an Rta protein mutated at the nuclear localization signal. *The Journal of general virology* 86, 317-322.
  50. Huang, S.Y., Hsieh, M.J., Chen, C.Y., Chen, Y.J., Chen, J.Y., Chen, M.R., Tsai, C.H., Lin, S.F., and Hsu, T.Y. (2012). Epstein-Barr virus Rta-mediated transactivation of p21 and 14-3-3sigma arrests cells at the G1/S transition by reducing cyclin E/CDK2 activity. *The Journal of general virology* 93, 139-149.
  51. Hung, C.H., Chen, L.W., Wang, W.H., Chang, P.J., Chiu, Y.F., Hung, C.C., Lin, Y.J., Liou, J.Y., Tsai, W.J., Hung, C.L., *et al.* (2014). Regulation of autophagic activation by Rta of Epstein-Barr virus via the extracellular signal-regulated kinase pathway. *Journal of virology* 88, 12133-12145.
  52. Jiang, J.H., Wang, N., Li, A., Liao, W.T., Pan, Z.G., Mai, S.J., Li, D.J., Zeng, M.S., Wen, J.M., and Zeng, Y.X. (2006). Hypoxia can contribute to the induction of the Epstein-Barr virus (EBV) lytic cycle. *Journal of clinical virology : the official publication of the Pan American Society for Clinical Virology* 37, 98-103.
  53. Jin, S.H., Akiyama, Y., Fukamachi, H., Yanagihara, K., Akashi, T., and Yuasa, Y. (2008). IQGAP2 inactivation through aberrant promoter methylation and promotion of invasion in gastric cancer cells. *International journal of cancer Journal international du cancer* 122, 1040-1046.
  54. Johansson, B., Klein, G., Henle, W., and Henle, G. (1970). Epstein-Barr virus (EBV)-associated antibody patterns in malignant lymphoma and leukemia. I. Hodgkin's disease. *International journal of cancer Journal international du cancer* 6, 450-462.
  55. Jones, J.F., Shurin, S., Abramowsky, C., Tubbs, R.R., Sciotto, C.G., Wahl, R., Sands, J., Gottman, D., Katz, B.Z., and Sklar, J. (1988). T-cell lymphomas containing Epstein-Barr viral DNA in patients with chronic Epstein-Barr virus

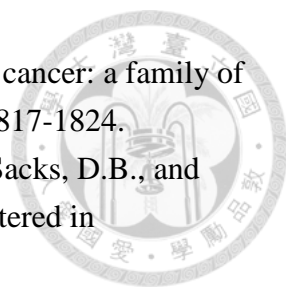
- 
- infections. *The New England journal of medicine* 318, 733-741.
56. Kallin, B., Luka, J., and Klein, G. (1979). Immunochemical characterization of Epstein-Barr virus-associated early and late antigens in n-butyrate-treated P3HR-1 cells. *Journal of virology* 32, 710-716.
  57. Kenney, S.C., and Mertz, J.E. (2014). Regulation of the latent-lytic switch in Epstein-Barr virus. *Seminars in cancer biology* 26, 60-68.
  58. Kim, J.H., Xu, E.Y., Sacks, D.B., Lee, J., Shu, L., Xia, B., and Kong, A.N. (2013). Identification and functional studies of a new Nrf2 partner IQGAP1: a critical role in the stability and transactivation of Nrf2. *Antioxidants & redox signaling* 19, 89-101.
  59. Kohno, T., Urao, N., Ashino, T., Sudhakar, V., Inomata, H., Yamaoka-Tojo, M., McKinney, R.D., Fukai, T., and Ushio-Fukai, M. (2013). IQGAP1 links PDGF receptor-beta signal to focal adhesions involved in vascular smooth muscle cell migration: role in neointimal formation after vascular injury. *American journal of physiology Cell physiology* 305, C591-600.
  60. Kraus, R.J., Perrigoue, J.G., and Mertz, J.E. (2003). ZEB negatively regulates the lytic-switch BZLF1 gene promoter of Epstein-Barr virus. *Journal of virology* 77, 199-207.
  61. Leung, J., Yueh, A., Appah, F.S., Jr., Yuan, B., de los Santos, K., and Goff, S.P. (2006). Interaction of Moloney murine leukemia virus matrix protein with IQGAP. *The EMBO journal* 25, 2155-2166.
  62. Li, Y., Webster-Cyriaque, J., Tomlinson, C.C., Yohe, M., and Kenney, S. (2004). Fatty acid synthase expression is induced by the Epstein-Barr virus immediate-early protein BRLF1 and is required for lytic viral gene expression. *Journal of virology* 78, 4197-4206.
  63. Liang, C.L., Chen, J.L., Hsu, Y.P., Ou, J.T., and Chang, Y.S. (2002). Epstein-Barr virus BZLF1 gene is activated by transforming growth factor-beta through cooperativity of Smads and c-Jun/c-Fos proteins. *The Journal of biological chemistry* 277, 23345-23357.
  64. Lin, C.T., Chan, W.Y., Chen, W., Huang, H.M., Wu, H.C., Hsu, M.M., Chuang, S.M., and Wang, C.C. (1993). Characterization of seven newly established nasopharyngeal carcinoma cell lines. *Laboratory investigation; a journal of technical methods and pathology* 68, 716-727.
  65. Lin, J.C., Sista, N.D., Besencon, F., Kamine, J., and Pagano, J.S. (1991). Identification and functional characterization of Epstein-Barr virus DNA polymerase by in vitro transcription-translation of a cloned gene. *Journal of virology* 65, 2728-2731.

- 
66. Lin, J.C., Wang, W.Y., Chen, K.Y., Wei, Y.H., Liang, W.M., Jan, J.S., and Jiang, R.S. (2004). Quantification of plasma Epstein-Barr virus DNA in patients with advanced nasopharyngeal carcinoma. *The New England journal of medicine* 350, 2461-2470.
  67. Liu, C., Sista, N.D., and Pagano, J.S. (1996). Activation of the Epstein-Barr virus DNA polymerase promoter by the BRLF1 immediate-early protein is mediated through USF and E2F. *Journal of virology* 70, 2545-2555.
  68. Liu, S., Liu, P., Borrás, A., Chatila, T., and Speck, S.H. (1997). Cyclosporin A-sensitive induction of the Epstein-Barr virus lytic switch is mediated via a novel pathway involving a MEF2 family member. *The EMBO journal* 16, 143-153.
  69. Logue, J.S., Whiting, J.L., Tunquist, B., Langeberg, L.K., and Scott, J.D. (2011a). Anchored protein kinase A recruitment of active Rac GTPase. *The Journal of biological chemistry* 286, 22113-22121.
  70. Logue, J.S., Whiting, J.L., Tunquist, B., Sacks, D.B., Langeberg, L.K., Wordeman, L., and Scott, J.D. (2011b). AKAP220 protein organizes signaling elements that impact cell migration. *The Journal of biological chemistry* 286, 39269-39281.
  71. Longnecker, R.M.K., Elliott.
  72. Cohen, Jeffery I. (2013). *Fields virology* (Philadelphia: Wolters Kluwer Health/Lippincott Williams & Wilkins).
  73. Lu, J., Qu, Y., Liu, Y., Jambusaria, R., Han, Z., Ruthel, G., Freedman, B.D., and Harty, R.N. (2013). Host IQGAP1 and Ebola virus VP40 interactions facilitate virus-like particle egress. *Journal of virology* 87, 7777-7780.
  74. Macsween, K.F., and Crawford, D.H. (2003). Epstein-Barr virus-recent advances. *The Lancet Infectious diseases* 3, 131-140.
  75. Manet, E., Rigolet, A., Gruffat, H., Giot, J.F., and Sergeant, A. (1991). Domains of the Epstein-Barr virus (EBV) transcription factor R required for dimerization, DNA binding and activation. *Nucleic acids research* 19, 2661-2667.
  76. Menezes, J., Leibold, W., Klein, G., and Clements, G. (1975). Establishment and characterization of an Epstein-Barr virus (EBC)-negative lymphoblastoid B cell line (BJA-B) from an exceptional, EBV-genome-negative African Burkitt's lymphoma. *Biomedicine / [publiee pour l'AAICIG]* 22, 276-284.
  77. Monteleon, C.L., McNeal, A., Duperret, E.K., Oh, S.J., Schapira, E., and Ridky, T.W. (2015). IQGAP1 and IQGAP3 Serve Individually Essential Roles in Normal Epidermal Homeostasis and Tumor Progression. *The Journal of investigative dermatology*.
  78. Nojima, H., Adachi, M., Matsui, T., Okawa, K., Tsukita, S., and Tsukita, S. (2008). IQGAP3 regulates cell proliferation through the Ras/ERK signalling cascade.

- 
- Nature cell biology *10*, 971-978.
79. Noritake, J., Fukata, M., Sato, K., Nakagawa, M., Watanabe, T., Izumi, N., Wang, S., Fukata, Y., and Kaibuchi, K. (2004). Positive role of IQGAP1, an effector of Rac1, in actin-meshwork formation at sites of cell-cell contact. *Molecular biology of the cell* *15*, 1065-1076.
  80. Noritake, J., Watanabe, T., Sato, K., Wang, S., and Kaibuchi, K. (2005). IQGAP1: a key regulator of adhesion and migration. *Journal of cell science* *118*, 2085-2092.
  81. Pallesen, G., Hamilton-Dutoit, S.J., Rowe, M., and Young, L.S. (1991). Expression of Epstein-Barr virus latent gene products in tumour cells of Hodgkin's disease. *Lancet* *337*, 320-322.
  82. Quinlivan, E.B., Holley-Guthrie, E.A., Norris, M., Gutsch, D., Bachenheimer, S.L., and Kenney, S.C. (1993). Direct BRLF1 binding is required for cooperative BZLF1/BRLF1 activation of the Epstein-Barr virus early promoter, BMRF1. *Nucleic acids research* *21*, 1999-2007.
  83. Ragoczy, T., and Miller, G. (2001). Autostimulation of the Epstein-Barr virus BRLF1 promoter is mediated through consensus Sp1 and Sp3 binding sites. *Journal of virology* *75*, 5240-5251.
  84. Raver, R.M., Panfil, A.R., Hagemeyer, S.R., and Kenney, S.C. (2013). The B-cell-specific transcription factor and master regulator Pax5 promotes Epstein-Barr virus latency by negatively regulating the viral immediate early protein BZLF1. *Journal of virology* *87*, 8053-8063.
  85. Rea, D., Fourcade, C., Leblond, V., Rowe, M., Joab, I., Edelman, L., Bitker, M.O., Gandjbakhch, I., Suberbielle, C., Farcet, J.P., *et al.* (1994). Patterns of Epstein-Barr virus latent and replicative gene expression in Epstein-Barr virus B cell lymphoproliferative disorders after organ transplantation. *Transplantation* *58*, 317-324.
  86. Ren, J.G., Li, Z., and Sacks, D.B. (2007). IQGAP1 modulates activation of B-Raf. *Proceedings of the National Academy of Sciences of the United States of America* *104*, 10465-10469.
  87. Reusch, J.A., Nawandar, D.M., Wright, K.L., Kenney, S.C., and Mertz, J.E. (2015). Cellular differentiation regulator BLIMP1 induces Epstein-Barr virus lytic reactivation in epithelial and B cells by activating transcription from both the R and Z promoters. *Journal of virology* *89*, 1731-1743.
  88. Robinson, A.R., Kwek, S.S., Hagemeyer, S.R., Wille, C.K., and Kenney, S.C. (2011). Cellular transcription factor Oct-1 interacts with the Epstein-Barr virus BRLF1 protein to promote disruption of viral latency. *Journal of virology* *85*, 8940-8953.

- 
89. Robinson, A.R., Kwek, S.S., and Kenney, S.C. (2012). The B-cell specific transcription factor, Oct-2, promotes Epstein-Barr virus latency by inhibiting the viral immediate-early protein, BZLF1. *PLoS pathogens* 8, e1002516.
  90. Roy, M., Li, Z., and Sacks, D.B. (2005). IQGAP1 is a scaffold for mitogen-activated protein kinase signaling. *Molecular and cellular biology* 25, 7940-7952.
  91. Sambrook, J. (2001). *Molecular cloning : a laboratory manual*, D.W. Russell, ed. (Cold Spring Harbor, N.Y. :: Cold Spring Harbor Laboratory Press).
  92. Sbroglio, M., Carnevale, D., Bertero, A., Cifelli, G., De Blasio, E., Mascio, G., Hirsch, E., Bahou, W.F., Turco, E., Silengo, L., *et al.* (2011). IQGAP1 regulates ERK1/2 and AKT signalling in the heart and sustains functional remodelling upon pressure overload. *Cardiovascular research* 91, 456-464.
  93. Schmidt, V.A., Chiariello, C.S., Capilla, E., Miller, F., and Bahou, W.F. (2008). Development of hepatocellular carcinoma in Iqgap2-deficient mice is IQGAP1 dependent. *Molecular and cellular biology* 28, 1489-1502.
  94. Schmidt, V.A., Scudder, L., Devoe, C.E., Bernardis, A., Cupit, L.D., and Bahou, W.F. (2003). IQGAP2 functions as a GTP-dependent effector protein in thrombin-induced platelet cytoskeletal reorganization. *Blood* 101, 3021-3028.
  95. Sharma, S., Findlay, G.M., Bandukwala, H.S., Oberdoerffer, S., Baust, B., Li, Z., Schmidt, V., Hogan, P.G., Sacks, D.B., and Rao, A. (2011). Dephosphorylation of the nuclear factor of activated T cells (NFAT) transcription factor is regulated by an RNA-protein scaffold complex. *Proceedings of the National Academy of Sciences of the United States of America* 108, 11381-11386.
  96. Shimizu, N., Tanabe-Tochikura, A., Kuroiwa, Y., and Takada, K. (1994). Isolation of Epstein-Barr virus (EBV)-negative cell clones from the EBV-positive Burkitt's lymphoma (BL) line Akata: malignant phenotypes of BL cells are dependent on EBV. *Journal of virology* 68, 6069-6073.
  97. Smith, J.M., Hedman, A.C., and Sacks, D.B. (2015). IQGAPs choreograph cellular signaling from the membrane to the nucleus. *Trends in cell biology* 25, 171-184.
  98. Sokol, S.Y., Li, Z., and Sacks, D.B. (2001). The effect of IQGAP1 on *Xenopus* embryonic ectoderm requires Cdc42. *The Journal of biological chemistry* 276, 48425-48430.
  99. Sun, C.C., and Thorley-Lawson, D.A. (2007). Plasma cell-specific transcription factor XBP-1s binds to and transactivates the Epstein-Barr virus BZLF1 promoter. *Journal of virology* 81, 13566-13577.
  100. Swart-Mataraza, J.M., Li, Z., and Sacks, D.B. (2002). IQGAP1 is a component of Cdc42 signaling to the cytoskeleton. *The Journal of biological chemistry* 277, 24753-24763.

- 
101. Takada, K., Horinouchi, K., Ono, Y., Aya, T., Osato, T., Takahashi, M., and Hayasaka, S. (1991). An Epstein-Barr virus-producer line Akata: establishment of the cell line and analysis of viral DNA. *Virus genes* 5, 147-156.
  102. Tekletsadik, Y.K., Sonn, R., and Osman, M.A. (2012). A conserved role of IQGAP1 in regulating TOR complex 1. *Journal of cell science* 125, 2041-2052.
  103. Thompson, M.P., and Kurzrock, R. (2004). Epstein-Barr Virus and Cancer. *Clinical Cancer Research* 10, 803-821.
  104. Tovey, M.G., Lenoir, G., and Begon-Lours, J. (1978). Activation of latent Epstein-Barr virus by antibody to human IgM. *Nature* 276, 270-272.
  105. Tsai, C.H., Liu, M.T., Chen, M.R., Lu, J., Yang, H.L., Chen, J.Y., and Yang, C.S. (1997). Characterization of Monoclonal Antibodies to the Zta and DNase Proteins of Epstein-Barr Virus. *Journal of biomedical science* 4, 69-77.
  106. Tsai, P.F., Lin, S.J., Weng, P.L., Tsai, S.C., Lin, J.H., Chou, Y.C., and Tsai, C.H. (2011). Interplay between PKCdelta and Sp1 on histone deacetylase inhibitor-mediated Epstein-Barr virus reactivation. *Journal of virology* 85, 2373-2385.
  107. Tsai, S.C., Lin, S.J., Chen, P.W., Luo, W.Y., Yeh, T.H., Wang, H.W., Chen, C.J., and Tsai, C.H. (2009). EBV Zta protein induces the expression of interleukin-13, promoting the proliferation of EBV-infected B cells and lymphoblastoid cell lines. *Blood* 114, 109-118.
  108. Tsurumi, T., Kobayashi, A., Tamai, K., Yamada, H., Daikoku, T., Yamashita, Y., and Nishiyama, Y. (1996). Epstein-Barr virus single-stranded DNA-binding protein: purification, characterization, and action on DNA synthesis by the viral DNA polymerase. *Virology* 222, 352-364.
  109. Wakatsuki, Y., Neurath, M.F., Max, E.E., and Strober, W. (1994). The B cell-specific transcription factor BSAP regulates B cell proliferation. *The Journal of experimental medicine* 179, 1099-1108.
  110. Wang, J.T., Yang, P.W., Lee, C.P., Han, C.H., Tsai, C.H., and Chen, M.R. (2005). Detection of Epstein-Barr virus BGLF4 protein kinase in virus replication compartments and virus particles. *The Journal of general virology* 86, 3215-3225.
  111. Wang, S., Watanabe, T., Noritake, J., Fukata, M., Yoshimura, T., Itoh, N., Harada, T., Nakagawa, M., Matsuura, Y., Arimura, N., *et al.* (2007). IQGAP3, a novel effector of Rac1 and Cdc42, regulates neurite outgrowth. *Journal of cell science* 120, 567-577.
  112. Weissbach, L., Settleman, J., Kalady, M.F., Snijders, A.J., Murthy, A.E., Yan, Y.X., and Bernards, A. (1994). Identification of a human rasGAP-related protein containing calmodulin-binding motifs. *The Journal of biological chemistry* 269, 20517-20521.

- 
113. White, C.D., Brown, M.D., and Sacks, D.B. (2009). IQGAPs in cancer: a family of scaffold proteins underlying tumorigenesis. *FEBS letters* 583, 1817-1824.
  114. White, C.D., Khurana, H., Gnatenko, D.V., Li, Z., Odze, R.D., Sacks, D.B., and Schmidt, V.A. (2010). IQGAP1 and IQGAP2 are reciprocally altered in hepatocellular carcinoma. *BMC gastroenterology* 10, 125.
  115. Xie, Y., Yan, J., Cutz, J.C., Rybak, A.P., He, L., Wei, F., Kapoor, A., Schmidt, V.A., Tao, L., and Tang, D. (2012). IQGAP2, A candidate tumour suppressor of prostate tumorigenesis. *Biochimica et biophysica acta* 1822, 875-884.
  116. Yamashiro, S., Abe, H., and Mabuchi, I. (2007). IQGAP2 is required for the cadherin-mediated cell-to-cell adhesion in *Xenopus laevis* embryos. *Developmental biology* 308, 485-493.
  117. Yang, T.-Y. (2013). EBV BGLF4 Induces Formation of Viral Cytoplasmic Assembly Compartment Through Rearrangement of Cytoskeleton. In Graduate Institute of Microbiology, College of Medicine (Taipei, Taiwan: National Taiwan University).
  118. Yao, Q.Y., Rickinson, A.B., and Epstein, M.A. (1985). A re-examination of the Epstein-Barr virus carrier state in healthy seropositive individuals. *International journal of cancer Journal international du cancer* 35, 35-42.
  119. Ye, J., Gradoville, L., and Miller, G. (2010). Cellular immediate-early gene expression occurs kinetically upstream of Epstein-Barr virus bzlfl1 and brlf1 following cross-linking of the B cell antigen receptor in the Akata Burkitt lymphoma cell line. *Journal of virology* 84, 12405-12418.
  120. Young, L.S., and Rickinson, A.B. (2004). Epstein-Barr virus: 40 years on. *Nature reviews Cancer* 4, 757-768.
  121. Yu, X., Wang, Z., and Mertz, J.E. (2007). ZEB1 regulates the latent-lytic switch in infection by Epstein-Barr virus. *PLoS pathogens* 3, e194.
  122. Zacny, V.L., Wilson, J., and Pagano, J.S. (1998). The Epstein-Barr virus immediate-early gene product, BRLF1, interacts with the retinoblastoma protein during the viral lytic cycle. *Journal of virology* 72, 8043-8051.
  123. Zalani, S., Coppage, A., Holley-Guthrie, E., and Kenney, S. (1997). The cellular YY1 transcription factor binds a cis-acting, negatively regulating element in the Epstein-Barr virus BRLF1 promoter. *Journal of virology* 71, 3268-3274.
  124. Zalani, S., Holley-Guthrie, E., and Kenney, S. (1995). The Zif268 cellular transcription factor activates expression of the Epstein-Barr virus immediate-early BRLF1 promoter. *Journal of virology* 69, 3816-3823.
  125. Ziegler, J.L., Drew, W.L., Miner, R.C., Mintz, L., Rosenbaum, E., Gershow, J., Lennette, E.T., Greenspan, J., Shillitoe, E., Beckstead, J., *et al.* (1982). Outbreak of

- Burkitt's-like lymphoma in homosexual men. *Lancet* 2, 631-633.
126. zur Hausen, H., O'Neill, F.J., Freese, U.K., and Hecker, E. (1978). Persisting oncogenic herpesvirus induced by the tumour promotor TPA. *Nature* 272, 373-375.
127. zur Hausen, H., Schulte-Holthausen, H., Klein, G., Henle, W., Henle, G., Clifford, P., and Santesson, L. (1970). EBV DNA in biopsies of Burkitt tumours and anaplastic carcinomas of the nasopharynx. *Nature* 228, 1056-1058.